

**A MUTATION IN THE SEMAPHORIN  
SIGNALLING PATHWAY AND ITS  
CONSEQUENCES IN PROSTATE CANCER**

**Jason Constantinou**

**A thesis submitted for the degree of MD(Res)**

**University College London**

**2010**

## **Declaration of originality**

I, Jason Constantinou confirm that the work presented in this thesis is my own.

Where information has been derived from other sources, I can confirm that this has  
been indicated in the thesis

## **Abstract**

Prostate cancer kills over 10,000 men every year in the UK, mainly as a consequence of the spread of the disease to other sites in the body. It is important to understand what controls the spread of prostate cancer cells, as this may lead to treatments that either slow down or prevent metastasis, and perhaps result in the cure of some of the advanced prostate cancers.

Semaphorins act as chemotactic cues for axon guidance and cell movement, via their transmembrane receptors, plexins. It has been found that semaphorins and their receptors are overexpressed in some human prostate cancer cell lines. These cell lines have been screened for mutations in genes in the semaphorin signalling pathway. 13 somatic missense mutations in the cytoplasmic domain of the Plexin B1 gene have been identified in clinical samples of primary and metastatic prostate cancers. One of the mutations C5662T was predicted to result in a substitution of a Proline to a Serine.

The aim of this research is to determine if the mutation C5662T in the Plexin B1 gene alters cell behaviour and contributes to prostate cancer progression.

This thesis describes the method of constructing an expression vector containing the mutation and transfecting the mutation into COS7 cells to produce stable and transient clones.

The effect of the mutation on cell collapse was examined. It was possible to show that Plexin B1 is involved in cell collapse and that Rnd1 is required for this process and this effect is independent of its ligand Semaphorin 4D (Sema4D). Although no functional difference between the wild type Plexin B1 and the mutant (C5662T) was observed, the rate of cell collapse may be important and more work will be needed to define whether this is a mutation that alters prostate cancer cell behaviour.

## Dedication

To Penny, Thomas and Xanthe for their love and support

## **Acknowledgements**

I would like to thank all the staff, especially Tharani Nitkunan, at the Prostate Cancer Research Centre, Institute of Urology Laboratories for their day-to-day help and support.

To Professor McNicholas, Mr Boustead, Mr Hanbury and Linda Fowler, Department of Urology at the Lister Hospital, Stevenage for their support, enthusiasm and generous financial assistance in making this thesis possible.

To Dr Magali Williamson, Mr Mark Feneley and Professor John Masters for their encouragement, insight and knowledge, and for being so supportive during the period of my study.

# CONTENTS

<b>Title</b>	<b>1</b>
<b>Declaration of originality</b>	<b>2</b>
<b>Abstract</b>	<b>3-4</b>
<b>Dedication</b>	<b>5</b>
<b>Acknowledgements</b>	<b>6</b>
<b>Contents</b>	<b>7-10</b>
<b>List of Figures</b>	<b>11-14</b>
<b>List of Tables</b>	<b>15</b>
<b>List of Abbreviations</b>	<b>16-17</b>
<b>Chapter 1      Introduction</b>	<b>18-65</b>
1.1 Prostate cancer	
1.1.1 Epidemiology of prostate cancer	
1.1.2 Pathology of prostate cancer	
1.1.3 Natural History of prostate cancer	
1.2 Cancer cell invasion and metastasis	
1.3 Semaphorins and Plexins	
1.3.1 Classification of Semaphorins	

- 1.3.2 Structure of Plexins
- 1.3.3 Interactions of Plexins
- 1.3.4 Semaphorin Functions
- 1.4 Semaphorin 4D and invasive growth
- 1.5 Plexin B1 and prostate cancer
- 1.6 Aims and Objectives

## **Chapter 2      Materials and Methods**

**66-100**

- 2.1 Materials and Methods
  - 2.1.1 DNA constructs
  - 2.1.2 Cell culture
  - 2.1.3 Site-directed in-vitro mutagenesis
  - 2.1.4 DNA Extraction
  - 2.1.5 PCR (Polymerase Chain Reaction)
  - 2.1.6 Digestion with Restriction Enzyme
  - 2.1.7 Cycle sequencing
  - 2.1.8 Cloning of CD2-vector pcDNA3
  - 2.1.9 Transfection
  - 2.1.10 Relative expression of Plexin B1 RNA in stable clones
  - 2.1.11 Protein Extraction
  - 2.1.12 Western Blotting
  - 2.1.13 Immunofluorescence



2.1.14 Preparation of Semaphorin 4D-Fc

2.1.15 Collapse assay

**Chapter 3      Generation of Mutant Plexin B1      101-156**

3.1 Introduction

3.2 Results

3.2.1 Generation of the mutation into Plexin B1 cDNA (full length-FL & truncated-CD2)

3.2.2 Confirmation of the mutation

3.2.3 Generation of stable clones of full length Plexin B1

3.2.4 Protein expression of Plexin B1

3.2.5 Expression of Semaphorin 4D and Plexin B1 in prostate cancer cell lines

3.3 Discussion

**Chapter 4      The Collapse assay      157-185**

4.1 Introduction

4.2 Results

4.2.1 Preparation of Semaphorin 4D-Fc

4.2.2 Optimising the Collapse assay

4.2.3 The Collapse Assay

4.3 Discussion

<b>Chapter 5</b>	<b>Discussion and future work</b>	<b>186-193</b>
5.1	Discussion	
<b>References</b>		<b>194-217</b>
<b>Appendix</b>		<b>218-224</b>
<b>Published work</b>		<b>225-231</b>

## **LIST OF FIGURES**

### **Chapter 1**

Figure 1.1 Age standardized incidence and mortality rates, prostate cancer, males, Great Britain, 1975-2006

Figure 1.2 The five Gleason grades of prostate cancer

Figure 1.3 The Semaphorin Family

Figure 1.4 Vertebrate Plexins

Figure 1.5 Structure of Plexin B1

Figure 1.6 Plexin B1/Rac interaction inhibits PAK activation and enhances Sema4D ligand binding

Figure 1.7 Mechanism by which plexins activate Rho via PDZ-Rho GEF

Figure 1.8 Pathway of Sema 3A signalling

### **Chapter 2**

Figure 2.1 Plexin B1 in pcDNA3

Figure 2.2 Site directed in-vitro mutagenesis

## Chapter 3

Figure 3.1 Extracted DNA of mutated full length Plexin B1 and truncated CD2 Plexin B1 run on 0.8% gel

Figure 3.2 PCR product of truncated CD2 Plexin B1 and full length Plexin B1

Figure 3.3 Digestion of CD2 Plexin B1 and full length Plexin B1 using the restriction enzyme Hae III

Figure 3.4 PCR product of DNA extracted from clones A-E CD2 Plexin B1 and clone A and B full length Plexin B1

Figure 3.5 Cycle sequencing of the mutant Plexin B1

Figure 3.6 Cycle sequencing of mutant full length Plexin B1 clone B

Figure 3.7 Relative expression of Plexin B1 RNA in clones

Figure 3.8 Checking the clones with Hae III digestion and cycle sequencing

Figure 3.9 Full length Plexin B1 showing the  $\alpha$  and  $\beta$  subunits

Figure 3.10 Western blot showing protein expression of endogenous Plexin B1

Figure 3.11 Protein expression of Plexin B1 using three protein extraction buffers – RIPA, EB, OBG with and without sodium butyrate (NaB) in wild type, mutant and vector only stable clones

Figure 3.12 COS1 cells transiently transfected with WT-CD2 Plexin B1

Figure 3.13 COS1 cells transiently transfected with WT-CD2 Plexin B1 (no 1<sup>o</sup> antibody)

Figure 3.14 COS1 cells transiently transfected with Mutant-CD2 Plexin B1

Figure 3.15 COS1 cells transiently transfected with Vector-CD2

Figure 3.16 COS1 cells mock transfected

Figure 3.17 3T3 cells transiently transfected with WT-CD2 Plexin B1

Figure 3.18 3T3 cells transiently transfected with WT-CD2 Plexin B1 (no 1° Ab)

Figure 3.19 3T3 cells transiently transfected with Mutant-CD2 Plexin B1

Figure 3.20 3T3 cells transiently transfected with Vector-CD2

Figure 3.21 3T3 cells mock transfected

Figure 3.22 Stable transfection of 3T3 cells with WT-CD2 Plexin B1

Figure 3.23 Stable transfection of 3T3 cells with Mutant-CD2 Plexin B1

Figure 3.24 Stable transfection of 3T3 cells with Vector-CD2

Figure 3.25 Mock transfected 3T3 cells

Figure 3.26 Confocal microscopy showing protein expression of CD2-Plexin B1 in

COS7 cells

Figure 3.27 RT-PCR of Semaphorin 4D mRNA in cell lines

Figure 3.28 RT-PCR of Plexin B1 mRNA in cell lines

## **Chapter 4**

Figure 4.1 Western Blot showing protein expression of Sema4D-Fc and Sema3A-Fc

Figure 4.2 Sema4D expression in COS7 cells transfected with Sema4D-Fc (with Triton X)

Figure 4.3 COS7 cells transfected with Sema4D-Fc (no Triton X)

Figure 4.4 Protein expression of Wild Type Full Length Plexin B1

Figure 4.5 Protein expression of Wild Type Plexin B1 (Confocal Image) a) with Triton X b) without Triton X

Figure 4.6 Protein expression of Mutant Plexin B1 (Confocal Image) a) with Triton X b) without Triton X

Figure 4.7 COS7 cells transfected with Rnd1 stained by immunofluorescence

Figure 4.8 COS7 cells transfected with Wild Type Plexin B1 with and without Sema4D-Fc (No Rnd1)

Figure 4.9 COS7 cells cotransfected with Wild Type Plexin B1 and Rnd1 a) without Sema4D-Fc b) with Sema4D

Figure 4.10 COS7 cells transfected with Mutant Plexin B1 without Rnd1 a) without Sema4D-Fc b) with Sema4D

Figure 4.11 COS7 cells cotransfected with Mutant Plexin B1 and Rnd1 a) without Sema4D-Fc b) with Sema4D

Figure 4.12 COS7 cells transfected with Rnd1 a) with Sema4D-Fc b) without Sema4D-Fc

Figure 4.13 Analysis of COS7 cell collapse (%)

Figure 4.14 Image J software

## **LIST OF TABLES**

### **Chapter 1**

Table 1.1 Position of the mutations found in Plexin B1

Table 1.2 Sequence conservation of Plexin B1

### **Chapter 2**

Table 2.1 Antibodies used in western blot

Table 2.2 Primary and secondary antibodies used for immunohistochemistry

Table 2.3 Antibodies used in the Collapse assay

### **Chapter 3**

Table 3.1 DNA concentration of individual colonies

Table 3.2 Transfection Efficiency (%). Percentage of COS7 cells expressing  $\beta$ -galactosidase

Table 3.3 Transfection Efficiency (%). Percentage of COS1 cells expressing  $\beta$ -galactosidase

Table 3.4 Transfection Efficiency (%). Percentage of NIH3T3 cells expressing  $\beta$ -galactosidase

## List of abbreviations

AR	Androgen receptor
BSA	Bovine serum albumin
CRIB	Cdc42/Rac interactive binding
DH	Dbl homology
ECL	Enhance chemiluminescent
ECM	Extracellular matrix
DMEM	Dulbecco's modified eagle medium
FBS	Foetal bovine serum
GAP	GTPase activating protein
GEF	Guanine nucleotide exchange factor
GPCR	G protein coupled receptor
GPI	glycosylphosphatidylinositol
HGF	Hepatocyte growth factor
Ig	Immunoglobulin
LARG	Leukemia associated Rho-GEF
MAPK	Mitogen-activated protein kinase
MRS	MET related sequence
OBG	n-Octyl-Beta-D-Glucopyranoside
PAK	p21 activated kinase
PCR	Polymerase chain reaction



PDZ	PSD-95/Dlg/ZO-1
PH	Pleckstrin homology
PIN	Prostatic intraepithelial neoplasia
RGS	Regulators of G protein signalling
PSA	Prostate specific antigen
Sema	Semaphorin
Sema4D	Semaphorin 4D
SSCP	Single strand conformation polymorphism
VEGF	Vascular endothelial growth factor
VESPR	Virus encoded semaphorin protein receptor

## **Chapter 1:**

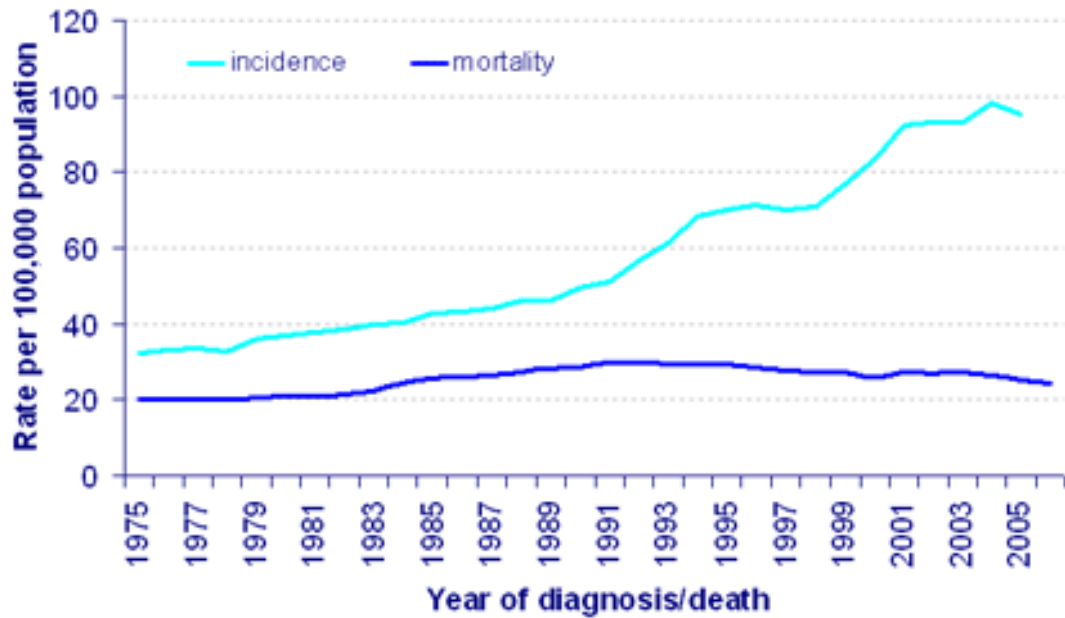
### **Introduction**

## **1.1 Prostate cancer**

### **1.1.1 Epidemiology of prostate cancer**

Prostate cancer is the most frequently diagnosed male cancer. In 2007 there were 10,239 deaths in the UK from prostate cancer (Office for National Statistics, 2009). In 2004, there were 34,986 new cases of prostate cancer diagnosed in the UK (Office for National Statistics, CSR). The incidence of prostate cancer is increasing steadily in almost all countries (Hsing et al. 2000). Over the last three decades prostate cancer rates have increased significantly in Great Britain. In Great Britain the age-standardized incidence rate almost trebled from 32 per 100,000 in 1975 to 95 per 100,000 in 2005. There was little change in death rates during the 1970's and death rates from prostate cancer only began to rise from 1980 onwards. The age standardized death rate peaked in 1995, and since then death rates from prostate cancer have declined (Figure 1.1) (Majeed et al. 2000).

The lifetime risk of being diagnosed with prostate cancer is 1 in 14 (Cancer research UK, [www.cancerresearchuk.org](http://www.cancerresearchuk.org)), the strongest risk factor is age. It is largely a disease of older men and is rare below the age of 50 (Cancer Research UK, [www.cancerresearchuk.org](http://www.cancerresearchuk.org)). Half of all cases are registered in men aged over 75. The median age of both diagnosis and mortality is 75 years (Chamberlain et al. 1997).



*Figure 1.1 Age standardized incidence and mortality rates of prostate cancer, males, Great Britain, 1975-2006 (Cancer Research UK). The number of prostate cancer cases diagnosed each year has been steadily rising. Much of this increase is due to the increased detection of prostate cancer by PSA testing and a growing awareness of the condition. Overall in the United Kingdom, prostate cancer mortality was fairly stable during the 1970s but began to increase in the early 1980s, however since 1995 the mortality has been declining. The reason for this is unclear but may be due to screening picking up the disease at an earlier stage.*

The incidence of prostate cancer varies widely between ethnic populations and countries. The lowest rates are in Asia, especially Chinese people in Tianjin, China (1.9 per 100 000 per year), and the highest are in North America and Scandinavia, especially in African-American people in the USA (137 per 100 000 per year) (Parkin et al. 1997). However, migration studies show that as men from low-risk countries move to high-risk countries the risk increases, suggesting that lifestyle plays an important role (Winter et al. 1999).

A family history of prostate cancer is an important risk factor. It is estimated that 5-10% of all prostate cancers are caused by inherited genes (Bratt, 2002). The relative risk of prostate cancer is increased 2-fold with one first degree relative diagnosed aged 70 or under and rises to 4-fold with two relatives, if one of them is diagnosed under the age of 65 (Cancer Research UK, [www.cancerresearchuk.org](http://www.cancerresearchuk.org)). The clustering of prostate cancer in families can be because of exposure to environmental factors, genetic susceptibility or chance since prevalence of this cancer is so high. A high concordance rate also exists in monozygotic twins. The site of the affected gene or genes is currently the subject of much investigation.

The lifestyle related factor that may play a part in the promotion of prostate cancer is diet. Studies suggest that prostate cancer is associated with a western diet that includes a high intake of fat and meat. However the results of these studies are conflicting except for a few dietary components that appear to be more promising such as lycopene (present in tomatoes), selenium and vitamin E (Gronberg 2003).

However, the Selenium and Vitamin E Cancer Prevention Trial (SELECT) recently showed that neither Selenium nor vitamin E prevented prostate cancer (Lippman et al. 2009).

The role of benign prostatic hypertrophy in the development of prostate cancer remains unclear. It is generally believed that the benign, hypertrophic prostatic cells do not directly transform into malignant cells (Carter et al. 1990). One possible contributory factor to the pathogenesis of prostate cancer is elevated serum testosterone concentrations. This hypothesis is supported by observations that prostate cancers are responsive to testosterone suppression. Black men have higher serum testosterone levels than white men, and the incidence of detectable prostate cancer, in eunuchs, who have below-average or negligible levels of testosterone, is low (Ross et al. 1986; Hill et al. 1979).

The prevalence of incidental tumours is characteristic of the prostate gland. Autopsies of men over the age of 50 years have revealed microscopic foci of well-differentiated adenocarcinoma in serial sections of prostate glands. It has been estimated that 9 out of 10 men who eventually develop clinically recognized prostate cancer had cancer that remained undetected for decades (Gittes 1991).

Despite progress in the diagnosis and local therapy of prostate cancer, many fundamental questions remain unanswered. What is the cause of this disease? How can we prevent it? Which cancers are clinically significant? Progress in the

management of prostate cancer requires ways to distinguish the harmless cancers from the potentially lethal, and developing effective ways to prevent or treat the potentially lethal cancers.

### **1.1.2 Pathology of prostate cancer**

High-grade prostatic intraepithelial neoplasia (PIN) is a clinically significant finding on prostate biopsies and is a well documented precursor to adenocarcinoma. PIN consists of architecturally benign prostatic ducts lined with cytologically atypical cells (McNeal 1969; McNeal et al. 1986). Low grade PIN, previously referred to as mild dysplasia or PIN-1, is of no prognostic significance and patients are at no greater risk of developing an invasive carcinoma. When high-grade PIN is found on needle biopsy, there is a 30 to 50 percent risk of finding carcinoma on subsequent biopsies (Keetch et al. 1995).

PIN itself does not give rise to elevated serum PSA levels (Ronnelt et al. 1993; Alexander et al. 1996; Ramos et al. 1999). The presence of high grade prostatic intraepithelial neoplasia indicates increased risk of prostate cancer somewhere in the prostate, but not necessarily at the site where the neoplasia was found at biopsy (Shepherd et al. 1996; Langer et al. 1996; Kamoj et al. 2000). Although high grade PIN appears to be a well recognized precursor lesion to prostate cancer, it is not a required precursor for carcinomas to arise within the prostate (Epstein et al. 1996).

Histologically, almost all prostate cancers are adenocarcinomas, derived from prostatic acinar cells. Approximately 75% will arise in the peripheral zone, 15% in the central zone and 10% in the transitional zone. Carcinomas tend to be multifocal and even if it appears to be unilateral on rectal examination, these lesions occur on both sides in approximately 70 percent of surgical specimens that are examined pathologically (Mostofi et al. 1992).

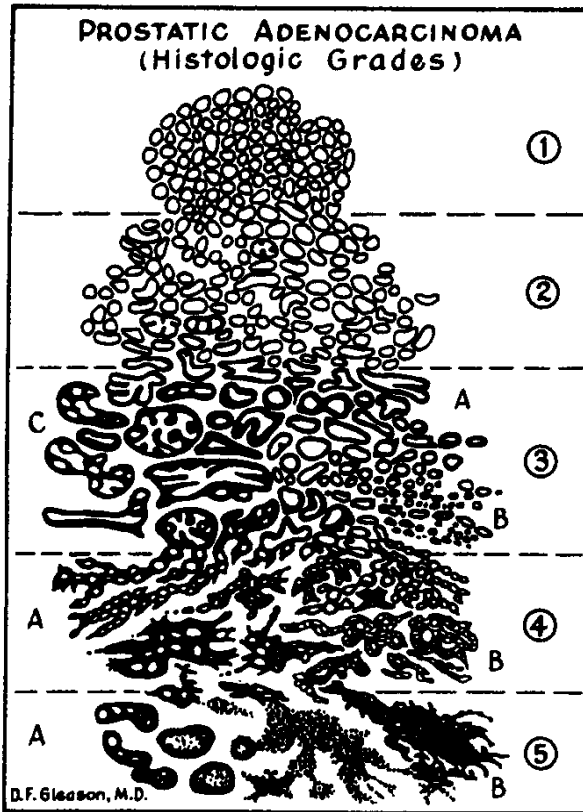
Similar to other cancers, prostate adenocarcinomas are graded by the pathologist according to their degree of differentiation and overall aggressiveness. The Gleason grading system is the most widely accepted. Patients are given a Gleason Score which is a number from 2-10. Dr. Gleason provided a diagram (Figure 1.2) to show the progressive deterioration of the cancer cell architecture, and the four dividing lines along this grading system which he discovered are able to identify patients with significantly different prognosis, derived from a study which included 2,900 patients (Gleason et al. 1974, 1992).

The Gleason grading system recognises the fact that prostate cancer is a multifocal disease with heterogeneous glandular patterns. It combines the two most dominant (primary and secondary) histological patterns of cancer within the sampled specimen. Each of the two most common patterns is assigned a grade from one to five, with one the most differentiated and least aggressive and five the least differentiated or most aggressive pattern. Gleason sum score is reported as the two scores added together. If the most common pattern of grading was a 3 pattern and the second most common pattern was a 4, the Gleason grade would be reported as



Gleason 3+4=7. The major prognostic shift is between 6 and 7 and Gleason score 7 tumours behave much worse than tumours scoring 5 or 6. The value of the Gleason grading system is its ability to predict survival rates. It correlates with all important pathological variables seen in the radical prostatectomy sample, with prognosis after radical prostatectomy, and with outcome after radiotherapy (McNeal et al. 1990; Epstein et al. 1996; Green et al. 1998).

The histology of the remaining few percent of prostate cancers is heterogeneous, arising from epithelial, stromal, or ectopic cells. Endometrioid carcinoma involves the prostatic urethra and periurethral prostatic ducts. This variant is aggressive and often is associated with metastatic disease. Similarly mucinous adenocarcinomas have a poor prognosis. Squamous cell carcinoma of the prostate accounts for 0.5% of cases and in these, serum tumour markers such as PSA tend to remain normal (Okamoto et al. 1996). Small cell carcinoma is another type of prostate cancer derived from neuroendocrine cells. These cancers tend to develop in men treated with long term hormonal ablation therapy. Primary transitional cell carcinoma of the prostate has also been reported, although secondary spread from the bladder is much more common (Reese et al. 1992).



*Figure 1.2 This illustration shows Dr. Gleason's own simplified drawing of the five Gleason grades of prostate cancer. The Gleason Score reflects how abnormal prostate cells look under the microscope. Abnormal-looking cells tend to grow and spread more quickly and have a worse outcome. A pathologist assigns a Gleason grade ranging from 1 through 5 based on how much the cancer cells under the microscope look like normal prostate cells. Those that look like normal cells are graded as 1, while those that look the least like normal cells are graded as 5.*

### **1.1.3 Natural history of prostate cancer**

Low-grade tumours can grow very slowly and remain localized to the gland for relatively long periods, during which they remain clinically undetectable. Tumours that become clinically significant arise mainly in the peripheral zone of the prostate gland and less frequently in the central zone or transition zone (Mostofi et al. 1992).

Prostate cancers may spread locally or distantly, typically they grow peripherally through the capsule along perineural sheaths that perforate the capsule at the upper outer corner and at the apex. Such tumours often invade the seminal vesicles and the neck of the urinary bladder. Extension through the prostatic capsule and into the rectum is rare, owing to separation of the bladder and rectum by Denonvilliers fascia (Gillenwater et al. 2002).

Distant metastatic spread is both lymphatic and haematogenous. Lymphatic spread occurs in a stepwise manner, first affecting the obturator lymph nodes, then advancing contiguously into the external iliac and hypogastric nodes, and finally involving the common iliac and periaortic nodes (Touijer et al. 2007). Haematogenous spread is also characteristically orderly. Bone is one of the most common site of metastasis and about 20% of newly diagnosed prostate cancer patients present with metastasis (Esper et al. 1999). Bone metastasis will occur in up to 85% of patients who die of prostate cancer (Narayan et al. 1995) and studies

show that 50%-70% of all prostate cancer patients will develop skeletal metastases during the course of their disease (Buckwalter et al. 1997; Hage et al. 2000). The axial skeleton is particularly vulnerable, this is followed by spread to the proximal appendicular skeleton. Bone metastases are typically osteoblastic. Only in advanced disease do pulmonary and hepatic metastases appear. Metastases to the brain and other visceral sites are uncommon. Paraneoplastic syndromes have been associated with disseminated prostate cancer and include disseminated intravascular coagulopathy and neuromuscular abnormalities.

## **1.2 Cancer cell invasion and metastasis**

Metastasis which is defined as the formation of progressively growing secondary tumour foci at sites discontinuous from the primary lesion, is the most clinically significant behavioural trait of malignant cancer (Welch et al. 1999). It is this dissemination of tumour cells which commonly defeats surgery, chemotherapy and radiotherapy that is responsible for a large proportion of cancer deaths.

The metastatic process is a complex cascade of many steps. The cancer cells must detach from the primary tumour, invade the surrounding stroma and enter the vasculature or lymphatic system. These cells must survive in the blood circulation before entering the capillary beds of distant organs. The disseminated cells must attach to the target endothelium, extravasate and invade the target tissue. The new tumour focus must then establish a blood supply before developing into a secondary

cancer (Souhami et al. 2002). Finally, the metastatic foci of tumour cells must evade eradication by immune responses. Since all of these steps are required for metastases, inhibition of any of these should prevent metastases from developing.

Metastasis formation is clearly a complex process and studies have shown it to be inefficient. A large number of tumour cells are shed into the vascular system of a primary tumour (Butler et al. 1975). It has been demonstrated that only a small number of metastatic tumour cells when injected intravenously will form tumour foci.

Cells, with few exceptions, stay in their tissue of origin. They remain in place by sticking to one another through cell-cell adhesion and by sticking to a meshwork of protein – the "extracellular matrix" – that fills the space between them. Cancer cells must evade the multiple controls in the body that keep normal cells in place.

It has long been recognised that tumours of different tissue origins have a predisposition to metastasise to specific target organs. Prostate cancer preferentially spreads to bone. The observation that metastases are organ-specific was first noticed by Dr. Stephen Paget. In 1889, he proposed that cancer cells shed from an initial tumour were dispersed randomly throughout the body by the circulatory system. He called these circulating cancer cells "seeds" and proposed that only some seeds fall onto fertile soil - organs where they can grow (Paget 1889). Evidence of the seed and soil theory was provided by the observation that B16

melanoma cells injected into mice metastasised to selective organs (Fidler et al. 1976).

James Ewing challenged Paget's theory by arguing that cancer cells don't spread randomly throughout the circulation in search of fertile soil. He suggested that circulating cancer cells become trapped in the first small blood vessels, or capillaries, they encounter and then grow in the surrounding organ (Ewing 1940). Using autopsy studies of cancer patients and measurements of blood flow to organs, Leonard Weiss showed that, on its own, neither Ewing's theory nor Paget's completely explained the pattern of cancer metastasis (Weiss et al. 1986, 1988).

A large amount of evidence now indicates that molecular factors that are present in each organ can influence the ability of each type of metastatic cancer cell to grow in that organ (Fidler 1995). Prostate cancer cells that arrive in bone may be stimulated to grow because of molecular interactions that occur between cancer cells and cells in the bone.

The study of chemokine receptors is providing important clues concerning why some cancers metastasise to particular organs. Studies have shown that tumour cells express patterns of chemokine receptors that match chemokines that are expressed in organs to which these cancers commonly metastasise (Muller et al. 2001). So it has been suggested that chemokines cause cancer cells to 'home' to specific secondary sites (Liotta 2001).

There is also research on the characteristics of adhesion molecules in an effort to understand the metastatic process. A variety of cell surface receptors that mediate cell-cell adhesion and interactions with the extracellular matrix have been characterised, including cadherins, integrins and CD44. Cell adhesion molecules on the cell's surface are unique to certain tissues or organs and identify where cells should reside. The initial escape of a tumour cell from its primary location requires the loss of the cell-cell attachment which maintains tissue cohesion. In epithelial tumours this is mediated by cadherins (Souhami et al. 2002). In cancer cells, cell adhesion molecules are altered or lost, allowing the cells to leave their appropriate location and re-establish themselves in a new environment. Cancer cells also lose the requirement of normal cells to anchor to the tissue matrix for survival.

As a primary tumour grows it needs to develop a blood supply that can support its metabolic needs – a process called angiogenesis (Holleb et al. 1972). Cancer cells promote angiogenesis by disrupting the normal balance between the naturally occurring molecules that stimulate this process and those that inhibit it (Holleb et al. 1972). A required early step in cancer growth is the "angiogenic switch," when this balance is lost and new blood vessel growth is promoted (Bergers et al. 2003).

Angiogenic peptides are released by neoplastic cells, such as vascular endothelial growth factor (VEGF). Researchers are developing agents that can impede the effects of angiogenesis-stimulating growth factors in the body; and developing new techniques to increase the production of naturally-occurring anti-angiogenic factors to prevent tumour spread. It has been shown that antibodies specific to the VEGF

peptide will inhibit the growth of different human tumour cell lines in recipient athymic mice (Kim et al. 1993).

The design of more effective therapies to treat metastatic cancer requires a better understanding of the molecular events and cellular processes that are involved in the process of metastasis.

## **1.3 Semaphorins and Plexins**

### **1.3.1 Classification of Semaphorins and Plexins**

Semaphorins are a large family of secreted and membrane-bound proteins (Semaphorin nomenclature committee, 1999). Semaphorin is derived from the word “semaphore” meaning to convey information by a signalling system. Over the past ten years since the identification of the first semaphorin, many different names and classification systems have been used. In 1999 the nomenclature for these proteins was standardized (Semaphorin nomenclature committee, 1999). More than 20 members are now known and they fall into eight subfamilies. These subfamilies are defined in Figure 1.3.

A distinctive protein module of 500 amino acids, called the sema domain, characterises all semaphorins (Kolodkin et al. 1993). This domain is known to mediate receptor-binding specificity of semaphorins (Feiner et al. 1997). The sema



domain is also present in other cell surface proteins, namely the plexins, which are the functional receptors for semaphorins, as well as the scatter factor receptors which control similar biological functions (Winberg et al. 1998; Artigiani et al. 1999).

In humans, there are at least nine different plexin genes, which are grouped into four subfamilies according to sequence similarities – A, B, C and D (Tamagnone et al. 1999) (Figure 1.4).

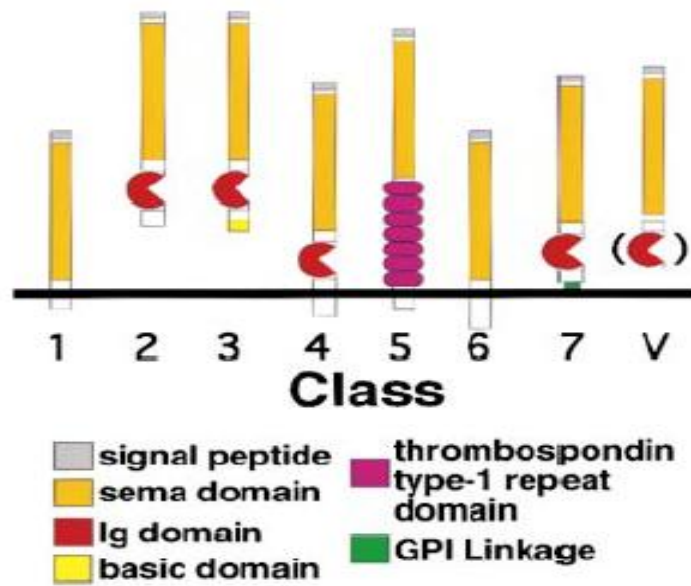
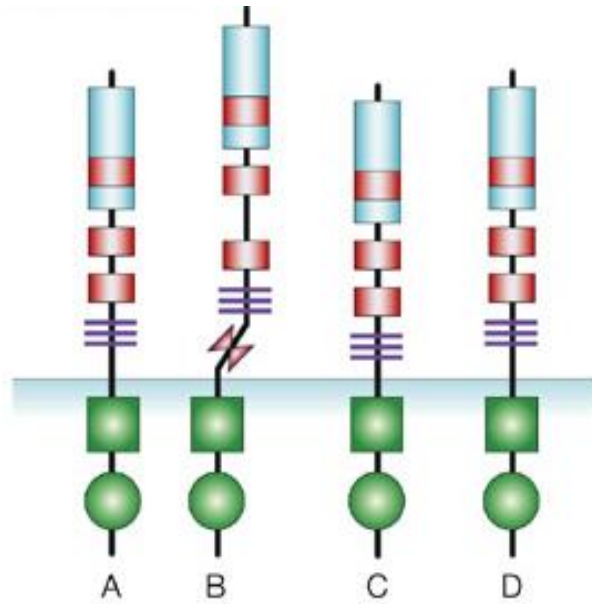


Figure 1.3 The Semaphorin Family (Semaphorin nomenclature committee, 1999).

- (1) Sema domain, transmembrane (TM) domain, and short cytoplasmic domain (found in invertebrates).
- (2) Sema domain, immunoglobulin domain (Ig), secreted (found in invertebrates).
- (3) Sema domain, Ig domain, short basic domain, secreted (found in vertebrates).
- (4) Sema domain, Ig domain, TM domain, and short cytoplasmic domain (found in vertebrates).
- (5) Sema domain, seven thrombospondin repeats (type 1 and type 1-like), TM domain, and a short cytoplasmic domain (found in vertebrates).
- (6) Sema domain, TM domain, and a cytoplasmic domain (found in vertebrates).
- (7) Sema domain, Ig domain, and a glycosylphosphatidylinositol (GPI) membrane anchor (found in vertebrates).
- (V) Viral semaphorins, including to date a truncated secreted sema domain

*(SEMAVA), and a sema domain followed by an Ig domain shown in parentheses  
(SEMAVB).*

**N-terminal**



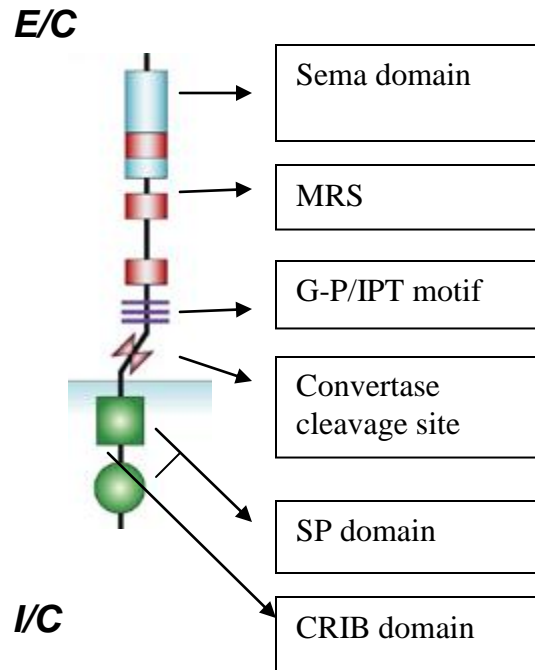
*Figure 1.4 Vertebrate plexins. Members of the Plexin A group bind Semaphorins of class 3, Plexin B1 binds Semaphorin 4D (Sema 4D), Plexin B2 binds Semaphorin 4C, Plexin C1 binds Semaphorin 7A and Plexin D1 binds Semaphorin 3E. (Trusolino et al. 2002).*

There are at least two families of semaphorin receptor, plexins and neuropilins which interact to form receptor complexes (Figure 1.5) (Tamagnone et al. 2000; Kolodkin et al. 1997). Secreted semaphorins bind to receptor complexes that include neuropilins and plexins whereas membrane bound semaphorins bind directly to plexins. Plexins alone seem unable to interact with secreted semaphorins and neuropilins are required for binding these ligands (Feiner et al. 1997). Plexin B1 is a high affinity receptor for Sema4D.

### **1.3.2 Structure of plexins**

Plexins are large transmembrane proteins that have a large extracellular region, a transmembrane area and a cytoplasmic region (Figure 1.5).

The extracellular domain of all plexins has features in common with scatter factor receptors and semaphorins (Winberg et al. 1998) and it contains the sema domain, the MRS domain, IPT/GP domain and the convertase cleavage site.



*Figure 1.5 Structure of Plexin B1. The extracellular domain of Plexin B1 can be divided into the sema domain, the MRS domain, IPT/GP domains and a cleavage site, indicating a heterodimeric structure. The cytoplasmic portion of Plexin B1 comprises a 600 amino acid module which consists of the SP domain and the CRIB domain. The CRIB domain is thought to be the binding site of Rac and Rnd (Trusolino et al. 2002).*

**Sema domain** – encompasses about 500 amino acids with 15 conserved cysteine residues spaced by stretches of conserved amino acids and a conserved potential glycosylation site (Winberg et al. 1998; Kolodkin et al. 1993). The sema domain has been identified in hepatocyte growth factor (HGF), semaphorins and viral proteins (virus encoded semaphorin receptors, VESPR) (Winberg et al. 1998; Kolodkin et al. 1993). The sema domains of plexins share 25%-30% amino acid identity between pairs of plexins (Winberg et al. 1998). The role of the sema domain is not entirely understood, however crosslinking of Met occurs only in the presence of the sema domain, suggesting it is necessary in receptor dimerisation (Kong-Beltran et al. 2004).

It has been speculated that the sema domain is crucial for biological activity and receptor specificity (Giger et al. 1998; Nakamura et al. 1998). The structure of the sema domain has recently been determined and is primarily composed of a seven bladed beta-propeller. Each blade comprises a four strand antiparallel beta sheet (Antipenko et al. 2003).

The sema topology reveals an unexpected homology with integrins (Love et al. 2003). There are strong parallels between integrin and semaphorin function. Integrins are cell adhesion molecules and there is evidence to suggest that their intracellular signalling pathways converge with those of semaphorins (Pasterkamp et al. 2003).

**MRS (Met Related Sequence)** – contains a cysteine- rich motif, and is named after the scatter factor receptor Met (Maestrini et al. 1996). It has also recently been found to be present in integrins (Bork et al. 1999). Plexins have three repeated MRS motifs, with the exception of Plexin C1 which has two. The MRS motifs are also known as PSI domains (Plexins, Semaphorins and Integrins) (Bork et al. 1999).

**G-P/IPT motif** – This was first described by Bork et al. 1999, the immunoglobulin-like fold shared by **p**lexins and **t**ranscription factors. It was found to contain a repeat sequence, rich in **g**lycine and **p**roline residues (Bork et al. 1999). The role of this domain is unknown.

**Convertase cleavage site** – located in the proximity of the transmembrane domain (Tamagnone et al. 1999). Plexin B1/B2 undergoes proteolytic processing in this region by proprotein convertases, thereby converting single-chain precursors into non-disulfide-linked, heterodimeric receptors. This processing of plexins occurs in a post-Golgi compartment, possibly at the cell surface. This conversion of Plexin B1 into a heterodimeric receptor appears to enhance the binding and the functional response to its ligand Semaphorin 4D (Artigiani et al. 2003).

The cytoplasmic domain is large, consisting of about 600 amino acids and it is conserved among family members and in evolution (Maestrini et al. 1996). It



consists of two SP domains and the CRIB domain. It contains stretches that are distantly related to GTPase activating proteins (Artigiani et al. 2003).

**SP domain** – This domain has no homology to other proteins and although it includes a number of tyrosine phosphorylation sites it lacks the typical motifs of catalytic tyrosine kinases (Tamagnone et al. 1999). The two SP (sex-plexin) domains are thought to play an important role in signal transduction. They are highly conserved within the plexin family and in evolution with over 50% similarity between invertebrates and humans (Tamagnone et al. 1999).

**CRIB domain (Cdc42/Rac interactive binding)** – The Cdc42/Rac interactive binding (CRIB) motif was identified between residues 1848 and 1890 of the intracellular region of Plexin B1 between the two SP domains (Vikis et al. 2000). This motif is thought to be essential for the binding of activated Rac. Mutation of three amino acid residues L1849G, V1850G and P1851A, in Plexin B1 abolishes the interaction of Plexin B1 with Rac (Vikis et al. 2000). The minimal Rac binding domain has been identified as the 215 residues between 1696 and 1910 (Vikis et al. 2000).

Rac is involved in growth cone guidance. Activation of Rac, a small GTPase, results in the formation of lamellipodia (Hall 1998). The CRIB domain is also the site at which Rnd (Oinuma et al. 2003) and R-Ras (Oinuma et al. 2004) bind.

More recently it has been suggested that the CRIB domain is not involved in the binding of Rac and Rnd. Instead the small GTPases bind to a region adjacent to the CRIB domain and this interaction may play a role in Plexin B1 activation (Tong et al. 2007).

### **1.3.3 Protein interactions of class B Plexins**

#### **Plexins and the small GTPases – Rho, Rac and Cdc42**

The mammalian Rho GTPase family consists of a number of distinct proteins, the three best characterized members of the family are Rho, Rac and Cdc42. These proteins act as molecular switches to control cellular processes by cycling between active, GTP-bound and inactive, GDP-bound states (Mackay et al. 1998). The Rho family of small GTPases are critical for the regulation of actin structures (Hall et al. 1998). In Swiss 3T3 cells, activation of Rho results in stress fiber formation (Ridley et al. 1992). Activation of Rac results in lamellipodia formation and Cdc42 results in filopodia formation. These small GTPases activate WASP/Wave1, which in turn activates Arp2/3 and this causes actin polymerization (Ridley et al. 2003).

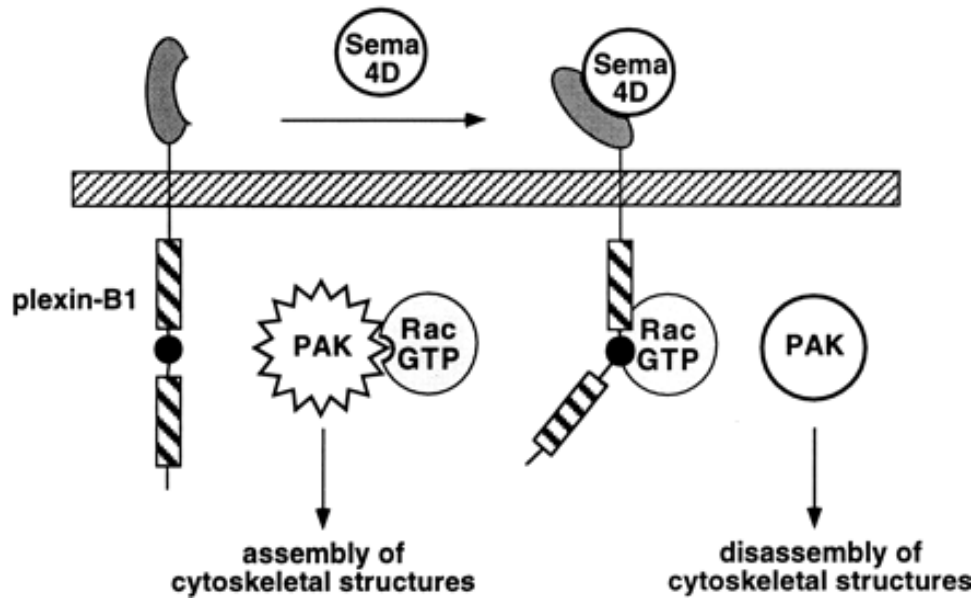
A direct interaction between Plexin B1 and activated Rac has been demonstrated, and it was found to occur at the Cdc42/Rac interactive binding (CRIB) motif in the cytosolic domain of Plexin B1, suggesting that Rac plays a role in mediating semaphorin signals, resulting in reorganisation of actin cytoskeletal structure (Vikis

et al. 2000). The same authors have shown that Plexin B1 and p21-activated Kinase (PAK) can compete for the interaction with active Rac and that Plexin B1 can inhibit Rac-induced PAK activation (Vikis et al. 2002) (Figure 1.6). The binding of Rac to Plexin B1 enhances the ability of Plexin B1 to interact with the ligand Sema4D by stimulating the localization of Plexin B1 to the cell surface (Vikis et al 2002).

Plexin B1 clustering induces assembly of actin and myosin filaments and cell contraction in fibroblasts, suggesting that Rho is also involved in Plexin B1 signalling (Driessens et al. 2001). Using a yeast two-hybrid system, the C-terminus of Plexin B1 activates Rho via PDZ-Rho-GEF (Driessens et al. 2001). Ligand binding of semaphorin to plexins causes activation of PDZ-Rho GEF via its PDZ domain, thereby stimulating the exchange of GDP for GTP on Rho, through its Dbl homology domain (DH) and Pleckstrin-homology domain (PH). A parallel input on PDZ-Rho GEF is established by ligand binding to G protein-coupled receptors activating  $G\alpha_{13}$ , which interacts with PDZ-Rho GEF through its RGS domain, thus catalysing the exchange of GDP for GTP on Rho (Driessens et al. 2002) (Figure 1.7).

Following this finding it was found that the PDZ domain of LARG is also directly involved in the interaction with the carboxy-terminal sequence of Plexin B1 (Aurandt et al. 2002). LARG (leukaemia-associated Rho GEF) is a Rho specific guanine nucleotide exchange factor that was initially identified in patients with primary acute myeloid leukaemia (Kourlas et al. 2000).

The mechanisms of signal transduction by plexins remains largely unknown, however a hallmark of semaphorin receptors is their interaction with multiple GTPases. It is this interaction that is likely to regulate cytoskeletal arrangements.



*Figure 1.6 Plexin B1/Rac interaction inhibits PAK activation and enhances Sema4D ligand binding (Vikis et al. 2002).*

*Treatment of Plexin B1 expressing neurons with Sema4D results in the recruitment and sequestration of active Rac. This inhibits the ability of Rac to activate PAK and thus results in the disassembly of cytoskeletal structures (Vikis et al. 2002). This suggests that a function of Plexin B1 is to inhibit PAK activation and this results in changes in the cytoskeletal structure, which in turn causes growth cone collapse.*

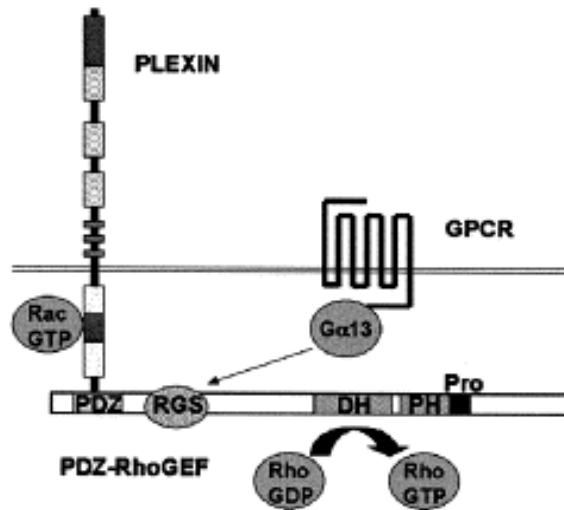


Figure 1.7 Mechanism by which plexins activate Rho via PDZ-Rho GEF (Driessens et al. 2002). (GPCR – G protein coupled receptor, RGS – regulators of G protein signalling).

Ligand binding of Sema 4D to Plexin B1 activates PDZ-Rho-GEF at the PDZ domain and this stimulates the exchange of Rho GDP for Rho GTP. Ligand binding to G-protein coupled receptors also activates PDZ-Rho GEF by binding of Ga13 to the RGS domain of PDZ-Rho GEF and this stimulates the exchange of Rho GDP for Rho GTP. This suggests there are two mechanisms whereby plexins and G-protein coupled receptors can stimulate Rho-dependent pathways.

### **Plexin B1 interacts with Rnd1**

Rnd1 is a member of the Rho family GTPases. Its expression in fibroblasts inhibits the formation of actin stress fibres and integrin based focal adhesions. By inducing the loss of cell-substrate adhesion it causes cell rounding (Nobes et al. 1998).

Rnd1 directly interacts with the cytoplasmic domain of Plexin B1 (Oinuma et al. 2003). In COS7 cells, coexpression of Rnd 1 and Plexin B1 induces cell contraction in response to Semaphorin 4D. The PDZ RhoGEF pathway appears to be directly involved in this morphological effect (Oinuma et al. 2003). Oinuma found that Rnd1 promoted the interaction between Plexin B1 and PDZ RhoGEF and thereby potentiated the Plexin B1 mediated Rho activation. The Rnd1 binding region in Plexin B1 appears to overlap with the region responsible for the interaction with Rac, since mutation of three amino acid residues in Plexin B1 (L1849G, V1850G and P1851A) abolishes the interaction of Plexin B1 with Rac and suppresses the interaction with Rnd 1 (Oinuma et al. 2003).

Rnd1 may act as a key regulator of the signal transduction of Plexin B1, leading to Rho activation during axon guidance and cell movement.

## **Plexins and R-Ras**

R-Ras belongs to the Ras superfamily of small GTP-binding proteins. It has been implicated in promoting cell adhesion and neurite outgrowth via integrins (Oinuma et al. 2004). Plexin B1 mediates Sema4D-induced repulsive axon guidance signalling by acting as a GTPase activating protein (GAP) for R-Ras. Plexin B1 stimulates the intrinsic GTPase activity of R-Ras and this action requires the interaction of Plexin B1 with Rnd1 (Oinuma et al. 2004). The downstream signalling of Plexin B1 mediated R-Ras GAP activity has been studied in further detail. Plexin B1 inactivates phosphatidylinositol-3-OH Kinase [PI(3)K] and dephosphorylates Akt and glycogen synthase kinase-3beta (GSK-3 beta) through R-Ras GAP activity and this induces growth cone collapse (Ito et al. 2006).

R-Ras activity is critical for ECM-mediated  $\beta$ 1 integrin activation and cell migration. Inactivation of R-Ras by Sema4D/ Plexin-B1-mediated R-Ras GAP activity controls cell migration by modulating the activity of  $\beta$ 1 integrins (Oinuma et al. 2006).

Plexin B1 also functions as an M-Ras GTPase activating protein during dendritic development (Saito et al. 2009). Plexin B1 is a dual function GAP for R-Ras and M-Ras, remodelling axon and dendrite morphology, respectively (Saito et al. 2009).



### **Plexin B1 interacts with Plexin A1**

The receptor for Sema 3A is neuropilin-1 (Kolodkin et al. 1997), but neuropilin does not contain cytoplasmic domains that initiate intracellular signalling cascades. Plexins that form complexes with neuropilin-1 are thought to be the receptors that transduce Sema 3A signals into cellular responses (Takahashi et al. 1999). Other classes of semaphorins do not utilize neuropilins and directly transduce their signal through plexins. Plexin B1 specifically interacts with Plexin-A1 at their cytoplasmic domains (Usui et al. 2002). The biological significance of this interaction is as yet unknown. However the proposed pathway for this interaction is Sema 3A binds to neuropilin-1 and then activates Plexin A1. Plexin A1 interacts with Plexin B1 probably by facilitating the function of Rho and Rac through Plexin B1 and this leads to the reorganization of the actin cytoskeleton (Usui et al. 2003) (Figure 1.8).

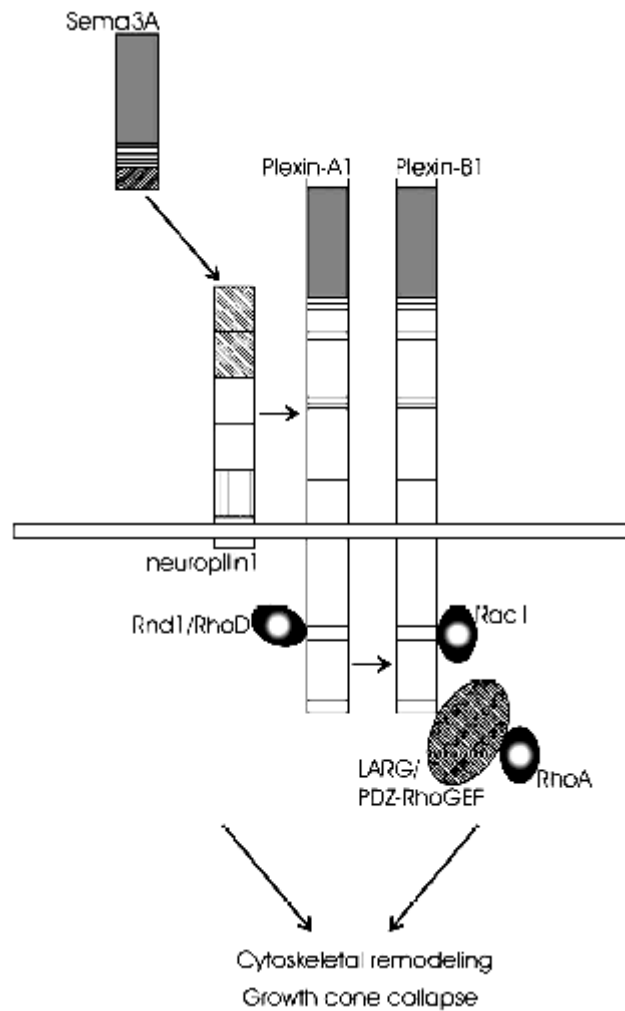


Figure 1.8 Pathway of Sema 3A signalling (Usui et al. 2002).

The receptor for Sema 3A is neuropilin 1 and on binding this activates Plexin A1. Plexin B1 interacts with Plexin A1 at their cytoplasmic domains and this interaction facilitates Rho and Rac which leads to the reorganization of the actin cytoskeleton. Since Plexin B1 directly interacts with Rac, this suggests that Plexin B1 is a mediator that links Plexin A1 to Rac.

### **Plexins couple with Met**

Semaphorins, plexins and scatter factor receptors share structural similarities and they are thought to derive from a common ancestor gene (Winberg et al. 1998). Plexins were identified through their homology to the extracellular domain of scatter factor receptors, all of which contain a conserved sequence of 500 amino acids (sema domain) and a cysteine rich motif of 80 amino acids (met related sequence, MRS) (Maestrini et al. 1996). Scatter factor receptors exist as heterodimers with intrinsic tyrosine kinase activity (Trusolino et al 2002). Met is the receptor for scatter factor 1 (also known as hepatocyte growth factor) which is encoded by the MET proto-oncogene (Giordano et al. 1989). Activation of the Met receptor induces 'invasive growth' (Trusolino et al 2002).

Plexin B1 forms a complex with Met. Met can be activated in a dual mode: either directly, through an interaction with its own ligand (SF 1) or indirectly, through recruitment to the Plexin B1-Sema4D complex (Giordano et al. 2002). Binding of Sema4D to Plexin B1 stimulates the tyrosine kinase activity of Met, which results in tyrosine phosphorylation of both receptors (Giardano et al. 2002). These observations suggest a possible involvement of semaphorins and plexins in cancer and metastasis.

### **Plexin B1 interacts with ErbB2**

ErbB2 (HER2/neu) is a receptor tyrosine kinase and is the only ErbB for which no ligand has been found (Franklin et al. 2004). Plexin B1 can associate with the receptor tyrosine kinases ErbB-2 and Met (Swiercz et al. 2007). The binding of Sema4D to Plexin B1 stimulates the intrinsic tyrosine kinase activity of ErbB-2, resulting in the phosphorylation of both Plexin B1 and ErbB-2. A dominant negative form of ErbB-2 blocks Sema4D-induced RhoA activation as well as axonal growth cone collapse in primary hippocampal neurons (Swiercz et al. 2004). Sema4D-induced activation and inactivation of RhoA require ErbB-2 and Met respectively (Swiercz et al. 2008).

### **Semaphorins and Integrins**

Integrins are a family of cell adhesion receptors that bind to extracellular matrix, cell-surface ligands and soluble ligands. Several integrins are involved in promoting tumour angiogenesis and tumour metastasis (Jin et al. 2004). They are known to associate with a large number of distinct proteins (Hynes 2002).

Integrins have recently been shown to mediate semaphorin responses. It was found that mutation of the Sema7A integrin binding motif blocks Sema7A mediated axon growth. At the same time it was found that class 3 semaphorins control vascular morphogenesis by inhibiting integrin function (Serini et al. 2003).

Integrins and Plexin B1 share homology in their PSI cysteine rich domains (Bork et al. 1999). Plexin B1 activation by Sema 4D induces disassembly of integrin based focal adhesive structures and this is followed by actin depolymerization and cell collapse (Barberis et al. 2004).

Plexin B1 promotes endothelial cell motility through RhoA and Rho Kinase by regulating integrin dependent signalling networks (Basile et al. 2007).

Although a direct interaction has not been shown for class B plexins and integrins, an interaction has been shown to occur via R-Ras. R-Ras becomes inactivated on Plexin B1 activation through its GTPase activity (Oinuma et al. 2006).

Several transmembrane and cytosolic proteins have been shown to bind to Plexin B1 and the precise mechanism by which these lead to modifications of the cytoskeleton remain poorly understood. However, as research continues on these interesting proteins new light is shed on the signalling network of plexins and semaphorins.

### **1.3.4 Semaphorin Functions**

Semaphorins were originally identified as axonal guidance cues. Increasing evidence has shown that semaphorins play additional roles in processes unrelated to

axonal development, including organogenesis, angiogenesis, immunity and neoplastic transformation.

### **Axon guidance**

The semaphorin family mediates axonal guidance in the nervous system. Guidance molecules can exhibit either attractive or repulsive effects, and different axons can respond differently to the same cue. Sema1A controls axonal elongation of peripheral neurons in grasshoppers (Kolodkin et al. 1992). Semaphorin 2A acts as a repulsive cue for axons when expressed ectopically in *Drosophila* (Matthes et al. 1995). Sema 3A has a potent inhibitory effect on axonal outgrowth from embryonic dorsal root ganglion (Luo et al. 1993). The extension versus retraction of different edges of the growth cone appears to be controlled by local changes in the dynamics of the actin cytoskeleton. But how do guidance cues regulate the actin cytoskeleton? There is evidence that Rho family GTPases regulate the actin cytoskeleton during axonal outgrowth and guidance (Dickson et al. 2001). Activation of Rac and Cdc42 induces lamellipodia and filopodia respectively, whereas Rho activation causes the formation of actin:myosin filaments and process retraction (Hall et al. 1998). One model postulates that attractive guidance cues activate Rac and Cdc42 in the growth cone, while repulsive guidance cues activate Rho. It has previously been discussed how plexins interact with the small GTPases (Vikis et al. 2000).

Although semaphorins and their receptors have emerged as important cellular cues in regulating the developing nervous system, the role of the plexin-B proteins is not

well understood. By developing Plexin B1 and Plexin B2 knock-out mice this role was further elucidated. Portions of the plexin B genes were deleted, which encoded the transmembrane domain of the respective plexin-B proteins or upstream sequences, to generate an early translational stop via a frameshift mutation. The development of the nervous system was normal in mice lacking Plexin B1, whereas mice lacking Plexin B2 demonstrated defects in closure of the neural tube and the embryonic brain was disorganized (Deng et al. 2007).

### **Organogenesis**

Mutations in the mouse semaphorin 3 gene cause certain embryonic bones and cartilaginous structures to develop abnormally, with vertebral fusions and partial rib duplications. The mice die shortly after birth owing to hypertrophy of the right ventricle of the heart and dilation of the right atrium (Behar et al. 1996).

Plexin B1 and Sema4D are expressed in epithelial and mesenchymal cells during the development of the ureteric collecting duct. Mice that lack Plexin B1 show anomalies in kidney development in vivo. These effects seem to be mediated via the Rho-A-ROCK pathway (Korostylev et al. 2008).

### **Immune cell response**

Evidence suggests that a subset of semaphorins called ‘immune semaphorins’ function in the immune system (Kumanogoh et al. 2001). Sema4D was originally found to induce B cells to aggregate (Hall et al. 1996). Since then semaphorins have

been found to influence monocyte migration, T-cell activation, B-cell survival as well as T/B and T/dendritic cell cooperation (Elhabazi et al. 2003).

### **Angiogenesis**

Semaphorin 4D has been identified as a potent proangiogenic molecule and this activity requires the coupling and activity of c-Met (Conrotto et al. 2005). The same group showed that the ability of cancer cells to grow is impaired in an environment lacking Sema4D. This observation is thought to be due to defective vascularisation within the tumour.

### **Semaphorins – signals for invasion**

Semaphorin overexpression is associated with the invasion and metastasis of tumours. Sema3E is overexpressed in metastatic cell lines in comparison with the non-metastatic parental population (Christensen et al. 1998). Sema3C is overexpressed in cancer cells resistant to radiation and cytostatic drugs in recurrent squamous carcinomas and in metastatic lung adenocarcinomas (Martin-satue et al. 1999; Yamada et al. 1997). Neuropilin 1 (receptor for Sema3A) expression in a prostate carcinoma cell line enhanced tumour growth and angiogenesis in vivo (Miao et al. 2000). Sema3F plays a role in adhesion in human lung cancer cell lines (Brambilla et al. 2000). Semaphorins Sema3F and its homologue Sema3B have been shown to be tumour suppressor genes, the expression of which are frequently lost in lung cancers (Tomizawa et al. 2001). Using a *Drosophila* screening system,



Sema5C was required for the proliferation of lethal(2)giant larvae [I(2)gl] tumours (Woodhouse et al. 2003).

More recently, Sema 3A, Sema 3D, Sema 3E and Sema 3G have been shown to display anti-tumourigenic and anti-angiogenic properties. This seems to be associated with the expression of Semaphorin 3 receptors by the tumour cells (Kigel et al. 2008).

In contrast to this, Christensen et al. 2005 suggest that Sema3E promotes tumour progression and metastasis. Sema3E is expressed in human cancer cell lines and solid tumours from breast cancer patients. In vivo, expression of Sema3E in mammary adenocarcinoma cells induces the ability to form experimental lung metastasis. In vitro, the Sema3E protein exhibits both migration and growth promoting activity on endothelial cells and pheochromocytoma cells (Christensen et al. 2005).

#### **1.4 Semaphorin 4D and invasive growth**

Although semaphorins were originally described in the nervous system for their roles in axon guidance, they are by no means limited to this role. They are expressed in various non-neuronal organs and tissues. However their ability to mediate cell contraction (Takahashi et al. 1999), adhesion and migration (Miao et al. 1999; Brambilla et al. 2000) as well as growth and differentiation establishes

parallel pathways with the invasive growth program. In addition, the conserved sema domain that is found in semaphorins and plexins is also present in Met, a well known inducer of invasive growth (Comoglio et al. 2002).

Semaphorin overexpression has been associated with the invasion and metastatic progression of tumours (Yamada et al. 1997; Christensen et al. 1998). However the available data implicating these proteins in tumour progression remains sparse compared with those for Met. Among the semaphorin receptors, Plexin B1 has the highest similarity (28%) to scatter factor receptors and is also present outside the nervous system in tissues and organs where Met is expressed (Tamagnone et al. 1999).

Two different ligand-receptor pairs join forces to promote invasive growth by cancer cells (Giordano et al. 2002). The first pair is Semaphorin 4D and Plexin B1. The second pair consists of a scatter factor, hepatocyte growth factor (HGF), and its receptor Met, a tyrosine kinase from the MET/RON/SEA oncogene family. Although HGF and Met are important during normal embryonic development, they have also been associated with malignancy when mutated. Plexin B1 and Met form a complex, and when Sema4D binds to its receptor, Plexin B1, this stimulates the tyrosine kinase activity of Met, resulting in tyrosine phosphorylation of both receptors (Giordano et al. 2002).

Giordano et al found that Sema4D could trigger a complex program for invasive growth, including cell-cell dissociation, anchorage-independent growth and branching morphogenesis. Semaphorin had no effect on cells where Met was not expressed indicating that this tyrosine kinase receptor is essential for semaphorin-stimulated invasive growth (Giordano et al. 2002).

This observation suggests a possible involvement of semaphorins in cancer and metastasis.

There is some controversy over the role of Met interaction with Plexin B1. Plexin B1 can associate with the receptor tyrosine kinases Met and ErbB-2. However, in breast carcinoma cells, Sema4D can have pro- and anti-migratory effects depending on the presence of ErbB-2 and Met. The exchange of the two receptor tyrosine kinases is sufficient to convert the cellular response to Sema4D from pro- to anti-migratory (Swiercz et al. 2008). The activation of Met by Sema4D/Plexin B1 inhibits migration, whereas activation of ErbB2 via Sema4D/Plexin B1 enhances migration.

Plexin B1 also acts as a tumour suppressor in melanoma cells. In primary melanoma cells, Plexin B1 blocked tumourigenesis as measured by growth of colonies in soft agar, spheroids in extracellular matrix and xenograft tumours (Argast et al. 2009).

## 1.5 Plexin B1 and prostate cancer

The association between prostate cancer and Plexin B1 has been investigated (Wong et al. 2007). The cytoplasmic domain and part of the extracellular domain (exons 1-5) of Plexins A1, A3 and B1 were sequenced using cDNA from the human prostate cancer cell lines PC3, DU145 and LNCaP. A single nucleotide change (A5359G) was found in Plexin B1 in LNCaP, which potentially changes threonine 1697 to an alanine. LNCaP is of Caucasian origin and the sequence change was absent from DNA from 60 control individuals, of Caucasian background. The rest of the Plexin B1 cDNA was sequenced in PC3, DU145 and LNCaP and no further mutations found.

To look for further mutations, the study was extended using SSCP (Single Strand Conformational Polymorphism) analysis of exons 22-29 of the cytoplasmic domain of the Plexin B1 gene in DNA microdissected from 89 primary prostate tumours treated by radical prostatectomy, 17 lymph node metastases and 9 prostate cancer bone metastases. Aberrant bands were excised from the gel and sequenced. 12 further missense mutations were found. Mutations were present in 89% (8/9) of prostate cancer metastases, in 41% (7/17) of lymph node metastases, and in 46% (41/89) of primary tumours. Forty percent of prostate cancers contained the same mutation. Mutations were also found in 6/30 breast cancer lymph node metastases (Wong et al. 2007).

The proportion of cells containing mutant Plexin B1 was higher in metastases than in primary tumour tissue. The mutations and their frequencies are shown in Table 1.1.

Together, the data suggest that cells carrying mutated Plexin B1 are selected for during prostate cancer progression.

One of the mutations was C5662T, that is predicted to result in a substitution of a proline to a serine at position 1798. This mutation was found in 1/9 prostate cancer metastases. The amino acid, at position 1798 is highly conserved in evolution. A proline is present in the protein in mouse, Drosophila and C elegans and other classes of the Plexin family- A1, A2, B2, B3 (Table 1.2).

Nucleotide	Amino acid	Bone metastases (total of 9)								LN metastases (total of 17)							1° (total of 89)	Total		
		1	2	3	4	5	6	7	8	1	2	3	4	5	6	7				
C5059T	P1597S											x	x	x				1	4	
C5060T	P1597L	x	x		x						x							x	4	9
G5074A	G1602R																	x		1
T5401A	F1711I																	1		1
C5468T	T1733I							x												1
A5474G	N1735S							x												1
A5596G	T1776A																	1		1
A5653G	T1795A	x	x	x	x	x		x	x						x	x		38		47
C5662T	P1798S								x											1
A5674G	T1802A			x																1
T5714C	L1815P	x				x		x										2		5
C5980T	R1904W										x									1
Total		8 of 9 (89%)								7 of 17 (41%)							41 of 89	73		

*Table 1.1 Mutations found in Plexin B1 (Wong et al. 2007).*

*On screening the cytoplasmic domain of Plexin B1 from human prostate cancer cell lines a single nucleotide change was found in Plexin B1 in LnCaP (A5359G). 12 further mutations were found in clinical samples of prostate cancer. Some of the mutations were found in many tumours, A5653G was found in 9 of 26 metastases and 38 of 89 primary prostate cancers. The C5662T mutation was found in 1 of 9 prostate cancer bone metastases.*

	<b>1796</b>	<b>1797</b>	<b>1798 (position of mutation)</b>
<i>Hs</i> PLXNB1	Q	R	<b>P</b>
<i>Mm</i> plex6	Q	R	<b>P</b>
<i>Dm</i> plexB	M	K	<b>P</b>
<i>Ce</i> plx-2	Q	R	<b>P</b>
<i>Hs</i> PLXNB3	Q	R	<b>P</b>
<i>Hs</i> PLXNB2	C	W	<b>P</b>
<i>Hs</i> PLXNA2	Q	R	<b>P</b>
<i>Hs</i> PLXNA1	Q	R	<b>P</b>

*S (AA change)*

*Table 1.2 Sequence conservation of Plexin B1 at amino acid position 1798.*

*The C5662T, that is predicted to result in a substitution of a proline to a serine at position 1798 is highly conserved in evolution. A proline is present in the protein in mouse, Drosophila, C elegans, Plexin A1, A2, B2, B3 suggesting functional significance.*

## 1.6 Aims and Objectives

The finding that mutations in Plexin B1 occur in a high proportion of prostate cancers, approximately half the primary cancers and nearly all the metastatic cancers, suggests that this pathway is involved in the progression of prostate cancer.

The aim of this research is to determine whether the mutation C5662T in the Plexin B1 gene alters cell behaviour and contributes to prostate cancer progression.

The objectives:

*Objective 1: Construct an expression vector containing the mutation.*

By using primers containing the point mutation, the altered sequence will be introduced into the wild type gene. The altered construct will be used to transform E.Coli. Colonies will be selected, grown up and the identity of the mutation will be confirmed by direct sequencing.

*Objective 2: Transfect the mutation into NIH3T3 cells and COS cells to produce stable and transient clones.*

In order to determine the effect of the mutation, it must first be transfected into suitable cells. Using lipofectamine transfection, the construct will be transfected into NIH3T3 cells and COS cells. Transfected cells will be selected in G418 and individual colonies will be expanded and frozen stocks produced. The presence of



the mutation will be confirmed and the level of protein expression measured by western blotting and immunofluorescence.

*Objective 3: Determine the effect of the mutation on cell collapse and downstream signalling.* In vitro assays will be used to assess the effect of the mutation on the behaviour of cells. At present it is not known which components of the semaphorin signalling pathway will be affected by the mutation. For example the mutation may affect the interaction with MET or downstream effectors such as Rho, Rac and cdc42.

## **Chapter 2:**

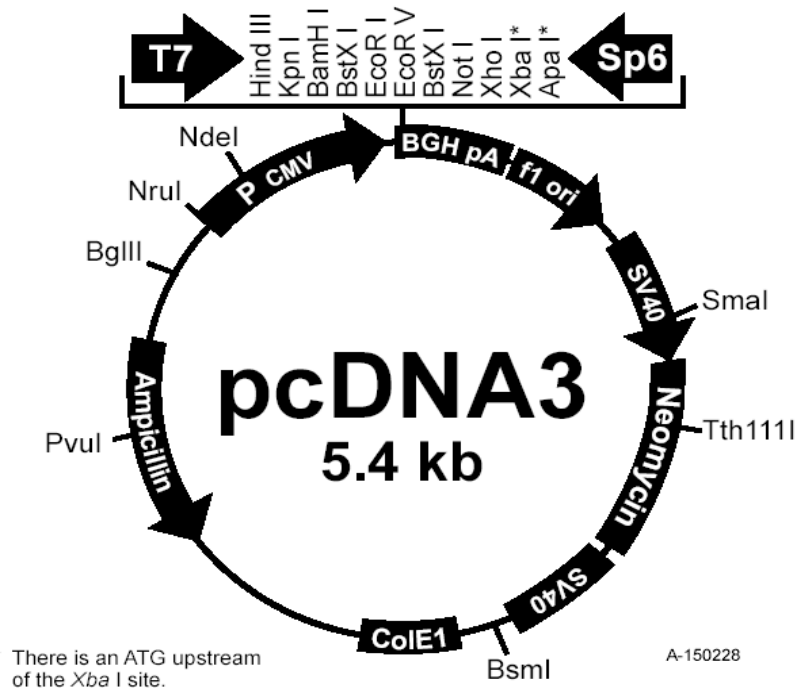
### **Methods and Materials**

## **2.1 Materials and Methods**

### **2.1.1 DNA constructs**

The following constructs were provided by Alan Hall (A.Hall, Memorial Sloan-Kettering Cancer Centre, New York, NY) and Mariette Driessens (The Netherlands Cancer Institute, Amsterdam; Driessens et al. 2001)

1. Full length Plexin B1 cDNA in the expression vector pcDNA3 (Figure 2.1)
2. Truncated Plexin B1 conjugated to CD2 in pcDNA3 (Driessens et al. 2001). The cytoplasmic domain (amino acids 1520–2135) of Plexin B1 (truncated Plexin B1) was fused to the transmembrane and extracellular domain of CD2 (a T lymphocyte antigen).



*Figure 2.1 Plexin B1 in pcDNA3 (Invitrogen). The expression vector pcDNA3 has 5446 nucleotides. It is designed for stable and transient expression in mammalian hosts. It has multiple cloning sites, Plexin B1 was cloned into the NOT1 site.*

*(CMV promoter: bases 209-863, T7 promoter: bases 864-882, Polylinker: bases 889-994, Sp6 promoter: bases 999-1016, BGH poly A: bases 1018-1249, SV40 promoter: bases 1790-2115, SV40 origin of replication: bases 1984-2069, Neomycin ORF: bases 2151-2945, SV40 poly A: bases 3000-3372, ColE1 origin: bases 3632-4305, Ampicillin ORF: bases 4450-5310).*

## **2.1.2 Cell culture**

Cell lines are immortal cell cultures that will proliferate indefinitely given appropriate fresh medium and space. A number of characterized cell lines are available.

LNCaP cells are human prostate adenocarcinoma cells derived from the left supraclavicular lymph node metastasis of a 50 year old caucasian male in 1977 (Horoszewicz et al. 1983). They were grown in RPMI medium 1640 (Gibco, Paisley, UK) with 8% foetal bovine serum (FBS; Labtech international).

PC3 cells were established from a bone marrow metastasis isolated post-mortem from a 62-year-old Caucasian man with poorly differentiated prostatic adenocarcinoma after androgen suppression therapy (Kaighn et al. 1979). They were grown in RPMI medium 1640 with 8% foetal bovine serum.

DU145 cells were derived from a patient with brain metastasis from prostate cancer (Stone et al. 1978). They were grown in RPMI medium 1640 with 8% foetal bovine serum.

1542-CPT3X cells were derived from primary prostate tumour (Housseau et al. 1999). 1542-NPTX epithelial cells were derived from normal prostate tissue of the

same radical prostatectomy specimen as 1542-CPT3X cells (Housseau et al. 1999). Pre2.8 were derived from Benign Prostatic Hyperplasia (BPH) epithelial cells and S2.13 derived from BPH stromal cells. They were grown in RPMI medium 1640 with 8% foetal bovine serum.

NIH3T3 cells are fibroblasts and were obtained from Swiss mouse embryo tissue in 1962 (Jainchill et al. 1969). They were grown in Dulbecco's Modified Eagle Medium (D-MEM; Gibco BRL, UK), with 8% newborn calf serum (Gibco, New Zealand).

COS1 and COS7 cells were derived from kidney cells of the African green monkey (Jensen et al. 1964). They were grown in D-MEM with 8% FBS. COS cells are amenable to transfection.

All Cell lines were grown at 37°C in 5% CO<sub>2</sub> and passaged when 80% confluent.

### **2.1.3 Site-directed in-vitro mutagenesis**

In vitro site-directed mutagenesis is used for studying protein structure-function relationships and gene expression and it allows the modification of a gene sequence.

The QuikChange XL Site-Directed Mutagenesis Kit (Stratagene) was used to introduce the C5662T mutation into the full length Plexin B1 construct and CD2 (truncated) Plexin B1 construct (Figure 2.2).

Mutagenic oligonucleotide primers were designed according to the mutation C5662T.

Plexin B1 sequence:

5'GAGTGCCTCTCACCCAGCGGCCAGACCCTCGCACCCCTTGATG3'

The following oligonucleotide primers were used:

5'GAGTGCCTCTCACCCAGCGGTCAGACCCTCGCACCCCTTGATG3' sense

5'CATCAAGGGTGCAGGGTCTGACCGCTGGGTGAGAGGCACTC3' Antise-  
nse

To optimise the process of mutagenesis primers were designed with the following considerations as set out in the Stratagene instruction manual. Both primers contained the desired mutation and anneal to the same sequence on opposite strands of the plasmid. Primers were between 25-45 bases in length and the melting temperature of the primers was calculated to be 78°C or greater (melting temperature =  $81.5 + 0.41(\%GC) - 675/N - \% \text{ mismatch}$ ). The desired mutation was placed in the middle of the primer and there was a minimum GC content of 40% (QuikChange XL Site-Directed Mutagenesis Kit, Stratagene).

Site directed in-vitro mutagenesis uses a supercoiled double stranded DNA vector and two synthetic oligonucleotide primers containing the desired mutation. During

temperature cycling the plasmid denatures and the primers anneal. Using PfuTurbo DNA polymerase, incorporation of the oligonucleotide primers generates a mutated plasmid. The product is treated with Dpn1 to digest the parental DNA template, leaving the DNA containing a mutation. This DNA is transformed into XL10-Gold ultracompetent cells.



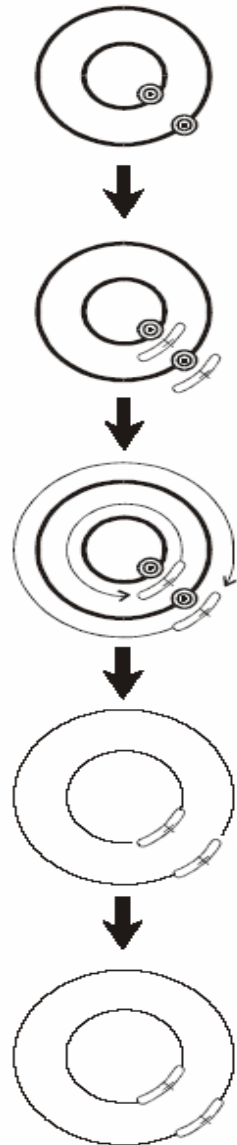
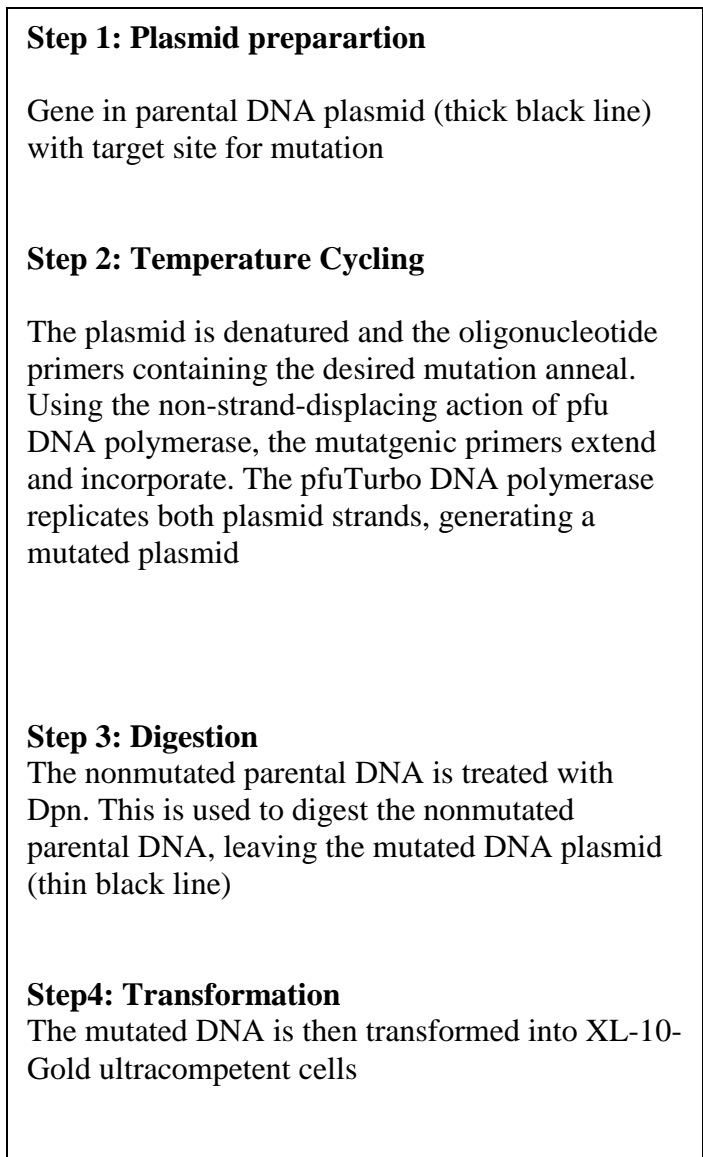


Figure 2.2 Site directed in-vitro mutagenesis

The control reaction was prepared using 5µl 10X reaction buffer, 1µl (10ng) dsDNA construct, 12.5µl (125ng) Primer 1, 12.5µl (125ng) Primer 2, 1µl dNTP mix, 3µl Quick solution, 15µl ddH<sub>2</sub>O and 1µl Pfu Turbo DNA polymerase. The PCR cycling parameters used were:

95°C	1minute		1 cycle
95°C	50seconds	}	18 cycles
60°C	50seconds		
68°C	24minutes		
68°C	7minutes		1 cycle

Following temperature cycling the reaction tubes were placed on ice for 2 minutes. The amplification products were then digested with 1µl of Dpn 1 (10U/µl) restriction enzyme and incubated at 37°C for 1 hour to digest the parental (nonmutated) DNA. XL10-Gold ultracompetent E.Coli cells (Invitrogen) were transformed with the constructs. The XL-10 E.Coli cells were thawed on ice. 15µl of the PCR product was added to 100µl of the E.Coli cells. The cells were incubated on ice for 20 minutes and heat-pulsed at 42°C. The cells were then incubated on ice for 2 minutes. 0.5mls NZY<sup>+</sup> broth (5g NZ amine, 2.5g yeast, 2.5g NaCl, 500mls H<sub>2</sub>O adjusted to pH 7.5) was added (preheated to 42°C) and incubated at 37°C for 1 hour with shaking at 250g. 250µl of each reaction mix was

then placed on LB ampicillin agar plates (20g LB agar, 500mls H<sub>2</sub>O), 250µl ampicillin) and incubated at 37°C for 16 hours.

10 colonies were then selected and grown in Luria-Bertani medium (12.5gLB broth, 500mls deionised H<sub>2</sub>O, 100µg/ml Ampicillin) and incubated at 37°C. The bacterial cells were then harvested by centrifugation at 6000g for 15 minutes and DNA was extracted.

#### **2.1.4 DNA Extraction**

The Qiagen plasmid purification kit protocol (Qiagen) was used to extract DNA. The bacterial pellet was resuspended in 10mls of Buffer P1 (50 mM Tris·Cl, pH 8.0, 10 mM EDTA 100 µg/ml RNase A). Then 10mls of Buffer P2 (200 mM NaOH, 1% SDS) was added and mixed by inverting 4-6 times. The reaction mixture was incubated at room temperature for five minutes. 10mls of chilled Buffer P3 (3.0 M potassium acetate, pH 5.5) was added and mixed immediately by inverting 4-6 times. The mixture was incubated on ice for 20 minutes. The mixture was then centrifuged at 20000g for 30minutes at 4°C. The supernatant containing plasmid DNA was then removed promptly. The supernatant was then re-centrifuged at 20000g for 15minutes at 4°C. The supernatant was applied to a QIAGEN-tip 500. This was equilibrated by applying 10ml of Buffer QBT [750 mM NaCl; 50 mM MOPS, pH 7.0; 15% isopropanol (v/v); 0.15% Triton® X-100 (v/v)]. The QIAGEN-tip was washed twice with 30mls of Buffer QC (1.0 M NaCl, 50 mM

MOPS, pH 7.0, 15% isopropanol (v/v). DNA was eluted with 15ml of Buffer QF (1.25 M NaCl, 50 mM Tris-Cl, pH 8.5, 15% isopropanol (v/v)). The eluted DNA was precipitated by adding 10.5ml of isopropanol. The mixture was centrifuged immediately at 15000 x g for 30 minutes at 4°C. The resulting DNA pellet was washed with 5ml of 70% ethanol and spun at 15000 x g for 10 minutes. The ethanol was decanted and the DNA pellet allowed to air-dry. The pellet was then dissolved in 0.5ml of TE (Tris-EDTA pH8). To determine the yield, the DNA concentration was measured by spectrophotometry and an agarose gel was used to confirm the presence of DNA.

#### **Analysis of DNA (Agarose gel analysis)**

To determine the presence of DNA, agarose gel electrophoresis was used (0.8% gel – 8mg agarose, 1ml 0.5% Tri-borate-EDTA, 0.5µg/ml ethidium bromide). The gel solution was placed into a tray with combs until set. The gel was placed in the electrophoresis tank (Electro-4gel tank, Thermo Electron Corporation) containing TBE (54g Tris base, 27.5g boric acid and 20ml 0.5M EDTA, pH 8.0 in 5 litres ddH<sub>2</sub>O). 2µl of DNA/loading buffer (0.25% bromophenol blue, 0.25% xylene cyanol FF, 30% glycerol in H<sub>2</sub>O) were added to each well and 1µl of a 1Kb DNA marker (Invitrogen) was used. 150V was applied to the tank containing the gel and ethidium bromide-DNA complexes were visualised under UV light (254-366nm) using an ultraviolet transilluminator (Gene Genius, Bio Imaging System).

## **Spectrophotometric measurement of nucleic acid concentration**

A spectrophotometer is a photometer (a device for measuring light intensity) that can measure intensity as a function of the wavelength of light.

Using 3 $\mu$ l of DNA mixed with 500 $\mu$ l of water, each sample was placed in the spectrophotometer and the concentration of DNA was calculated. Measurements were taken using a quartz cuvette (Qiagen).

Spectrophotometric conversions for calculating the concentration of nucleic acids from their absorbance at 260nm ( $A_{260}$ ) are given below:

dsDNA                      50 $\mu$ g/ml

RNA                              40 $\mu$ g/ml

Conc. of DNA sample = 50 x  $A_{260}$  x dilution factor

Conc. of RNA sample = 40 x  $A_{260}$  x dilution factor

The purity of DNA was calculated by  $A_{260} / A_{280}$

### **2.1.5 PCR (Polymerase Chain Reaction)**

PCR is a technique used to amplify the number of copies of a specific region of DNA in order to produce enough DNA to be tested. There are three basic steps in a PCR, which are repeated for 30 or 40 cycles. During denaturation the double strand

melts open to single stranded DNA, and all enzymatic reactions stop. The primer then binds to the DNA template, annealing. The final step, DNA replication, starts the process of “multiplying” the amount of DNA.

PCR was used to amplify a segment of DNA containing the C5662T mutation. The following primers were used:

Plexin B1 sense                      5'-GCCAGTGGACAGTGTGAC-3'  
Plexin B1 antisense                5'-CTGCCTCACCAAGCATGTGC-3'

PCR reagents:

10X buffer	2.5µl
Primer 1 sense (10pmol/µl)	2.5µl
Primer 2 antisense (10pmol/µl)	2.5µl
MgCl <sub>2</sub> (25mM)	1.5µl
dNTPs (10mM)	0.5µl
Taq (5U/µl)	0.25µl
DNA	100ng
ddH <sub>2</sub> O	to make up to 25µl

PCR conditions (Perkin Elmer PCR machine) :

94°C	5minutes	1 cycle
94°C	1minute	} 30 cycles
60°C	1minute	

74°C	1minute	
74°C	7minutes	1 cycle

### **2.1.6 Digestion with Restriction Enzyme**

To confirm the presence of the mutation, the PCR product was digested with a restriction enzyme, Hae III (New England Biolabs).

Hae III recognises and cuts at GG/CC. (5'...GG<sup>^</sup>CC...3' and 3'...CC<sup>^</sup>GG...5').

Using the webcutter program (Webcutter 2004: internet communication) Hae III recognises 6 sites in the wild type plexin B1 PCR product. In the mutant (C5662T) Hae III recognises 5 sites.

The reagents for Hae III digestion were:

PCR product	14µl
10X Buffer	2µl
Hae III	1µl
H <sub>2</sub> O	3µl

Following incubation at 37°C for 4 hrs the product was run on a 3% agarose gel.

### **2.1.7 Cycle sequencing**

The purpose of sequencing is to determine the order of the nucleotides and involves three major steps (like PCR), which are repeated for 30 or 40 cycles. During

denaturation the double strand melts open to single stranded DNA and all enzymatic reactions stop. The primer binds to the DNA template (annealing). In sequencing only one primer is used, so there is only one strand copied (unlike PCR: two primers are used, so two strands are copied). The polymerase then allows extension of the fragment.

PCR products were loaded on a 1.8% agarose gel and run until the bands separated. The bands were cut from the gel under UV light and using the Qiagen gel extraction kit the DNA was purified and extracted.

The gel slice was weighed and 6 volumes of buffer QG was added to 1 volume of gel. The gel slice was incubated at 50°C for 10 minutes and to help dissolve the gel, the mixture was vortexed every 2 minutes. One gel volume of isopropanol was added to the sample to increase the yield of DNA fragments and centrifuged. To elute the DNA 50µl of buffer EB (10mM Tris-Cl, pH8.5) was added and centrifuged at 13000g for 1 minute.

2µl of purified product was loaded onto an agarose gel to check that extraction had been successful and to estimate the DNA concentration.

The ABI Prism dRhodamine terminator cycle sequencing ready reaction kit with AmpliTaq DNA polymerase (Applied Biosystems) was used for cycle sequencing.

The following reaction mix was set up on ice:

Primer	4 picomoles
Purified PCR product	10µl
Sequencing reaction mix	5µl (added last)





### **2.1.8 Cloning of CD2-vector pcDNA3**

CD2 alone in vector pcDNA3 was produced by digestion of Plexin B1-CD2 with the restriction enzyme *NotI* (New England BioLabs, Inc). The bands were separated on a 0.8% agarose gel and the larger band was cut out and purified using QIAquick gel extraction kit protocol (Qiagen). The purified linear product was ligated using T4 DNA ligase (New England BioLabs, Inc). The reaction was as follows:

DNA	4 $\mu$ l
Buffer 10x	1.5 $\mu$ l
T4 DNA ligase	1 $\mu$ l
ddH <sub>2</sub> O	8.5 $\mu$ l

The reaction mixture was incubated at 15°C for 30 minutes.

### **2.1.9 Transfection**

Lipofectamine 2000 is a cationic liposome that facilitates transfection of nucleic acids into eukaryotic cells giving a high level of expression and transfection efficiency for a broad range of cell types. Cationic liposomal transfection reagents

are the most common method of transfection, mainly due to their ease of use and high degree of success. They are based upon packaging the DNA into liposomes, which fuse with the plasma membrane and release the DNA into the cell. Lipofectamine 2000 (Invitrogen) was used to transfect NIH3T3, COS1 and COS7 cells with mutant Plexin B1, wild type Plexin B1, vector only and mock (no DNA). Both stable and transient transfections were performed.

The main advantage of using Lipofectamine 2000 is its ability to transfect a range of different cell types coupled with a high efficiency of transfection.

Transfection protocol:

On Day 1 cells were plated into 6 well plates with 2mls medium, so that they would be 90% confluent at the time of transfection. To sterilise the DNA, 4µg of DNA was added to 4µl of NaAC and 80µl of ethanol. This was placed on ice for 10 minutes and then spun at 13000g for 20 minutes. The supernatant was removed and 100µl of 70% ethanol added. This material was spun for a further 5 minutes and the supernatant removed. The pellet was allowed to air dry for 5 minutes and was resuspended with 250µl of Optimem 1.

The following day 10µl Lipofectamine 2000 was added to 240µl Optimem 1 with glutamax-1 (Gibco, UK) and left for 5minutes at room temperature (for each transfection sample). 4µg DNA (diluted in 250µl Optimem 1) was added to the

Lipofectamine 2000 mix (above) and left for 30 minutes at room temperature. The 500µl mix was added to the cells and incubated for 24 hours at 37°C.

On day 3, for stable cell lines, cells were transferred to two T80 flasks.

The following day, 1mg/ml (300µl) Geneticin (Gibco, UK) was added to each T80 flask and media was changed until the mock transfected cells died (upto 5 days).

Clones were then selected by ring cloning and each clone was grown separately. Ring cloning was performed by removing the top of the flask using a heated blade. The medium was removed and the cells were washed with PBS. A perspex ring coated with silicon grease was pressed onto the flask to surround a clone. Cells from each clone were transferred, using trypsin (50µl), into a new flask containing media.

Each clone was grown and the relative expression of Plexin B1 was determined. To ensure the sequence had not been altered during the transfection process, and the mutation was still present, cycle sequencing and digestion with HaeIII were performed (see previous methods).

To obtain the highest transfection efficiency and low non specific effects the transfection conditions were optimised. This was done by varying the DNA and

Lipofectamine 2000 concentrations, and cell density. The DNA ( $\mu\text{g}$ ):Lipofectamine 2000 ( $\mu\text{l}$ ) ratios were varied from 1:0.5 to 1:5 (see results section).

### **2.1.10 Relative expression of Plexin B1 RNA in stable clones**

RNA was extracted using the RNeasy mini protocol kit (Qiagen). All reagents were provided by Qiagen in the RNeasy mini protocol kit. Cells were initially grown in a monolayer and were trypsinized and collected as a cell pellet. The cell pellet was loosened by flicking and 600 $\mu\text{l}$  of Buffer RLT (RNeasy Lysis Buffer) was added (to  $5 \times 10^6$  cells). The sample was homogenised. The lysate was loaded on a QIAshredder spin column and centrifuged for 2 minutes at maximum speed. 600 $\mu\text{l}$  of 70% ethanol was added to the homogenised lysate and mixed by pipetting. 700 $\mu\text{l}$  of the sample was applied to an RNeasy mini column and centrifuged for 15 seconds at 10000g. The flow through was discarded. 350 $\mu\text{l}$  Buffer RW1 (composition unknown) was added to the RNeasy mini column and centrifuged for 15 seconds at 10000g to wash. The flow through was discarded. In a separate tube 10 $\mu\text{l}$  of DNase 1 stock solution was added to 70 $\mu\text{l}$  Buffer RDD (composition unknown). This combination was mixed gently by inverting and left for 15 minutes. 350 $\mu\text{l}$  Buffer RW1 was placed into the RNeasy mini column and centrifuged for 15 seconds at 10000g. The flow through was discarded. Buffer RPE (composition unknown) was added and centrifuged for 15 seconds at 10000g. To elute, 50 $\mu\text{l}$  RNase free water was added and centrifuged at 10000g for 1 minute.

The RNA concentration was estimated using spectrophotometry and the formula:

$$\text{RNA concentration} = \text{spectrophotometric reading} \times A_{260} \times \text{dilution factor}$$

First strand cDNA synthesis was carried out on the samples. The following components were added to a microcentrifuge tube:

Oligo(dT) <sub>12-18</sub> (500µg/ml)	1µl
Total RNA	5µg
H <sub>2</sub> O	to make up to 12µl

The mixture was incubated at 70°C for 10 minutes then quickly chilled on ice. The following components were added to the incubated mixture.

5X First strand buffer	4µl
0.1M DTT	2µl
10mM dNTP mix	1µl (dNTP = 10mM dATP, dGTP, dCTP, dTTP)

These components were further incubated at 42°C for 2 minutes. 1µl of Superscript II (reverse transcriptase) was added and incubated for 50 minutes at 42°C. The procedure was repeated without Superscript II, as a control. This mixture was then heated to 70°C for 15 minutes to inactivate the reactions and the cDNA was stored at -20°C or was used for PCR.

30ng of cDNA was used for the PCR reaction.

PCR reagents:

10X buffer	2.5µl
Primer 1 sense (10pmol/µl)	2.5µl
Primer 2 antisense (10pmol/µl)	2.5µl
MgCl <sub>2</sub> (25mM)	1.5µl
dNTPs (10mM)	0.5µl
Taq (5U/µl)	0.25µl
DNA	30ng
ddH <sub>2</sub> O	to make up to 25µl

PCR conditions:

94°C	5minutes	1 cycle
94°C	1minute	} 30 cycles
60°C	1minute	
74°C	1minute	
74°C	7minutes	1 cycle

6µl of the product was run on a 0.8% agarose gel to determine the relative expression of Plexin B1 mRNA in the stable clones.

### **2.1.11 Protein Extraction**

Plexin B1 was extracted from transfected cells using different protein extraction buffers containing a number of protease inhibitors. These included RIPA buffer, EB buffer (used by Atigiani et al. 2003) and OBG. These buffers were chosen since they enable efficient cell lysis and protein solubilization while avoiding protein degradation. The buffer that yielded the most protein during the extraction process was used thereafter. Sodium butyrate was also used to increase the amount of membrane protein extracted (see below). Once the medium was removed, the T80 flask was washed with PBS. In each T80 flask 400µl of the buffer was added, the cells left on ice for 30 minutes and using a cell scraper the cells were removed and placed in an eppendorf. The cells were then spun (10000g for 10minutes at 4°C) and the supernatant placed in a new eppendorf and stored at -70°C.

Buffers used:

#### **RIPA Buffer**

50mM Tris-HCl pH 8 (buffering agent prevents protein denaturation)

150mM NaCl (salt prevents non-specific protein aggregation)

5mM EDTA (chelator of magnesium and calcium ions)

1% (v/v) NP40 (detergent to extract protein)



0.5% (w/v) sodium deoxycholate (detergent to extract protein)

0.1% (w/v) SDS

10% (v/v) glycerol (cryoprotectant)

#### EB buffer

20mM Tris-HCl pH 7.4 (buffering agent prevents protein denaturation)

150mM NaCl (salt prevents non-specific protein aggregation)

5mM EDTA (chelator of magnesium and calcium ions)

1% Triton X-100 (detergent to extract membrane proteins)

10% glycerol (cryoprotectant)

#### OBG (n-Octyl-Beta-D-Glucoopyranoside)

OBG (AG Scientific Inc) is a biological detergent used for solubilizing membrane bound proteins in their native state.

Anti-proteases were added to each buffer in the quantities shown:

PMSF(Phenylmethyl sulfonyl fluoride) 20µg/ml (inhibits serine proteases)

Aprotinin 10µg/ml (inhibits serine proteases)

Leupeptin 10µg/ml (inhibits serine and cysteine proteases)

Pepstatin A 5µg/ml (inhibits aspartic proteases)

#### Sodium Butyrate

Sodium butyrate can act to increase the efficiency of transfection and expression of both transient and stable transfections. It is a potent inhibitor of histone acetylation,

therefore its addition leads to histone hyperacetylation and a chromatin structure on the incoming plasmid DNA that is predisposed to transcription. Cells transfected with Plexin B1 were grown in 7mM sodium butyrate and then protein was extracted as described previously.

### **Estimation of protein concentration**

The Modified Lowry Protein Assay was used for protein quantitation (Pierce Biotechnology, Illinois). The Lowry protein assay is a biochemical assay for determining the total level of protein in a solution. The total protein concentration is exhibited by a colour change of the sample solution in proportion to protein concentration, which can then be measured using colorimetric techniques. Protein standard solutions were made up using bovine serum albumin. 1 ml of Modified Lowry reagent was added to the test protein samples and standard solutions. After 10 minutes Folin-Ciocalteu reagent (a reagent that uses phosphomolybdotungstate for the colorimetric detection of proteins) was added to each sample. After 30 minutes the absorbance at 750nm was measured for each sample, using water as the reference.

A range of protein standard solutions were made up using bovine serum albumin from concentrations of 50µg/ml to 400µg/ml and a standard bovine serum albumin (BSA) curve was plotted. Using the standard curve, the protein concentration was determined for each unknown sample.

### 2.1.12 Western Blotting

Western blot is a technique used to detect proteins in a sample. Using gel electrophoresis, it separates proteins according to the length of polypeptides. The proteins are then probed using antibodies specific to the target protein.

SDS-PAGE gels were made using the mini protean II gel kit (Bio-Rad laboratories, California). SDS-PAGE, sodium dodecyl sulfate polyacrylamide gel electrophoresis, is a technique used to separate proteins according to their electrophoretic mobility.

#### Resolving gel

Gel	6%	8%	10%	13%
H <sub>2</sub> O (ml)	5.3	4.6	3.9	3.0
30% acrylamide (ml)	2.0	2.7	3.4	4.3
1.5M Tris pH 8.8 (ml)	2.5	2.5	2.5	2.5
10% SDS (ml)	0.1	0.1	0.1	0.1
10% ammonium persulfate (ml)	0.1	0.1	0.1	0.1
TEMED (μl)	8.0	8.0	8.0	8.0

7mls of the resolving gel mixture was poured into the assembled gel plates and left to polymerise for 15 minutes. The water was then poured off.

Varying amounts of acrylamide were used to separate different sized proteins. The greater volume of acrylamide in the higher percentage gel enabled the separation of smaller proteins.

#### Stacking gel

H <sub>2</sub> O (ml)	3.0
30% acrylamide (ml)	0.67
1.0M Tris pH 6.8 (ml)	0.25
10% SDS (μl)	40
10% ammonium persulfate (μl)	40
TEMED (μl)	6

2mls of the stacking gel mixture was poured into the gel plate and a comb was inserted and the gel was allowed to set for 15 minutes.

Protein samples were prepared (20-40μg protein) in 20μl of RIPA buffer with 10μl of SDS-PAGE loading buffer (4ml distilled water, 1ml 0.5M Tris pH 6.8, 0.8ml glycerol, 1.6ml 10% SDS, 0.4ml 2-mercaptoethanol, 0.2ml 2% bromophenol blue) and heated to 96°C for 6 minutes (using a Perkin Elmer PCR machine). Gels were assembled in the electrophoresis tank and the reservoirs filled with SDS-PAGE running buffer (7.5g Tris base, 36g Glycine, 2.5g SDS, 500ml deionized water). Samples were loaded and run at 140v until the bromophenol blue line was near the

bottom of the gel. A rainbow protein size marker (10µl) was also run alongside the samples.

#### Electroblotting onto PVDF membrane



The gels and membranes were assembled as shown above and were soaked in 1X transfer buffer (10% methanol, Tris base 150g, Glycine 720g, 10 litres deionized water). PVDF membranes (Polyvinylidene Difluoride, Sigma-Aldrich) were pre-wet in 100% methanol for 15 seconds then soaked in transfer buffer before use. The sandwich shown was placed in a cassette in a western tank containing 1X transfer buffer and run at 40V overnight at 4°C.

#### Probing the membrane with antibodies

The membranes were taken off the gels and rinsed with distilled water. They were placed in a bath of Ponceau S for two minutes, and the presence of bands confirmed protein transfer. Ponceau S is a sodium salt of a diazo dye that may be used to prepare a stain for rapid reversible detection of protein bands on PVDF membranes. The Ponceau S was rinsed off with PBS. The membranes were blocked in 5% Marvel (dried milk) in PBS + 0.1% Tween at room temperature for 1 hour. They were then incubated in primary antibody for 1 hour at room temperature. Membranes were washed with 0.1% PBS-Tween three times and then secondary antibody was added for 1 hour at room temperature (Table 2.1). The membrane was washed again with PBS-Tween three times and the Tween was removed by washing with PBS alone. Enhanced chemiluminescence was used to visualize the protein. 2mls of ECL reagent A (substrate solution containing tris buffer) was added to 2mls of ECL reagent B (acridan substrate solution in dioxane and ethanol) (Pierce & Warriner) and the membrane added and incubated for 5 minutes. The membranes were wrapped in cling film and exposed to hyperfilm ECL (Amersham) in a dark room. The films were developed.

Table 2.1 Antibodies used in western blot

	<b>1° Ab</b>	<b>2° Ab</b>
Antibody	IC2	Goat anti rabbit with HRP
Species	Rabbit polyclonal	Goat
Against	Intracellular domain	Rabbit

of plexin B1

Company

Artigiani et al, 2003

Santa Cruz Biotec Inc.

### **2.1.13 Immunofluorescence**

Immunofluorescence is a technique allowing the visualization of a specific protein in cells or tissue sections by binding a specific antibody chemically conjugated with a fluorescent dye such as fluorescein isothiocyanate (FITC).

Borosilicate glass coverslips of 13mm diameter were sterilised and coated with fibronectin (Sigma). 10µg/ml of fibronectin was added to each well. The coverslips were incubated with fibronectin for 2 hours at room temperature and cells were seeded to 70-80% confluence. The cells were left overnight at 37°C. Cells were transiently transfected with 0.8µg of DNA per well using Lipofectamine 2000 as described previously.

On day 3, the medium was aspirated and the cells transfected with CD2-Plexin B1 were activated using a mouse monoclonal antibody against CD2 (OX34, Abcam). Cells were incubated at 37°C for 30 minutes. The cells were washed three times with PBS. The OX34 antibodies were crosslinked using an anti-mouse IgG for 15 minutes at 37°C. The cells were washed in PBS and fixed with 4% paraformaldehyde (PAF) for 10 minutes. The cells were washed in PBS and to solubilise the cell membrane 0.2% Triton X 100 was added for 10 minutes at room

temperature. After washing the cells with PBS (3x5mins) on a shaker, 2% horse serum was used to block the cells for 20 minutes at room temperature.

The primary antibody (Table 2.2) was then added and allowed to incubate for 1 hour at room temperature on a shaker. The cells were washed three times for 5 minutes with PBS and then incubated with secondary antibody for 1 hour at room temperature on the shaker in the dark. After washing the cells, the coverslips were mounted on slides using 2 $\mu$ l Vectashield with DAPI and stored at 4°C. The cells were viewed using a fluorescent microscope (Nikon, C-SHG1 with epifluorescent attachment).

Table 2.2 Primary and secondary antibodies used for immunohistochemistry

<b>Antibody</b>	<b>Dilution</b>	<b>Species</b>	<b>Against</b>	<b>Company</b>
OX34	1/400	Mouse monoclonal	CD2	Abcam
anti-VSV	1/200	Rabbit polyclonal	VSV	Abcam
Goat anti-mouse FITC	1/200	Goat	Mouse	Southern Biotechnology
Phalloidin TRITC	1/500	<i>Amanita phalloides</i>	F-Actin	Sigma
Goat anti-rabbit TRITC	1/100	Goat	Rabbit	Sigma



### **2.1.14 Preparation of Semaphorin 4D-Fc**

Recombinant Sema4D were prepared by protein-A sepharose affinity chromatography from the conditioned medium of transiently transfected COS7 cells (Turner et al. 2006). The Sema4D was fused to the Fc fragment of human IgG, to enable the proteins to be efficiently purified using protein-A (Turner et al. 2006).

Three T80 flasks of COS7 cells were grown to 70% confluence and transiently transfected with 20 $\mu$ g of Sema4D-Fc (provided by Laura turner). Cells were cultured in medium containing 10% ultra low IgG FBS (Invitrogen) to prevent isolation of IgG's during the preparation. This provided 50mls of conditioned medium containing chimeric protein which was harvested 72 hrs post transfection and stored at  $-20^{\circ}\text{C}$  until required.

Conditioned medium was centrifuged at 3000g for 10 min to remove cell debris and the supernatant was transferred to 50 ml Falcon tubes containing 2 ml of Buffer A (500mls of water, 0.15M NaCl<sub>2</sub>, 0.02M NaH<sub>2</sub>PO<sub>4</sub>, 0.1% sodium azide, adjusted to pH 8.0) and 250mg of Protein-A immobilised on Sepharose CL-4B (Sigma, P3391; binding capacity approximately 20 mg human IgG/ml lyophilised powder) and rotated overnight at 4 $^{\circ}\text{C}$ . A further 48mls was rotated in a 1ml Protein-A agarose suspension (Invitrogen, 15918-014). Both suspensions were poured through a

disposable column (Amersham Biosciences, 2745700) at 4°C to allow the sepharose/agarose to accumulate and then the column was washed with 15ml cold PBS. Bound semaphorins were eluted using 2.5 ml of 100mM glycine, pH 2.7. The elutes were collected in 15 ml Falcon tubes containing 250µl of 1 M Tris, pH 9.0 and placed on ice. The protein concentration and purity were assessed by western blotting in comparison to known concentrations of Sema 3A-Fc (R&D systems). The concentration of recombinant semaphorin was estimated by comparison of the band intensities of known volumes of semaphorin with known quantities of BSA standards (Turner et al. 2006).

### **2.1.15 Collapse assay**

Borosilicate glass coverslips, 13mm diameter, were placed in each well of a 24 well plate (Nunc).  $1.5 \times 10^5$  COS7 cells were counted using a haemocytometer. The COS7 cells were then seeded in each well. The cells were incubated overnight at 37°C. When the COS7 cells were 80% confluent they were transiently transfected with 0.8µg of the appropriate construct to be studied, per well using Lipofectamine 2000. 10µl Lipofectamine 2000 was added to 240µl Optimem 1 with glutamax-1 (Gibco, UK) and left for 5minutes at room temperature (for each transfection sample). 0.8µg DNA (diluted in 250µl Optimem 1) was added to the lipofectamine 2000 mix (above) and left for 30 minutes at room temperature. The 500µl mix was added to the cells and incubated for 24 hours at 37°C.

48 hours post transfection, 50  $\mu$ l of medium and 2 $\mu$ g/ml of Sema4D-Fc were placed on parafilm and the coverslips were laid upside down on top of this mixture and incubated for 5 minutes at 37°C. The coverslips were placed in a 24 well plate and washed once with PBS. 4% paraformaldehyde (2g in 50mls PBS heated to 60°C for one hour adjusted to pH 7.4) was added for 20 minutes to fix the cells. The wells were washed with PBS and 0.2% Triton X 100 was added for 10 minutes at room temperature to permeabilise the membrane. The wells were washed with PBS (3 x 5 minutes). 2% horse serum in PBS (blocking buffer) was added for 20 minutes at room temperature on a shaker. The cells were incubated for 1 hour at room temperature with the primary antibody (Table 2.3) diluted in 2% horse serum and then washed with PBS (3 x 5 minutes). The secondary antibody diluted in 2% horse serum was added for 1 hour in the dark at room temperature with goat anti-mouse FITC and phalloidin conjugated TRITC. The wells were then washed with PBS (3 x 5 minutes) and a drop of Vectashield with DAPI (Vector Labs, H-200) was placed onto the slides. The coverslips were removed from each well and allowed to dry for 2 minutes and then placed over the top of the Vectashield. The coverslips were sealed onto the slides using clear nail varnish. The stained cells were then examined using a fluorescent microscope and pictures were taken (Nikon Diaphot 200 with epifluorescent attachment, C-SHG1). The images were taken using each of the three fluorescent filters and using Photoshop (Adobe) each image was assigned a colour (Red-TRITC, green-FITC, blue-DAPI). The images were merged and then opened using image J to calculate their area.

The number of collapsed COS7 cells, defined as rounded cells having a diameter  $<350\mu\text{m}^2$  were counted (Oinuma et al. 2003). The area of each cell was calculated by using Image J, version 1.38 (Image J\ plugins\Particle counting\Cell\_Area.txt). Collapsed cells were counted as a percentage of the total number of transfected cells and the results are the mean of three independent experiments, with 50 cells sized per experiment.

Confocal images were generated using a confocal microscope (Zeiss LSM 510W upright confocal microscope).

Table 2.3 Antibodies used in the Collapse Assay

<b>Antibody</b>	<b>Dilution</b>	<b>Species</b>	<b>Against</b>	<b>Company</b>
1° Plexin B1	1/200	Rabbit Polyclonal IgG	Plexin B1	Santa Cruz
2° Goat anti-rabbit TRITC	1/100	Goat	Rabbit IgG	Southern Biotech
2° Anti-mouse FITC	1/200	Goat	Mouse IgG	Southern Biotech
PhalloidinTRITC	1/5000	Amanita phalloides	F-actin	Sigma
Phalloidin FITC	1/5000	Amanita phalloides	F-actin	Fluka

## **Chapter 3**

### **Generation of Mutant Plexin B1**

### **3.1 Introduction**

Semaphorins are a large family of secreted or membrane-bound proteins (Nakamura et al. 2000), whose function is mediated by plexins. Plexin B1 has been identified as the receptor for Semaphorin 4D (Tamagnone et al. 1999). Semaphorins are known to regulate axonal pathfinding in the developing nervous system (Tessier-Lavigne & Goodman, 1996). However evidence suggests that semaphorins are involved in the regulation of cell-cell interactions (Tamagnone et al. 1999) and there is increasing data suggesting that semaphorins and their receptors may play a regulatory role in tumorigenesis.

The membrane anchored class 4 semaphorin has become a focus of intensive research. Wong et al. have found that semaphorins and their receptors are widely expressed in prostate cancer with overexpression of Plexin B1 in the cell line LNCaP. Thirteen somatic missense mutations have been found in the cytoplasmic domain of the Plexin B1 gene (Wong et al. 2007).

In order to determine the functional significance of Plexin B1 mutations, a mutation was introduced into the wild type gene. Two constructs were provided by Alan Hall and Mariette Driessens, full length Plexin B1 in pcDNA3 and truncated Plexin B1

conjugated to CD2 in pcDNA3, respectively. These constructs had been used previously by Driessens et al. 2001 and Turner et al. 2006. PcDNA3 is an expression vector, a circular piece of DNA that can be transformed into a host for the purpose of producing the protein coded for by the DNA. The mutation C5662T is predicted to result in a substitution of a proline to a serine at position 1798. The altered construct was used to transform E.coli. Colonies were selected, grown up and the identity of the mutation confirmed using restriction enzymes and direct sequencing. To determine the effect of the mutation it was transfected into mammalian cells. Transfection is a method by which experimental DNA may be put into a cultured cell. The expression of these constructs was confirmed using reverse transcription PCR, western blotting and immunofluorescence.

## **3.2 Results**

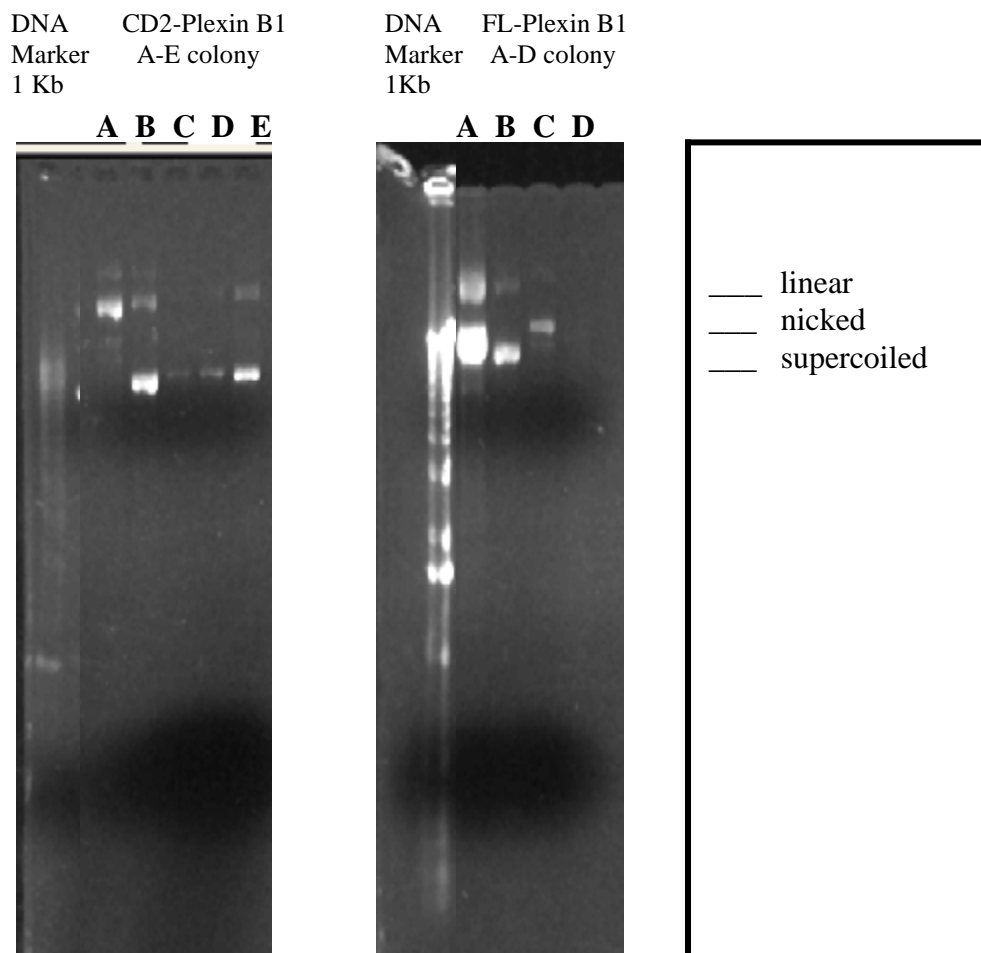
### **3.2.1 Generation of the mutation in Plexin B1 cDNA (full length-FL and truncated-CD2)**

The C5662T mutation in the Plexin B1 gene, which is predicted to result in a substitution of a proline to a serine at position 1798, was generated in full length and truncated Plexin B1 constructs. The QuikChange XL Site-Directed Mutagenesis Kit (Stratagene) was used to introduce the mutation into the two constructs.

Once the mutation had been introduced using site directed mutagenesis the vector DNA incorporating the desired mutation was transformed into XL10 – Gold ultracompetent cells. Transformed E-coli were grown on agar plates with ampicillin and colonies were picked for each construct. DNA was extracted for each construct and 1µl of DNA was run on an 0.8% agarose gel (Figure 3.1).

All five colonies of the CD2 construct and three colonies (A-C) of the full length (FL) construct showed the expected pattern of linear, nicked and supercoiled DNA. Colonies may have different quantities of these subtypes of DNA and will therefore show different patterns on the agarose gel. Plasmid DNA isolated using miniprep and maxiprep kits is a mixture of linear, nicked and supercoiled DNA and they can all exist in a single plasmid preparation. No product was seen in colony D full length Plexin B1 suggesting that it had not been transformed with Plexin B1.





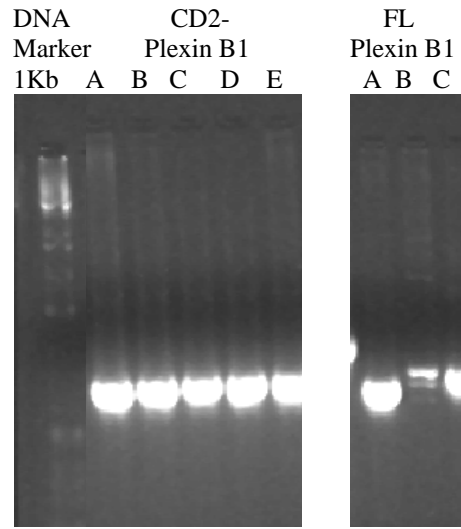
*Figure 3.1 Mutated full length Plexin B1 and truncated CD2 Plexin B1 DNA run on an 0.8% gel. Mutated Plexin B1 was transformed into E. coli cells and grown on agar plates. Following DNA extraction using the Qiagen plasmid purification method five colonies of the CD2 construct and three of the full length Plexin B1 construct are shown, in their supercoiled, nicked and linear forms.*

Spectrophotometry was used to calculate the DNA concentration in the samples using the formula described (Table 3.1).

Using the appropriate primers (Plexin B1 sense and antisense) for the mutation, PCR was used to amplify the segment of DNA containing the C5662T mutation and the product was run on a 1.8% gel using 6 $\mu$ l of PCR product (Figure 3.2). This confirmed the presence of DNA in the mutant full length Plexin B1 (colonies A-C) and in the CD2 Plexin B1 construct (colonies A-E).

<b>Sample</b>	<b>Ab 260nm</b>	<b>DNA concentration (µg/ml)</b>
CD2 A	0.0038	31.7
CD2 B	0.0147	122.5
CD2 C	0.0025	20.8
CD2 D	0.0093	77.5
CD2 E	0.0048	40.0
FL A	0.0577	480.8
FL B	0.0095	79.2
FL C	0.0039	32.5

*Table 3.1 DNA concentration of individual colonies. The concentration of the extracted DNA of the mutated full length Plexin B1 and truncated CD2 Plexin B1 was calculated according to the formula: Conc. of DNA sample = spectrophotometric conversion  $\times$   $A_{260}$   $\times$  dilution factor. 3µl of DNA was combined with 500µl of water – giving a dilution factor of 167. The spectrophotometric conversion for DNA was 50 (1  $A_{260}$  unit of double-stranded DNA=50 µg/ml).*



*Figure 3.2 PCR product of truncated CD2 Plexin B1 and full length Plexin B1. The PCR product was run on a 1.8% gel using a 1Kb DNA marker. 6 $\mu$ l of PCR product with 2 $\mu$ l of loading buffer were loaded in each well. The presence of DNA in the five CD2 plexin B1 and three full length Plexin B1 mutant clones was confirmed.*

### 3.2.2 Confirmation of the mutation

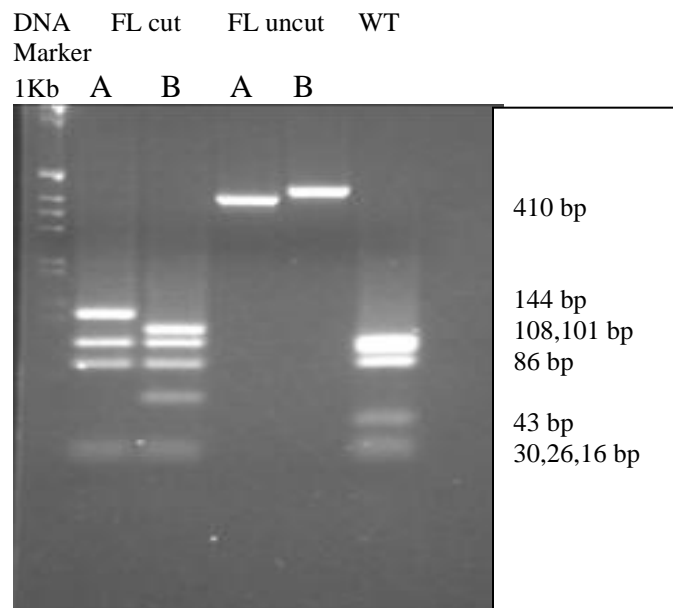
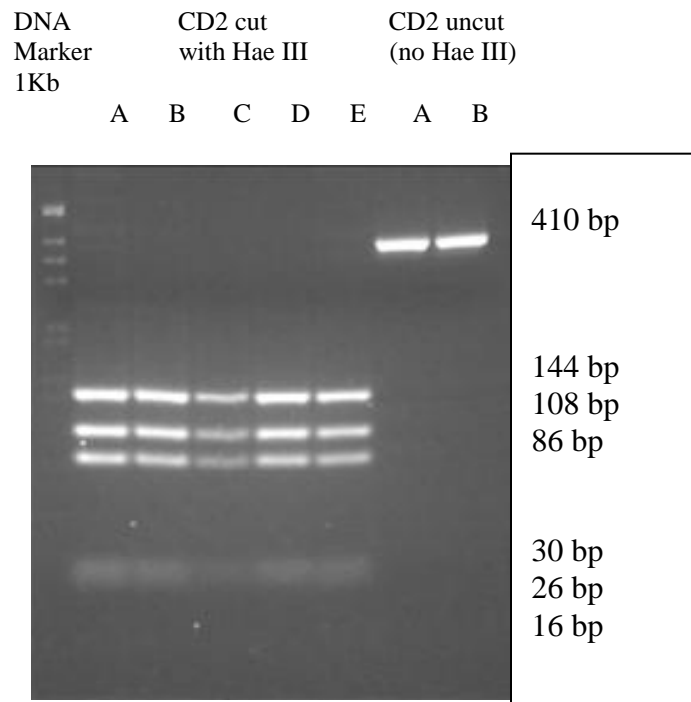
To check that the mutation had been introduced into the Plexin B1 constructs and no new mutations had been introduced, two methods were used:

#### 1. Digestion with Restriction Enzyme – Hae III

A restriction enzyme recognizes and cuts DNA at a particular sequence of nucleotides. For example, the bacterium *Hemophilus aegypticus* produces an enzyme named HaeIII that cuts DNA wherever it encounters the sequence 5'...GG<sup>^</sup>CC...3' and 3'...CC<sup>^</sup>GG...5'.

Using the webcutter program (Webcutter 2004: internet communication) Hae III recognises 6 sites in the wild type (full length Plexin B1-without mutation) Plexin B1 PCR product. In the mutant (C5662T) Hae III recognises 5 sites.

The digested products were run on a 3% agarose gel (Figure 3.3). The total number of base pairs in the uncut product is 410. The wild type Plexin B1 as expected has seven bands and the mutant has six bands. The lower bands had not separated entirely on the 3% agarose gel. Digestion with Hae III had shown that the full length clone A was not the same as full length clone B. The mutation was known to be present in the 144 length band and therefore the C5662T mutation appeared to be present in all of the CD2 Plexin B1 clones and the full length Plexin B1 clone A.



*Figure 3.3 Digestion of CD2 Plexin B1 and full length Plexin B1 using the restriction enzyme Hae III. PCR products, including wild type (WT) full length Plexin B1, mutant CD2 Plexin B1 and mutant full length Plexin B1 digested with*

*Hae III as well as uncut (No Hae III) CD2 Plexin B1 and full length Plexin B1 were run on a 3% agarose gel. Digestion of the constructs with Hae III had confirmed the presence of the mutation in clones A-E of the truncated CD2 Plexin B1 and Clone A of the full length Plexin B1. The total number of base pairs in the uncut PCR product is 410. The mutation was present in the 144 base pair band. The smaller bands had not separated as expected and this was probably a reflection of their size and having not been run for long enough. Despite using a higher percentage gel and running the product for a longer time in the electrophoresis tank, the lower bands could not be separated (WT = wild type cut, bp = base pairs).*

## 2. Cycle sequencing

To independently confirm the presence of the mutation and that no new mutations had been introduced, cycle sequencing was used. Using the appropriate primers for the mutation a PCR was performed and the product run on a 1.8% gel. (Figure 3.4).

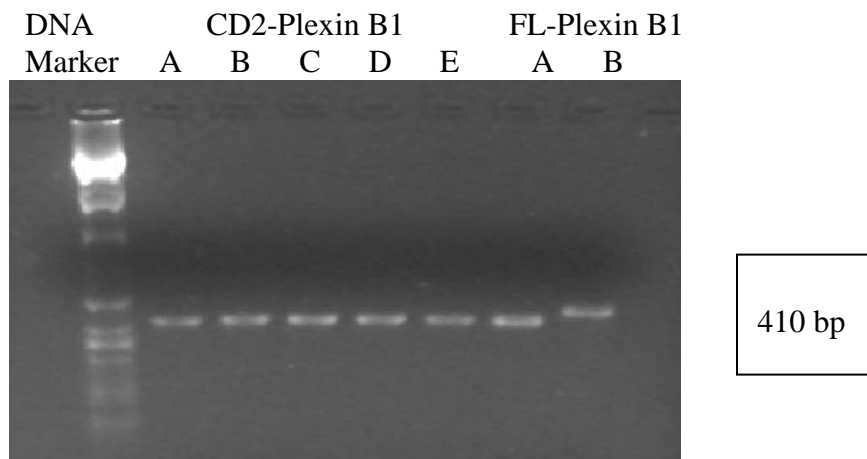
This reaction confirmed the presence of DNA in the PCR product, which was also the correct size at 410 base pairs. Again it appeared that the FL B clone was a slightly larger product than FL A clone.

Using the PCR products formed from the appropriate primers for the C5662T mutation, cycle sequencing was carried out (Figure 3.5). The samples could not be analysed in the laboratory where this research was carried out and had to be sent to a centre which had a sequence analyser.

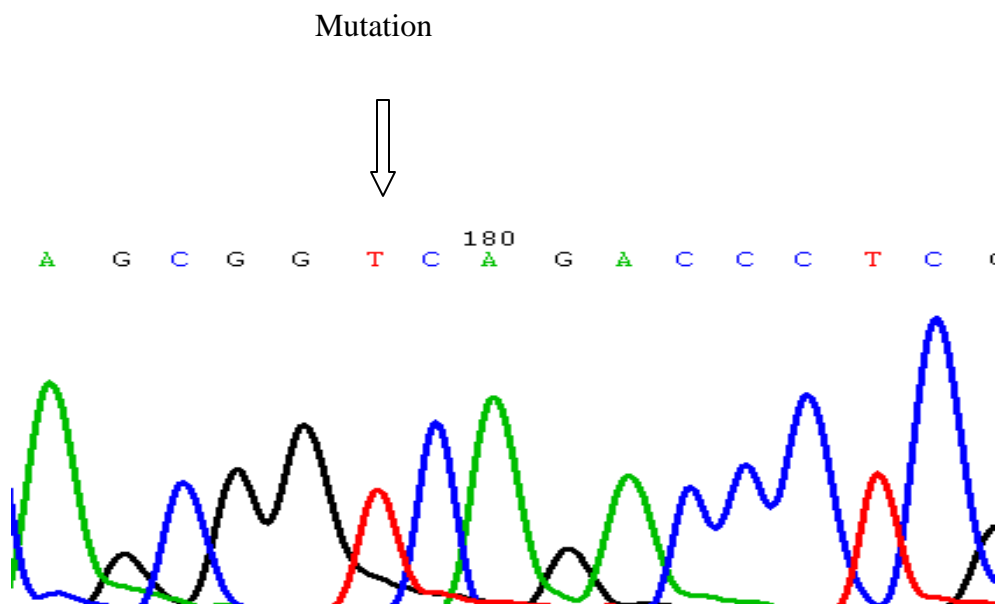
The mutation was confirmed in the CD2 construct in clones A to E and the full length construct in clone A. A Cytosine had been changed to a Thymine at the correct position.

From the cycle sequencing it became evident that the full length Plexin B1 clone B was not identical to clone A. It appeared that part of the sequence had been duplicated during mutagenesis and therefore it was no longer used (Figure 3.6).

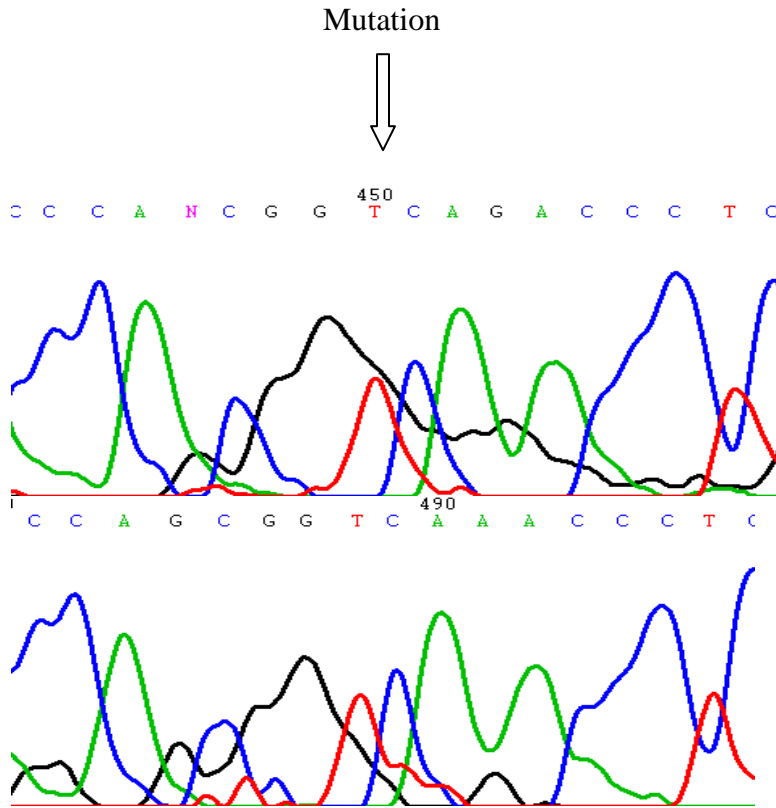




*Figure 3.4 PCR products of DNA extracted from clones A-E CD2 Plexin B1 and clone A and B full length Plexin B1. PCR products were loaded on to a 1.8% agarose gel. As expected the length of the PCR product was 410 base pairs and all of the clones were of the same size except the full length Plexin B1 clone B. With this consistent discrepancy in clone B of the full length Plexin B1 it was no longer used in future experiments (bp = base pairs).*



*Figure 3.5 Cycle sequencing of the mutant Plexin B1 (C5662T). An automated DNA sequencing machine was used to analyze the DNA fragments produced. This directly confirmed that the mutation had been introduced into the constructs. The base Cytosine had been altered to a Thymine in all five of the CD2 Plexin B1 clones and clone A of the full length Plexin B1.*



*Figure 3.6 Cycle sequencing of mutant full length Plexin B1 clone B. The results of the mutant full length Plexin B1 showed two separate sequences both containing the mutation. The reason for this was not clear but it was thought that part of the sequence had been duplicated possibly during mutagenesis, which would explain the larger size of the PCR product on gel electrophoresis.*

The entire cytoplasmic domain of the wild type Plexin B1 and the mutant clones were then sequenced using five sets of primers to cover 2200 base pairs. The presence of the mutation was confirmed in the mutant clones and that no new mutations had been introduced and there were no changes in the wild type clones (results not shown).

The primers used for sequencing the entire cytoplasmic domain of Plexin B1 and their sequence is shown below. See Appendix for positions of the primers on the gene sequence.

B1-52 S	TGGGTCACGTGCAGTATGAC
B1-52 AS	AGTGACCTGGTTGCCAGT
B1-2S	CTCACCGTGGCACTGCATG
B1-2AS	GATGTTGAGTGGCGGTCTGGG
B1-3S	AGGAGTGCCTCTCACCCAGCG
B1-3AS	GACCTGCTGGATGAGCAGGC
B1-4S	TGCCGCTCGCTGTGAAGTAC
B1-4AS	GCAGATTGCAGCTGCTGTGG
Sp6 S	CCCTGCATGAACTCTACAAG
Sp6 AS	TAGTGTCACCTAAATG

### **3.2.3 Generation of stable clones of full length Plexin B1**

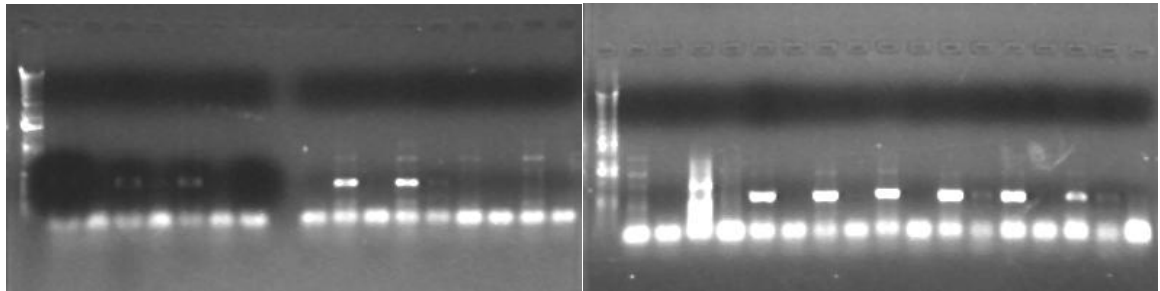
The vector, mutant and wild type full length Plexin B1 constructs were transfected into NIH3T3 cells. Stable clones were selected using geneticin and ring cloned. The clones were then grown up individually and stored at -80°C or in liquid nitrogen.

The relative expression of Plexin B1 RNA in each stable clone was then determined by RT-PCR+/- superscript II (Figure 3.7).

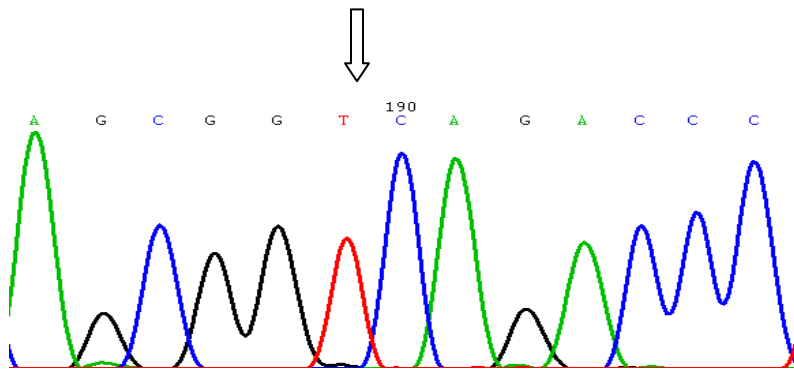
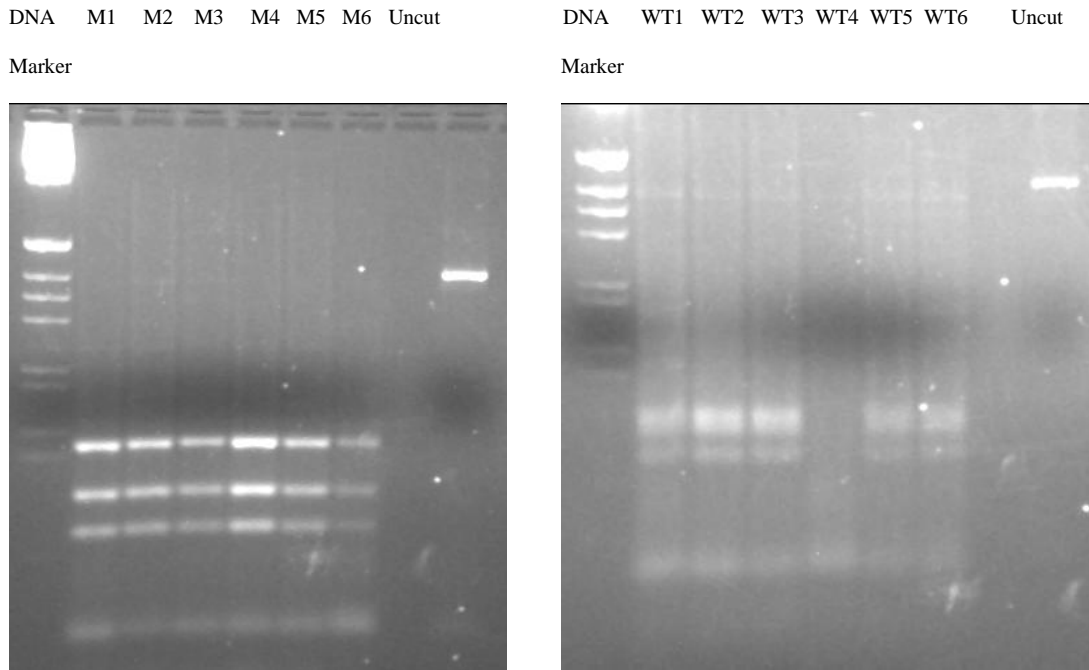
Most of the wild type (WT) clones and all of the mutant (M) clones strongly express Plexin B1. The vector (V) controls were negative, proving that there was no endogenous Plexin B1 being expressed. The control samples without superscript were all negative, showing that there was no cloned Plexin B1 cDNA present in the RNA samples.

Digestion with Hae III and sequencing were used to prove the presence of the mutation in each stable clone. Following the digestion with Hae III all the mutant clones showed the correct sized bands, as did the wild type (except WT4). Sequencing confirmed the presence of the mutation in the mutant clones and that no new mutations had been introduced in the wild type clones (Figure 3.8).

DNA	WT1	WT2	WT3	WT4	WT5	WT6	V1	V2	DNA	V3	V4	M1	M2	M3	M4	M5	M6
Marker	+/-	+/-	+/-	+/-	+/-	+/-	+/-	+/-	Marker	+/-	+/-	+/-	+/-	+/-	+/-	+/-	+/-



*Figure 3.7 Relative expression of Plexin B1 RNA in stable clones by RT-PCR. The constructs had been transfected into NIH3T3 cells and grown up individually and stored at -80°C. RNA was extracted and first strand cDNA synthesis was carried out on the samples. Following PCR, 6µl product was run on an 0.8% agarose gel. A 1Kb DNA marker was used. Two of the wild type Plexin B1 clones (WT4 and WT5) and all of the mutant Plexin B1 clones express Plexin B1 at a range of levels. The control samples without reverse transcriptase (Superscript II) confirmed that there was no contaminated Plexin B1 DNA in the RNA samples. The vector controls demonstrated that no endogenous Plexin B1 RNA was present (WT – Wild type Plexin B1, V – vector, M – mutant, +/- with and without superscript II).*



*Figure 3.8 Checking the clones with Hae III digestion and cycle sequencing. Samples were run on a 3% agarose gel. All six of the mutant clones showed the correct sized bands following digestion with Hae III as did five of the wild type clones. The total number of base pairs in the uncut PCR product was known to be 410 and this was confirmed on the DNA marker. Cycle sequencing had also confirmed the presence of the mutation and no new mutations had been introduced.*

### 3.2.4 Protein expression of Plexin B1

Western blotting and immunofluorescence was used to show the protein expression of full length Plexin B1 in stable clones.

In 2003 Artigiani found that Plexin B1 undergoes proteolytic processing converting it into a heterodimeric receptor, this occurs in a post golgi compartment and likely at the cell surface. This processing may increase the binding and functional response of Plexin B1 to its ligand Semaphorin 4D. The group showed that Plexin B1 was cleaved into an  $\alpha$  subunit of approximately 200KDa and a  $\beta$  subunit of approximately 100KDa (Figure 3.9) (Artigiani et al. 2003). The cleavage of Plexin B1 is mediated by proprotein convertases.

No commercial antibody against Plexin B1 was available at the time of doing this work. However Artigiani et al. had raised a rabbit polyclonal antibody (IC2) against the  $\beta$  subunit of Plexin B1. Therefore IC2 antibody against the intracellular region of Plexin B1 was used to detect the  $\beta$  subunit and the unprocessed Plexin B1 of 300KDa.



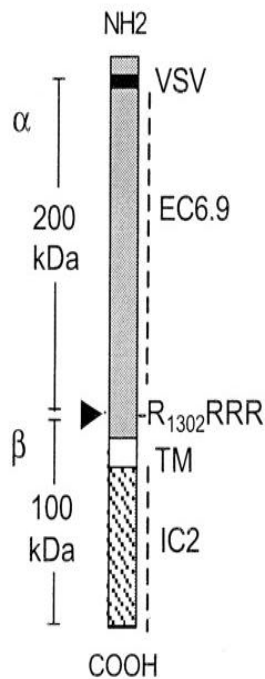


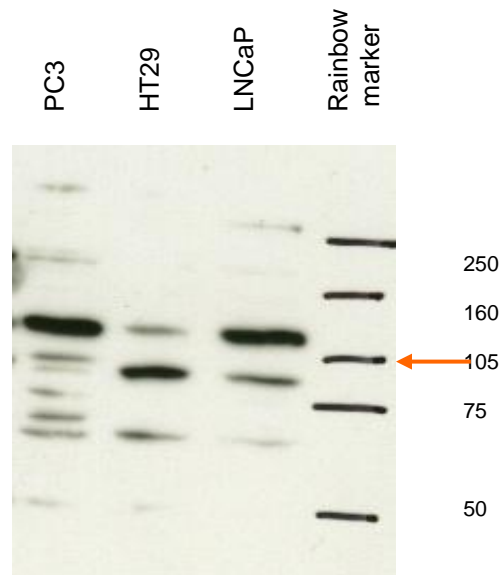
Figure 3.9 Full length Plexin B1 showing the  $\alpha$  and  $\beta$  subunits (Artigiani et al. 2003). In this schematic representation of Plexin B1, the arrow shows the predicted processing site resulting in an extracellular moiety (molecular mass 200KDa) and a transmembrane/ cytoplasmic moiety (100KDa). Cells that had been transfected with Plexin B1 were found to express both the full length (300KDa) and two cleaved subunits (200 and 100KDa) at the cell surface. The  $\beta$  subunit was detected using the IC2 antibody (Artigiani et al. 2003). This suggested that Plexin B1 undergoes proteolytic processing converting it into an heterodimeric receptor. This process increases the binding and the functional response of Plexin B1 to its ligand Sema4D (Artigiani et al. 2003).

Using protein from HT29 cells (human colon adenocarcinoma cell line) known to express Plexin B1 (Artigiani et al. 2003) as a positive control a western blot showed that a 100kDa product was present in LNCaP, PC3 and HT29 (Figure 3.10). The concentrations of primary and secondary antibody used were a personal communication by V Blanc. However there were many non-specific bands seen on the western blot. This problem is usually due to a non specific antibody, a poor primary antibody quality/ old antibody, inadequate blocking or the protein is detected but degraded.

Attempts were made to visualize the membrane protein Plexin B1 in stable transfected cells. Various techniques were used to solve the problem of too many bands. Different protein extraction buffers were tried, replacing the antibody with a fresh stock, blocking with BSA prior to adding antibody and using sodium butyrate to increase the intensity of Plexin B1 100KDa band. To increase antibody specificity and reduce the background, different antibody concentrations were used and a variety of blocking agents were tried. However, the problem of non specific bands continued. The use of sodium butyrate with the extraction buffer, RIPA, produced the brightest bands (Figure 3.11).

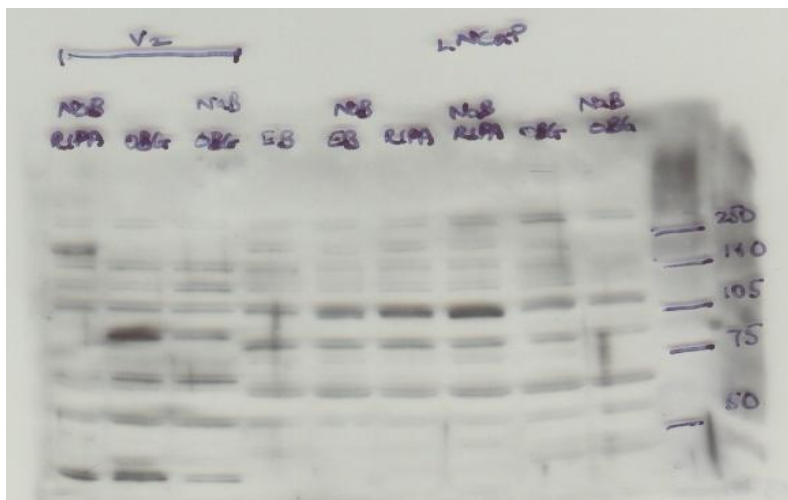
It was not possible to conclude from the western blot experiments that Plexin B1 was being expressed in the stable transfections as numerous bands from the vector control group were also seen on the western blots. This was thought to be because the IC2 antibody was non specific and/or the stable transfections were switching off

the expression of the protein. At the time of doing these experiments, there was no other antibody available and no further experiments were performed to verify these bands.

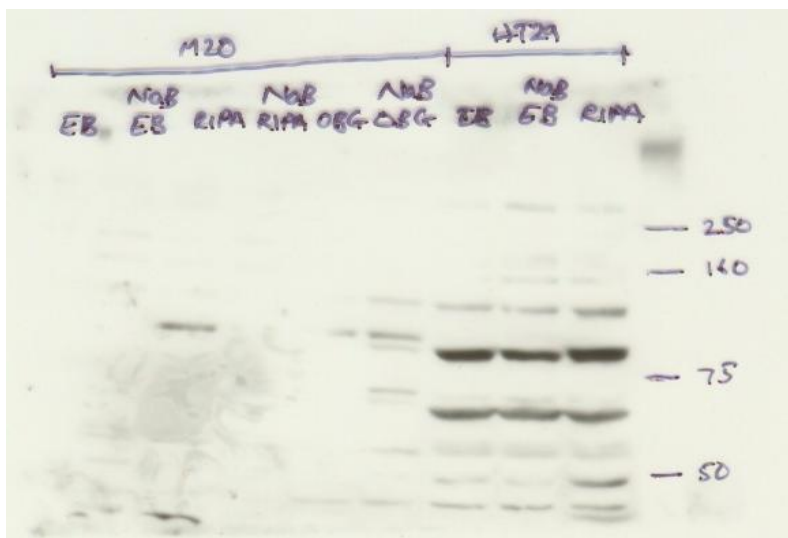


*Figure 3.10 Western blot showing protein expression of endogenous plexin B1 (26 $\mu$ g protein loaded using RIPA buffer and run on an 8% SDS-PAGE gel). Using a specific anti-Plexin B1 antibody raised against the cytoplasmic domain of the protein (IC2) a protein is detected on western blot with a molecular mass of 100KDa, corresponding to the truncated form of the Plexin B1 receptor. HT29 cells which are known to express endogenous Plexin B1 were used as a control. However, many non specific bands were seen on the western blot, suggesting there was non-specific binding of primary or secondary antibodies.*

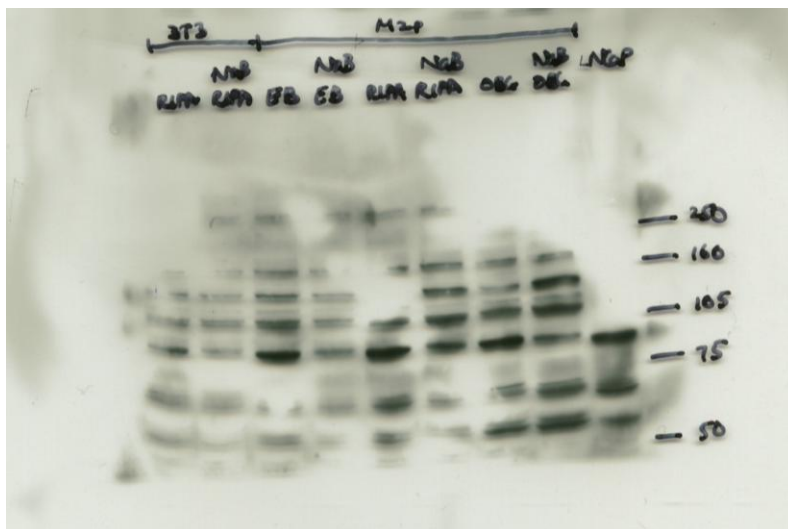
a) Vector +/- NaB                      LNCaP +/- NaB  
RIPA OBG EB                      EB RIPA OBG



b) Mutant +/- NaB                      HT29 + NaB  
EB RIPA OBG                      EB OBG RIPA



c) NIH3T3 + NaB                      WT +/- NaB  
RIPA OBG EB                      RIPA OBG EB



*Figure 3.11 a,b,c. Protein expression of Plexin B1 using three protein extraction buffers Different extraction buffers RIPA, EB and OBG with and without sodium butyrate (NaB) were used. Using stable transfected NIH3T3 cells with wild type (WT) Plexin B1, mutant Plexin B1, vector only (HT29 and LNCaP cells as controls) western blots were carried out. 40µg of protein was loaded onto 8% SDS-page gels. Non specific bands were seen on each western blot and there was insufficient evidence to say that the stable transfected cells expressed either construct.*

Western blotting was found to be unreliable most likely due to a non-specific antibody and so the research was now focused on a newly acquired antibody. The antibody to CD2 could be used to detect the truncated CD2 Plexin B1.

Semaphorin 4D, the transmembrane ligand for Plexin B1, is thought to activate plexin receptors through clustering (Driessens et al. 2001). The chimeric molecule CD2-Plexin B1, in which the cytoplasmic domain of Plexin B1 was fused to CD2 (a T lymphocyte antigen) was used. Driessens et al. 2001 had shown that when the DNA of CD2-Plexin B1 was microinjected into 3T3 cells and antibodies to CD2 added this led to the formation of stress fibers and cell contraction thus mimicking ligand binding.

DNA of Vector-CD2, Wild type (WT)-CD2 Plexin B1 and Mutant-CD2 Plexin B1 was extracted and transfected into COS1 cells and 3T3 cells (as described previously). Immunofluorescence was used to assess protein expression of these constructs using the anti-CD2 antibody (CD2 antibody, product name OX34, mouse monoclonal, Abcam).

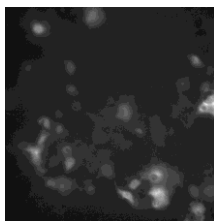
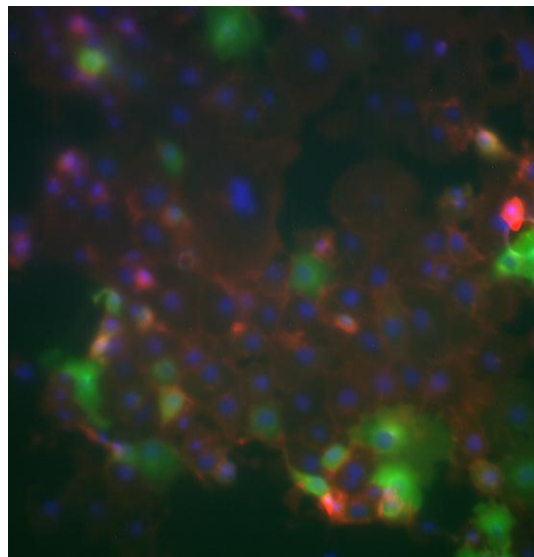
The results show membranous and nuclear staining indicating that both wild type and mutant transiently transfected cells express Plexin B1 and that the protein is

transported to the cell surface (Figure 3.12 – 3.21). The results suggest that the mutation does not have an effect on the protein expression of truncated Plexin B1.

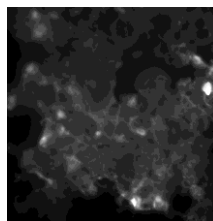
For each transfection three photographs were taken using filters to look at nuclear staining (blue), actin staining (red) and staining for Plexin B1 (green). A combined image was then taken (larger image). The cells were viewed using a fluorescent microscope (Nikon, C-SHG1 with epifluorescence attachment). OX34 primary antibody stained CD2, F-actin staining was with phalloidin TRITC and nuclear staining was with DAPI.



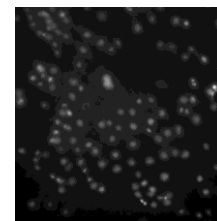
*Figure 3.12 COS1 cells transiently transfected with WT-CD2 Plexin B1. Nuclear staining – DAPI; CD2 staining – OX34 primary antibody diluted 1/400, Abcam; goat anti-mouse FITC secondary antibody diluted 1/200, Southern Biotechnology; F-actin staining – phalloidin TRITC diluted 1/500, Sigma. The protein expression of truncated Plexin B1 conjugated with CD2 was detected using immunofluorescence with the anti-CD2 antibody. Membranous and nuclear staining was seen indicating that the protein is transported to the cell surface. Nuclear staining may be due to over expression of the protein. A low transfection efficiency was observed. Three photographs were taken using filters to look at nuclear staining (blue), actin staining (red) and staining for Plexin B1 (green). A merged image was then taken (larger image).*



CD2 Plexin B1

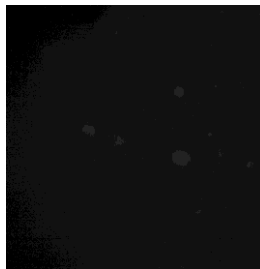
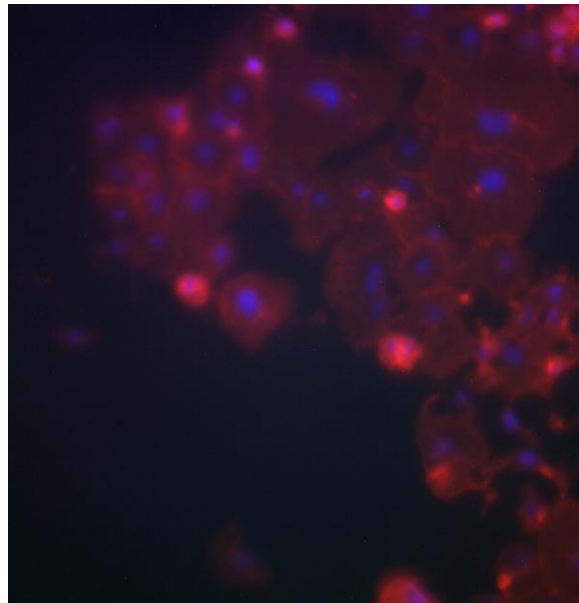


Actin

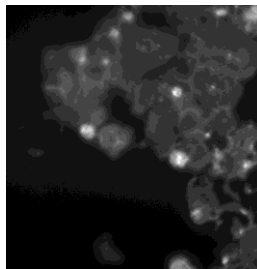


Nuclear

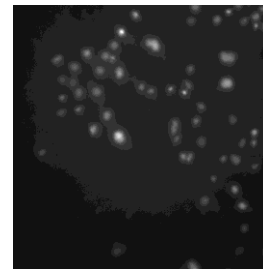
*Figure 3.13 COS1 cells transiently transfected with WT-CD2 Plexin B1 (no 1° antibody). Nuclear staining – DAPI; goat anti-mouse FITC secondary antibody diluted 1/200, Southern Biotechnology; F-actin staining – phalloidin TRITC diluted 1/500, Sigma. As a control, when no primary antibody is added (anti CD2 antibody), protein expression of CD2 Plexin B1 is not detected. Three photographs were taken using filters to look at nuclear staining (blue), actin staining (red) and staining for Plexin B1 (green). A merged image was then taken (larger image).*



CD2 Plexin B1

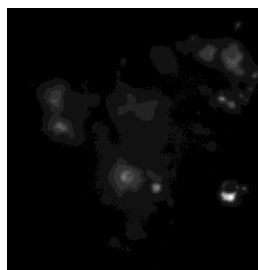
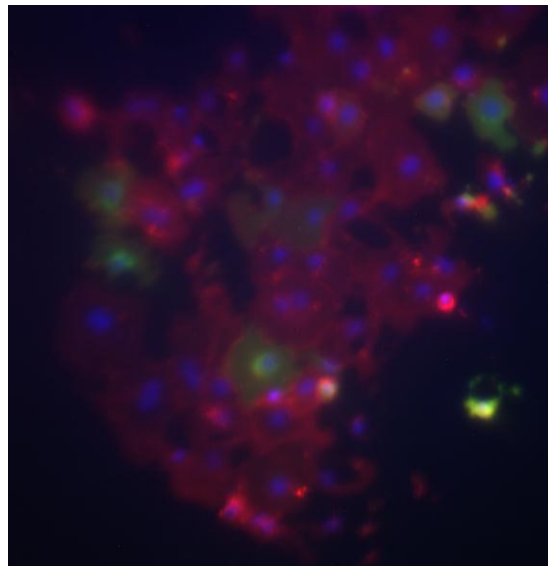


Actin

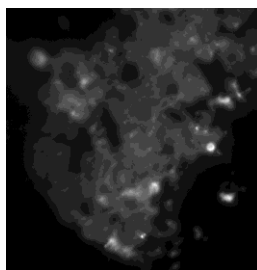


Nuclear

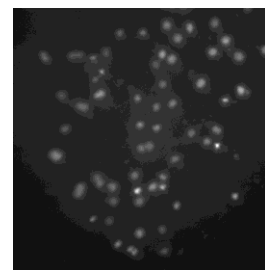
*Figure 3.14 COS1 cells transiently transfected with Mutant-CD2 Plexin B1. Nuclear staining – DAPI; CD2 staining – OX34 primary antibody diluted 1/400, Abcam; goat anti-mouse FITC secondary antibody diluted 1/200, Southern Biotechnology; F-actin staining – phalloidin TRITC diluted 1/500, Sigma. The protein expression of truncated Mutant Plexin B1 conjugated with CD2 was detected using immunofluorescence with the anti-CD2 antibody. Membranous staining was seen indicating that the protein is transported to the cell surface. A low transfection efficiency was observed. Three photographs were taken using filters to look at nuclear staining (blue), actin staining (red) and staining for Plexin B1 (green). A merged image was then taken (larger image).*



CD2 Plexin B1

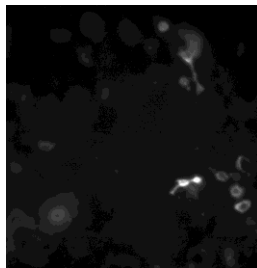
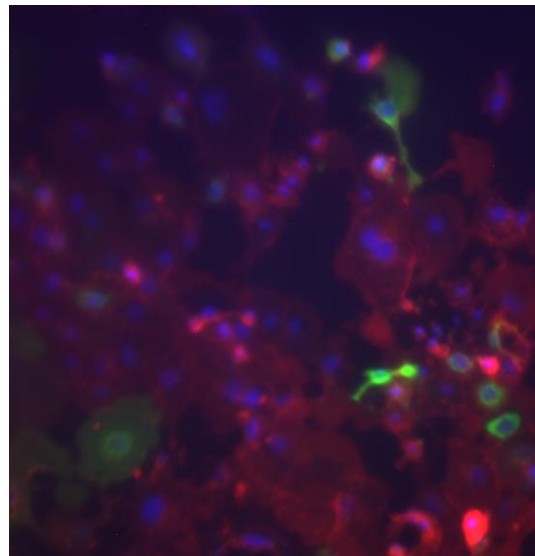


Actin

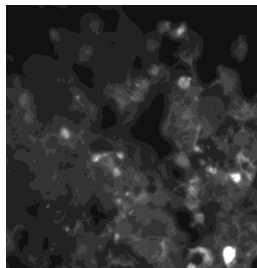


Nuclear

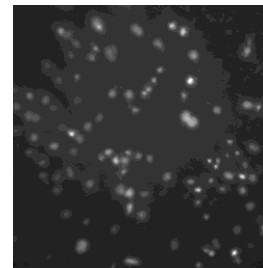
*Figure 3.15 COS1 cells transiently transfected with Vector-CD2. Nuclear staining – DAPI; CD2 staining – OX34 primary antibody diluted 1/400, Abcam; goat anti-mouse FITC secondary antibody diluted 1/200, Southern Biotechnology; F-actin staining – phalloidin TRITC diluted 1/500, Sigma. The protein expression of vector-CD2 was detected using immunofluorescence with the anti-CD2 antibody. Membranous and nuclear staining was seen indicating that the protein is transported to the cell surface. Nuclear staining may be due to over expression of the protein. A low transfection efficiency was observed. Three photographs were taken using filters to look at nuclear staining (blue), actin staining (red) and staining for Plexin B1 (green). A merged image was then taken (larger image).*



CD2 Plexin B1

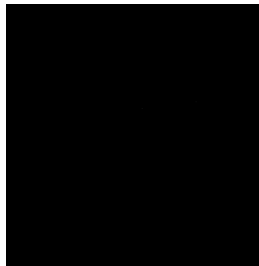
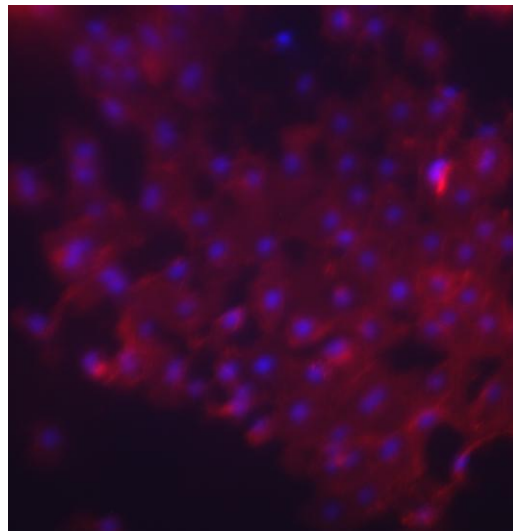


Actin

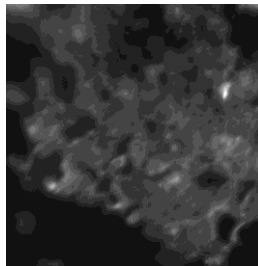


Nuclear

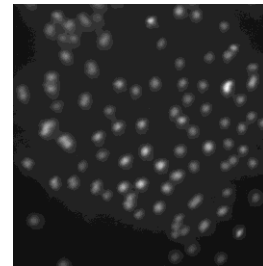
*Figure 3.16 COS1 cells Mock transfected. Nuclear staining – DAPI; CD2 staining – OX34 primary antibody diluted 1/400, Abcam; goat anti-mouse FITC secondary antibody diluted 1/200, Southern Biotechnology; F-actin staining – phalloidin TRITC diluted 1/500, Sigma. Protein expression of CD2 Plexin B1 is not detected when COS1 cells are mock transfected (no DNA). This indicates that COS1 cells do not express endogenous CD2-Plexin B1. Three photographs were taken using filters to look at nuclear staining (blue), actin staining (red) and staining for Plexin B1 (green). A merged image was then taken (larger image).*



CD2 Plexin B1

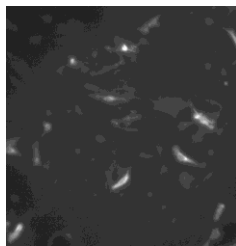
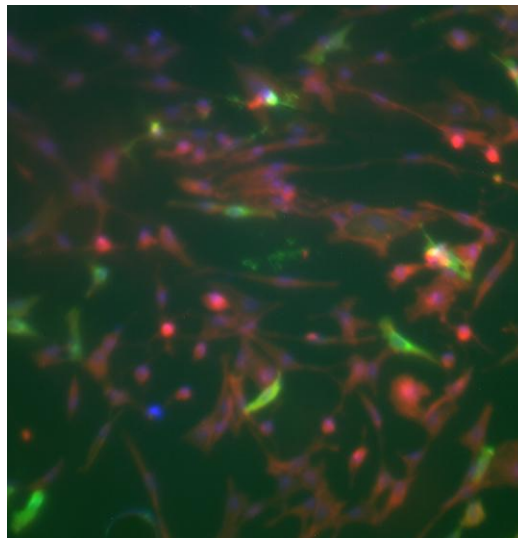


Actin

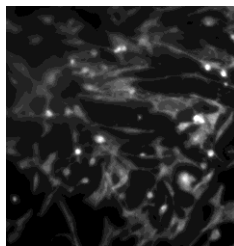


Nuclear

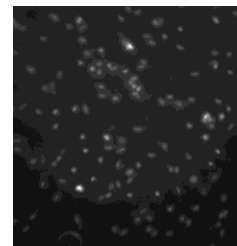
*Figure 3.17 3T3 cells transiently transfected with WT-CD2 Plexin B1. Nuclear staining – DAPI; CD2 staining – OX34 primary antibody diluted 1/400, Abcam; goat anti-mouse FITC secondary antibody diluted 1/200, Southern Biotechnology; F-actin staining – phalloidin TRITC diluted 1/500, Sigma. 3T3 cells were transiently transfected with wild type-CD2 Plexin B1. The protein expression of truncated Plexin B1 conjugated with CD2 was detected using immunofluorescence with the anti-CD2 antibody. Membranous and nuclear staining was seen indicating that the protein is transported to the cell surface. Nuclear staining may be due to over expression of the protein. A low transfection efficiency was observed. Three photographs were taken using filters to look at nuclear staining (blue), actin staining (red) and staining for Plexin B1 (green). A merged image was then taken (larger image).*



CD2 Plexin B1

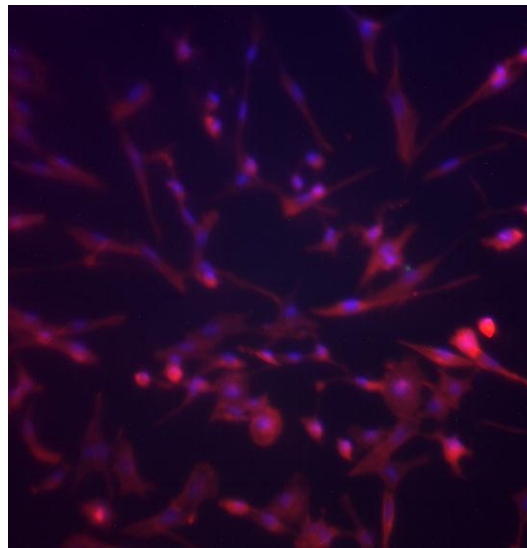


Actin

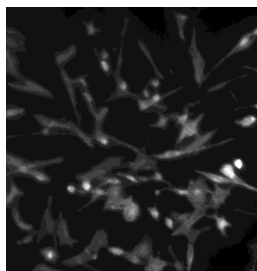


Nuclear

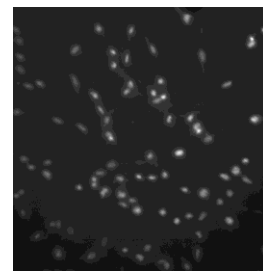
*Figure 3.18 3T3 cells transiently transfected with WT-CD2 Plexin B1 (no 1° Ab). Nuclear staining – DAPI; goat anti-mouse FITC secondary antibody diluted 1/200, Southern Biotechnology; F-actin staining – phalloidin TRITC diluted 1/500, Sigma. As a control, when no primary antibody is added (anti CD2 antibody), protein expression of CD2-Plexin B1 is not detected. Three photographs were taken using filters to look at nuclear staining (blue), actin staining (red) and staining for Plexin B1 (green). A merged image was then taken (larger image).*



CD2 Plexin B1

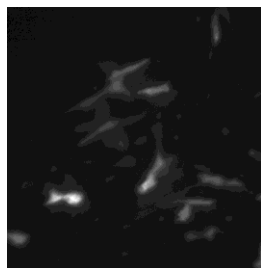
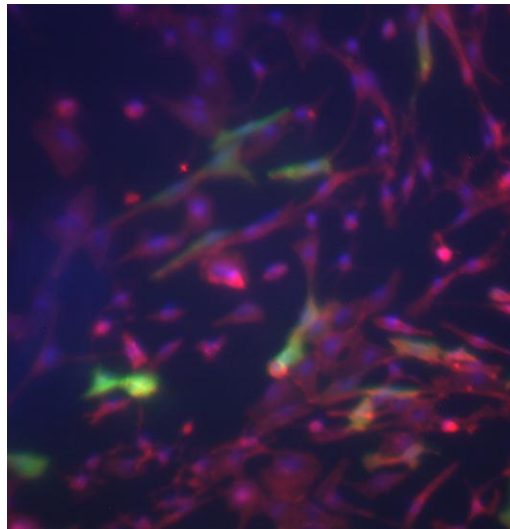


Actin

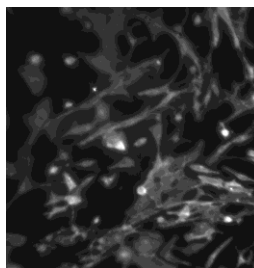


Nuclear

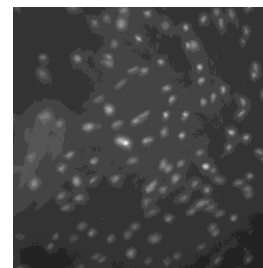
*Figure 3.19 3T3 cells transiently transfected with Mutant-CD2 Plexin B1. Nuclear staining – DAPI; CD2 staining – OX34 primary antibody diluted 1/400, Abcam; goat anti-mouse FITC secondary antibody diluted 1/200, Southern Biotechnology; F-actin staining – phalloidin TRITC diluted 1/500, Sigma. The protein expression of truncated Mutant Plexin B1 conjugated with CD2 was detected using immunofluorescence with the anti-CD2 antibody. Membranous staining was seen indicating that the protein is transported to the cell surface. A low transfection efficiency was observed. Three photographs were taken using filters to look at nuclear staining (blue), actin staining (red) and staining for Plexin B1 (green). A merged image was then taken (larger image).*



CD2 Plexin B1



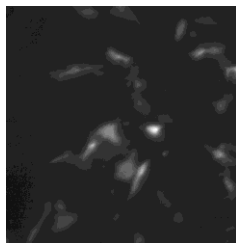
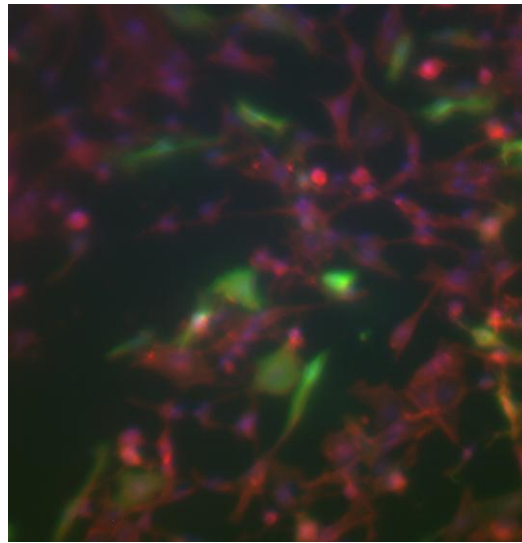
Actin



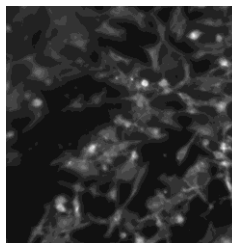
Nuclear



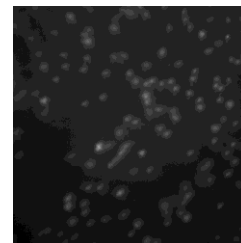
*Figure 3.20 3T3 cells transiently transfected with Vector-CD2. Nuclear staining – DAPI; CD2 staining – OX34 primary antibody diluted 1/400, Abcam; goat anti-mouse FITC secondary antibody diluted 1/200, Southern Biotechnology; F-actin staining – phalloidin TRITC diluted 1/500, Sigma. The protein expression of vector-CD2 was detected using immunofluorescence with the anti-CD2 antibody. Membranous and nuclear staining was seen indicating that the protein is transported to the cell surface. Nuclear staining may be due to over expression of the protein. A low transfection efficiency was observed. Three photographs were taken using filters to look at nuclear staining (blue), actin staining (red) and staining for Plexin B1 (green). A merged image was then taken (larger image).*



CD2 Plexin B1

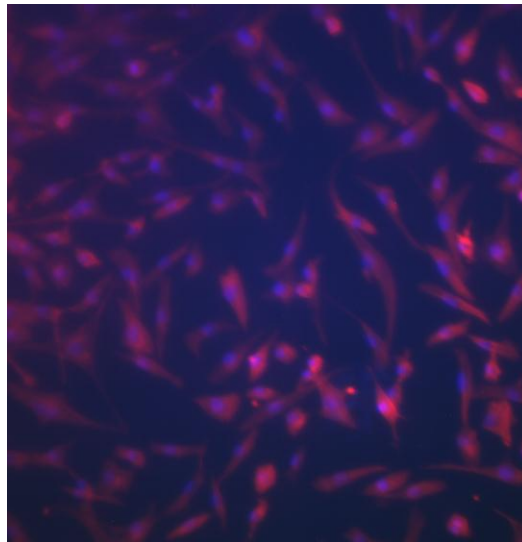


Actin

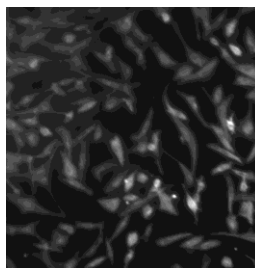


Nuclear

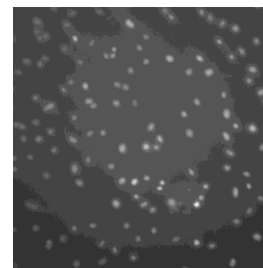
*Figure 3.21 3T3 cells Mock transfected. Nuclear staining – DAPI; CD2 staining – OX34 primary antibody diluted 1/400, Abcam; goat anti-mouse FITC secondary antibody diluted 1/200, Southern Biotechnology; F-actin staining – phalloidin TRITC diluted 1/500, Sigma. Protein expression of CD2 Plexin B1 is not detected when 3T3 cells are mock transfected (no DNA). This indicates that 3T3 cells do not express endogenous CD2-Plexin B1. Three photographs were taken using filters to look at nuclear staining (blue), actin staining (red) and staining for Plexin B1 (green). A merged image was then taken (larger image).*



CD2 Plexin B1



Actin



Nuclear

The protein expression of truncated CD2 Plexin B1 was detected with the anti-CD2 antibody using immunofluorescence. The wild type, mutant and vector constructs showed membranous and nuclear staining when transiently transfected in COS1 and 3T3 cells. Plexin B1 expression was not detected in the samples when no primary antibody was added. From the immunofluorescence results the transfection efficiency in the transiently transfected cells was low (approximately 15%). The *B*-Gal Kit (Invitrogen) was used to optimize the transfection efficiency by varying the concentrations of DNA and Lipofectamine and varying the confluence of the cells.

The *B*-Gal staining kit provides reagents required to determine the percentage of cells transfected with a plasmid expressing lacZ. LacZ is a bacterial gene used as a reporter construct in eukaryotic transfection and the gene product B-galactosidase is easily assayed. B-galactosidase catalyses the hydrolysis of B-galactosides i.e X-gal. This produces a blue colour that can be visualised. The steps for this involve transfecting cells with a plasmid expressing lacZ. The cells are fixed to the plates. They are then washed and incubated with an X-gal containing solution. The cells are then examined to determine the percentage of cells staining blue to estimate the transfection efficiency (Tables 3.2, 3.3, 3.4).







The percentage of cells expressing B-galactosidase was calculated, using the formula:

$$\frac{\text{Total no. of blue cells}}{\text{Total no. of cells}} \times 100$$

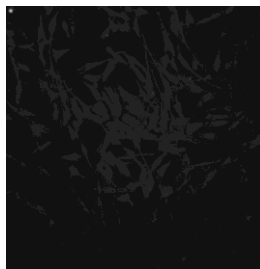
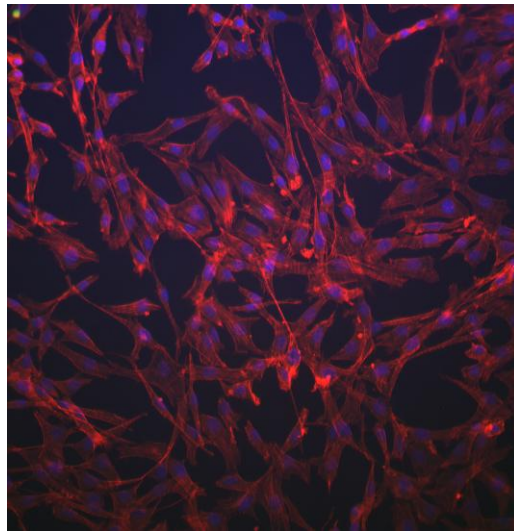
Total no. of cells

Using the *B*-Gal staining Kit, the DNA:Lipofectamine ratio that gave the best transfection rate was 1:2.5 for each cell line with the cells being highly confluent (approx. 90%).

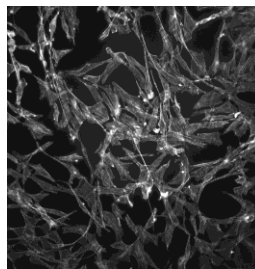
During the above optimisation, stable clones were grown up of truncated CD2-Plexin B1 to examine the protein expression in 3T3 cells (Figure 3.22 – 3.25). As previously described, for each transfection three photographs were taken using filters to look at nuclear staining (blue), actin staining (red) and staining for Plexin B1 (green). A merged image was then taken (larger image).

The results suggest that the stable transfections do not express CD2 Plexin B1 or that they express Plexin B1 at a very low level that could not be detected.

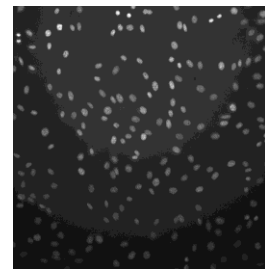
*Figure 3.22 Stable transfection of 3T3 cells with WT-CD2 Plexin B1. Nuclear staining – DAPI; CD2 staining – OX34 primary antibody diluted 1/400, Abcam; goat anti-mouse FITC secondary antibody diluted 1/200, Southern Biotechnology; F-actin staining – phalloidin TRITC diluted 1/500, Sigma. Stable transfected 3T3 cells with wild type CD2 Plexin B1 do not express Plexin B1. Three photographs were taken using filters to look at nuclear staining (blue), actin staining (red) and staining for Plexin B1 (green). A merged image was then taken (larger image).*



CD2 plexin B1



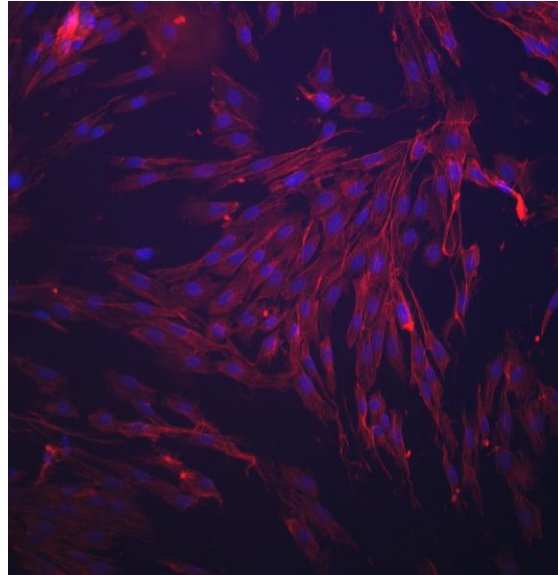
Actin



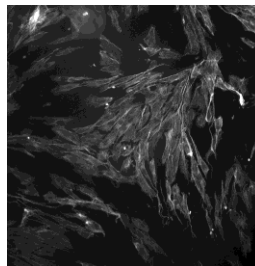
Nuclear



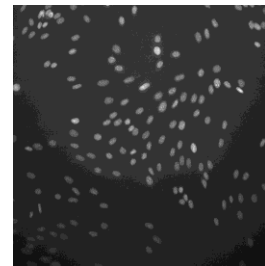
*Figure 3.23 Stable transfection of 3T3 cells with Mutant-CD2 Plexin B1. Nuclear staining – DAPI; CD2 staining – OX34 primary antibody diluted 1/400, Abcam; goat anti-mouse FITC secondary antibody diluted 1/200, Southern Biotechnology; F-actin staining – phalloidin TRITC diluted 1/500, Sigma. Stable transfected 3T3 cells with Mutant CD2 Plexin B1 do not express the mutant Plexin B1. Three photographs were taken using filters to look at nuclear staining (blue), actin staining (red) and staining for Plexin B1 (green). A merged image was then taken (larger image).*



CD2 plexin B1

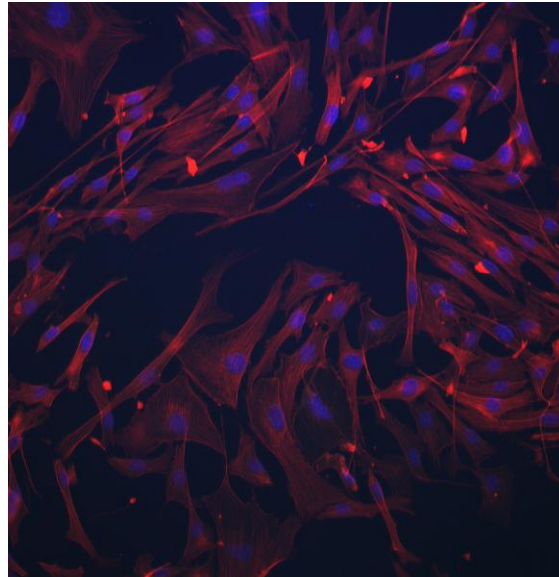


Actin

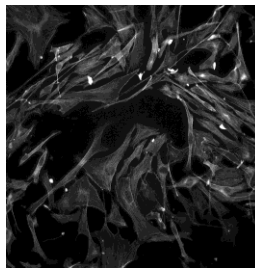


Nuclear

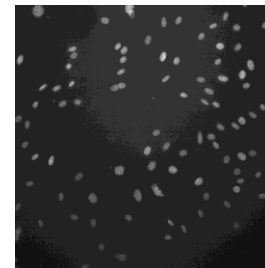
*Figure 3.24 Stable transfection of 3T3 cells with Vector-CD2. Nuclear staining – DAPI; CD2 staining – OX34 primary antibody diluted 1/400, Abcam; goat anti-mouse FITC secondary antibody diluted 1/200, Southern Biotechnology; F-actin staining – phalloidin TRITC diluted 1/500, Sigma. Stable transfected 3T3 cells with Vector CD2 do not express Plexin B1. Three photographs were taken using filters to look at nuclear staining (blue), actin staining (red) and staining for Plexin B1 (green). A merged image was then taken (larger image).*



CD2 plexin B1

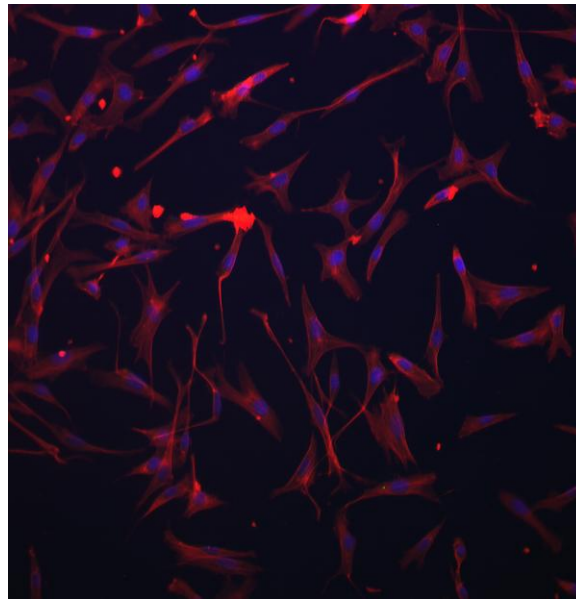


Actin

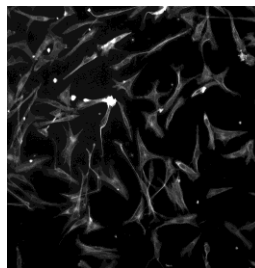


Nuclear

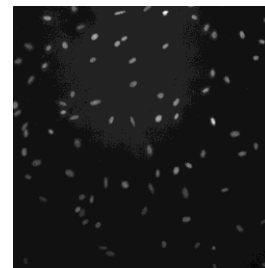
*Figure 3.25 Mock transfected 3T3 cells. Nuclear staining – DAPI; CD2 staining – OX34 primary antibody diluted 1/400, Abcam; goat anti-mouse FITC secondary antibody diluted 1/200, Southern Biotechnology; F-actin staining – phalloidin TRITC diluted 1/500, Sigma. Protein expression of CD2 Plexin B1 is not detected when 3T3 cells are mock transfected (no DNA). This indicates that 3T3 cells do not express endogenous CD2-Plexin B1. Three photographs were taken using filters to look at nuclear staining (blue), actin staining (red) and staining for Plexin B1 (green). A merged image was then taken (larger image).*



CD2 plexin B1



Actin

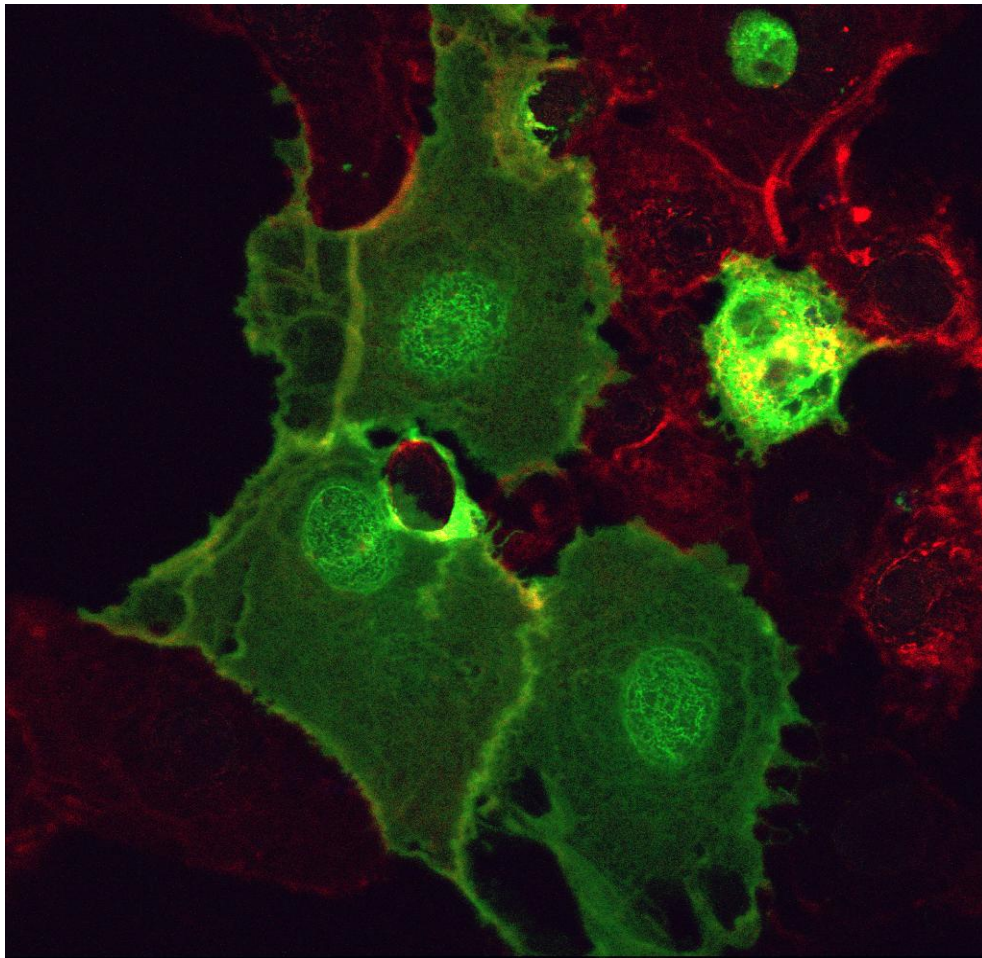


Nuclear

The stable transfections did not express CD2 Plexin B1. The experiments to optimise the transient transfection efficiency showed that COS7 cells gave the best transfection rate when highly confluent and therefore these were used for further assays.

Using a confocal microscope (Zeiss LSM 510W), Wild type (WT) CD2-Plexin B1 transiently transfected in COS7 cells showed membranous staining of CD2-Plexin B1 (Figure 3.26).

*Figure 3.26 Confocal microscopy showing protein expression of CD2-Plexin B1 in COS7 cells (x40 Magnification). Nuclear staining – DAPI; CD2 staining – OX34 primary antibody diluted 1/400, Abcam; goat anti-mouse FITC secondary antibody diluted 1/200, Southern Biotechnology; F-actin staining – phalloidin TRITC diluted 1/500, Sigma. COS7 cells transiently transfected with CD2 Plexin B1 showing expression of CD2 Plexin B1. Membranous and nuclear staining was seen indicating that the protein is transported to the cell surface.*



### **3.2.5 Expression of Semaphorin 4D and Plexin B1 in Prostate cancer cell lines**

Since mutations were found in Plexin B1 in prostate cancer cell specimens, the mRNA of Sema4D and Plexin B1 in prostate cell lines was determined. RT-PCR was used to analyse the expression of Semaphorin 4D and Plexin B1 mRNA in normal and prostate cancer cell lines. The PCR reaction was carried out using 3 $\mu$ l (30ng) of cDNA, 2.5 $\mu$ l of Reaction IV 10x buffer, 1.5 $\mu$ l of 25mM MgCl<sub>2</sub>, 0.5 $\mu$ l of 10mM deoxynucleoside triphosphates, 25pmol of each primer and 1.25U of *Taq* DNA polymerase on a Eppendorf thermocycler. The cycling conditions were 94°C for 5 minutes to activate the *Taq* polymerase followed by 40 cycles of 94°C for 45s, the annealing temperature 58°C for 45s, 72°C for 60s, and a final extension at 72°C for 7min. PCR products were electrophoresed on 0.8% agarose gels. GAPDH was used as a control as it was known to express Plexin B1 and Sema 4D.

Semaphorin 4D and Plexin B1 mRNA were expressed in all normal and prostate cancer cell lines (Figures 3.27 and 3.28). A PCR product was seen for PC3 cells using the 5' set of primers, and not the 3' set. This may be due to a splice variant in this cell line. Alternative splicing was first observed in 1977 (Berget et al. 1977). It was found that the primary RNA transcript produced by adenovirus type 2 was spliced in different ways, resulting in mRNAs encoding different viral proteins (Berget et al. 1977). Since then, alternative splicing has been found to be ubiquitous in eukaryotes (Black et al. 2003). To further investigate the splicing pattern in PC3,

more Sema4D primers would need to be designed to span the entire cDNA. Work would then need to be carried out to determine whether this affects the function of the protein. If the transmembrane domain is involved this could generate a protein that was secreted and not membrane bound and this would alter the function of the protein.

Figure 3.27 RT-PCR of Semaphorin 4D mRNA in cell lines. PCR products were electrophoresed on 0.8% agarose gels. GAPDH was used as a control. Semaphorin 4D (30ng cDNA) was expressed in all cell lines used. No PCR product was seen with the 3' primers in PC3 cells. This may be due to a splice variant in this cell line.

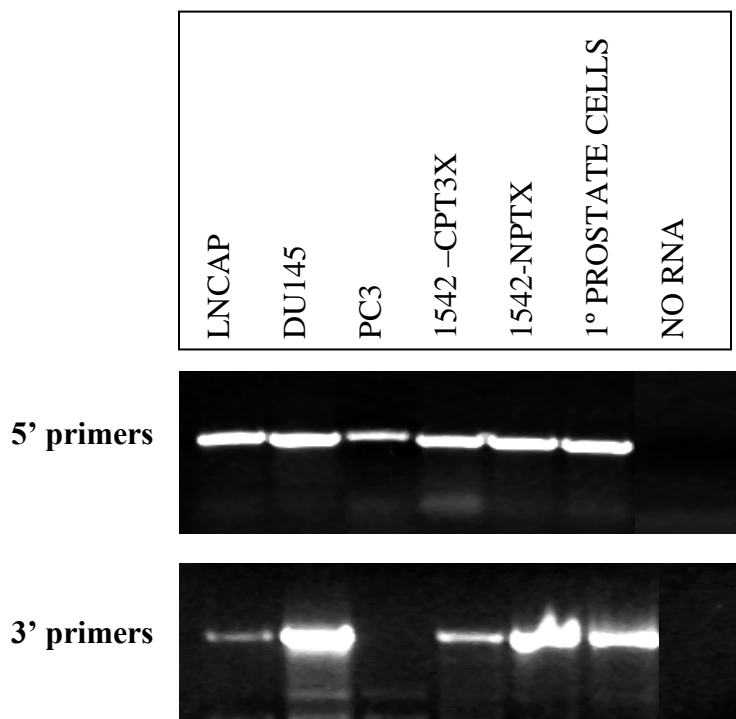
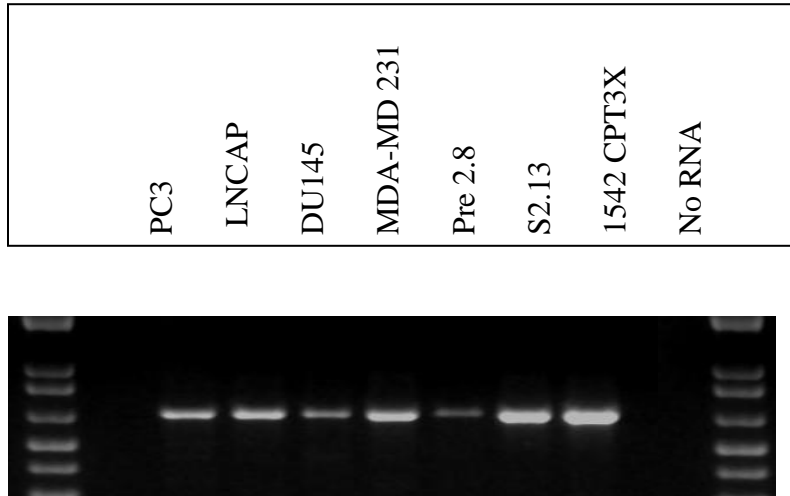




Figure 3.28 RT-PCR of Plexin B1 mRNA in cell lines. PCR products were electrophoresed on 0.8% agarose gels. GAPDH was used as a control. Plexin B1 was expressed in all cell lines. This data was provided by M. Williamson.



### **3.3 Discussion**

The aim of this research was to determine whether the mutation, C5662T, in the Plexin B1 gene at position 1798 contributes to prostate cancer progression. This section concentrates on the generation of vectors that expresses the wild type and mutant Plexin B1. Initially the mutation C5662T needed to be introduced into an expression vector. Two expression vectors had been provided. One had the full length cDNA of Plexin B1 cloned into the vector pcDNA3 and the other had only the cytoplasmic domain of Plexin B1 fused with CD2 (a T lymphocyte antigen) cloned into the vector pcDNA3. .

Primers were specifically designed so as to contain the mutation and site directed mutagenesis was used to generate a single base change in the constructs, so as to create the mutation. DNA was then extracted and the constructs were then checked using two methods. Digestion with the restriction enzyme Hae III, was able to confirm the mutation had been introduced. Cycle sequencing confirmed the presence of the mutation and also ensured that no other mutation had been introduced.

The mutant, wild type (no mutation), vector (no plexin B1) and mock cells were transfected into NIH3T3 cells and stable clones were generated. The relative expression of Plexin B1 RNA was estimated. This confirmed expression of mutant and wild type RNA.

Protein expression was initially measured by western blotting, however despite various attempts to optimize the western blot, it was not possible to reliably show that the protein was expressed in the full length constructs.

Possible reasons for this include:

- a) The stable clones do produce low levels of RNA and protein, but only the RNA is detected as reverse transcription is more sensitive than western blotting
- b) The antibody used in the western blot was non specific
- c) The stable clones expressed a low level of protein that was unable to be observed in the western blot
- d) The stable transfections switched off the expression of the protein

Stable transfections of 3T3 cells transfected with CD2-Plexin B1 were then examined by immunofluorescence. The results suggest that the stable transfections do not express Plexin B1.

Transient transfections of the truncated CD2-Plexin B1 in 3T3 cells and COS1 cells did show expression of the protein using the anti CD2 antibody. Wild type Plexin B1, mutant Plexin B1 and vector only constructs (containing CD2) showed membranous and nuclear staining indicating that the wild type and mutant express CD2-Plexin B1.

The issue with the transient transfections was a low transfection efficiency when using Lipofectamine, COS1 cells and 3T3 cells. This was overcome by optimizing the transfection efficiency using the *B-gal* staining kit and using COS7 cells which gave a better transfection efficiency.

Since the CD2 truncated construct did not have an extracellular domain, it would not be able to interact with other proteins such as Met, which may make the functional analysis difficult. For that reason the full length Plexin B1 would be more useful in the functional assays. During the optimisation of the immunofluorescence a commercial antibody for Plexin B1 became available, anti-Plexin B1 (#H300, Santa Cruz).

In the following chapter the protein expression of full length Plexin B1 is shown in transiently transfected COS7 cells.

In order to establish whether the semaphorin signalling pathway has any role in prostate cancer development or metastasis, an expression profile of components of this pathway in prostate cancer cells was performed. The endogenous mRNA expression of Plexin B1 and Sema4D in prostate cancer cell lines were studied using RT-PCR. Sema4D and Plexin B1 mRNA were expressed in these cell lines. The mRNA expression of Sema4D was altered in the PC3 cell line, this may be due to a splice variant of Sema4D in the metastatic cell line PC3.

## **Chapter 4**

### **The Collapse Assay**

## 4.1 Introduction

Semaphorins have a variety of functions from axon guidance where they were initially implicated to cardiac and skeletal development, immune function, morphogenesis and cancer progression.

The molecular mechanisms mediating semaphorin function are poorly understood. Recent studies suggest that Rho family small GTPases are involved in the downstream signalling of plexins (Etienne-Manneville et al. 2002). Rho family small GTPases are well known key regulators of the actin cytoskeleton in different cell types (Etienne-Manneville et al. 2002). Many Rho proteins have been identified including Rho (A,B, and C), Rac, Cdc42 and Rnd. Rho causes growth cone collapse (Negishi et al. 2002). Constitutively activated forms of Rho, Rac and Cdc42 induce the assembly of contractile actin and myosin filaments (stress fibres), actin-rich surface protrusions (lamellipodia), and finger-like membrane extensions (filopodia) respectively, when introduced into fibroblasts (Nobes and Hall, 1995).

Plexin B1 activates RhoA and induces growth cone collapse through PDZ-RhoGEF (Oinuma et al. 2003). Coexpression of Rnd and Plexin B1 induces cell contraction in COS7 cells in response to Semaphorin 4D (Oinuma et al. 2003). In dorsal root ganglia, Sema3A induced collapse has been shown to require Rac activity and Sema3A induced collapse of COS7 cells expressing Plexin A1 also requires Rac and Cdc42 activity (Turner et al. 2004).

The collapse assay is used as the standard functional assay for semaphorins and plexins (Barberis et al. 2004; Turner et al. 2004; Oinuma et al. 2004). In this study, the assay was used to determine whether the mutant Plexin B1 transiently transfected into COS7 cells behaved differently to the wild type Plexin B1 when activated by its ligand Semaphorin 4D. Semaphorin 4D was required for the collapse assay and this was purified from medium of Sema4D-Fc expressing COS7 cells. Oinuma et al. have shown that collapse in COS7 cells is dependent on Rnd1 and that collapse occurs after the addition of Sema4D. The morphology of the collapsed cell, is a rounded COS7 cell that has been defined as having an area of less than  $350\mu\text{m}^2$  (Oinuma et al. 2003). Using the same definition, a collapsed COS7 cell was defined as a cell with a surface area of less than  $350\mu\text{m}^2$  (Oinuma et al. 2003).

Protein expression of the truncated CD2 Plexin B1 has already been shown. There were initial difficulties showing the expression of full length Plexin B1 due to problems with antibodies. These problems were overcome once a suitable antibody became available.

## **4.2 Results**

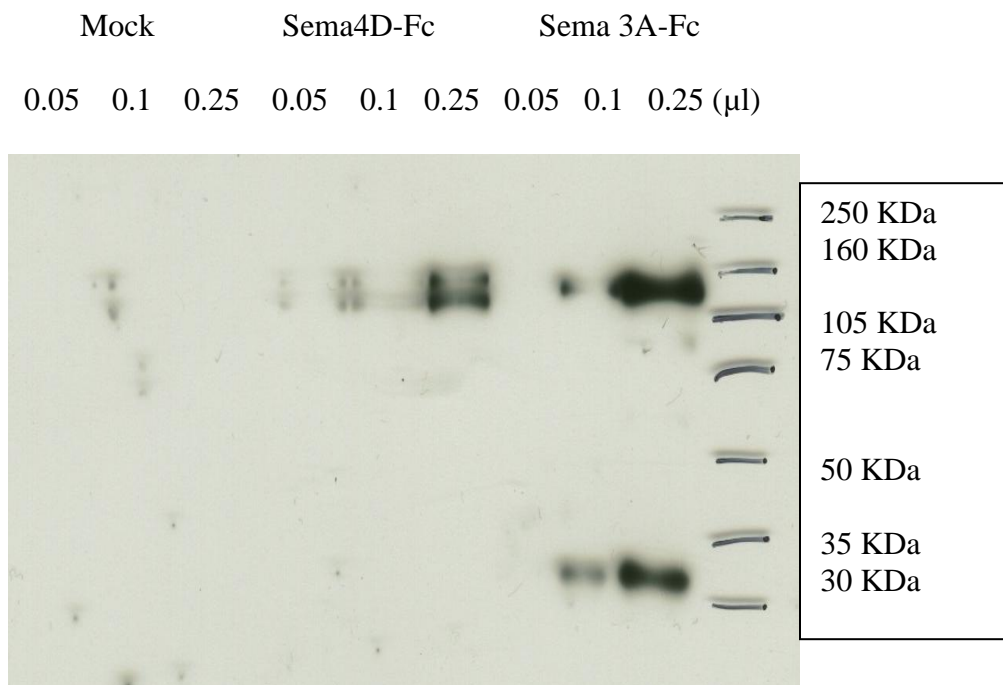
### **4.2.1 Purification of recombinant Sema 4D-Fc**

For the collapse assay a soluble form of Sema4D expressed as a fusion protein with the Fc fragment of human IgG was harvested from the medium of transiently transfected COS7 cells (see materials and methods). Purified Sema4D-Fc was run on an 8% SDS-PAGE gel with Sema3A-Fc. On western blot analysis, Sema3A-Fc (R&S systems) was known to produce two protein bands representing the full length Sema3A-Fc (130KDa) and the Fc fragment (35KDa) (Kumanogoh et al. 2001).

The Sema4D-Fc product showed a double band at around 150KDa compared to the 130KDa Sema3A-Fc product (Figure 4.1). The double band is likely to represent the precursor and a proteolytically cleaved form of Sema4D-Fc, as described by Turner et al. 2006. The full length Sema4D was 150KDa and a cleaved form of Sema4D which occurs at the transmembrane domain was 140KDa. The 35KDa band is the size of the Fc fragment alone (not shown for Sema4D). The concentration of purified Sema4D-Fc could be estimated from the known concentration of Sema3A-Fc (200µg/ml, R&D systems) by comparing the density of the western blot bands. The protein concentration of Sema4D-Fc was estimated to be 100µg/ml.



*Figure 4.1 Western Blot showing protein expression of Sema4D-Fc and Sema3A-Fc. Primary Antibody was goat anti-human IgG Fc Ab, 1:10000 (Jackson ImmunoResearch Laboratories); secondary antibody was mouse anti-goat, 1:5000 (Santa Cruz). Recombinant Sema4D-Fc was harvested from transiently transfected COS7 cells and purified using protein A as described previously. The purified Sema4D-Fc was run on an 8% SDS-PAGE gel. This showed a doublet band at 150KDa which represents the precursor and cleaved forms of Sema4D-Fc (Turner at al. 2006). The concentration of Sema4D was estimated by comparing the band brightness with the known concentration of Sema3A-Fc (200µg/ml).*



#### **4.2.2 Optimising the collapse assay**

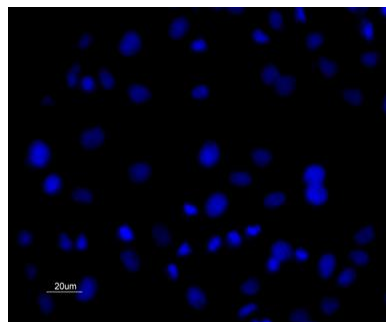
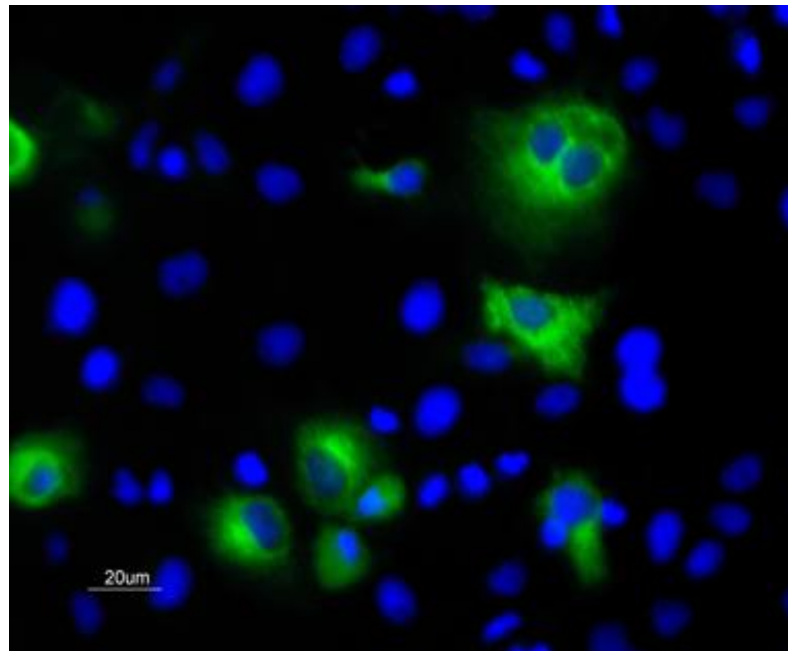
Using the purified Sema4D-Fc the next step was to optimize the conditions for the collapse assay. COS7 cells were used, when compared with NIH3T3 and COS1 cells they were found to give the highest transfection rates (Table 3.2). COS7 cells had been used for collapse assays by previous teams and they had successfully shown collapse on addition of Sema4D when transfected with Plexin B1 (Onuma et al. 2003, Turner et al. 2006).

COS7 cells were transiently transfected with Plexin B1, Sema4D was added and the percentage of collapsed cells scored. In the protocol set out by Turner et al. 2006, cells that were transfected with Plexin B1 could be detected using an antibody against the ligand Sema4D-Fc. The antibody used was against the Fc fragment of Sema4D-Fc (Jackson ImmunoResearch labs, PA). To optimize the immunocytochemistry conditions for detection of Sema4D, COS7 cells were transiently transfected with Sema4D-Fc and varying concentrations of the primary antibody (goat anti-human Fc) and the secondary antibody (mouse anti-goat) were used to detect the protein. The ideal concentration of the primary antibody was 20µg/ml.

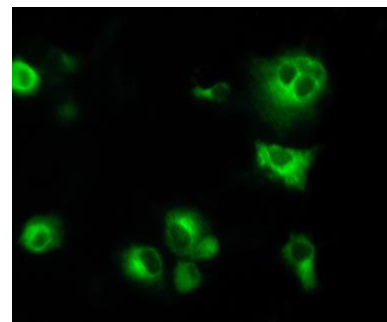
Figure 4.2 shows Sema4D expression in COS7 cells transfected with Sema4D-Fc with the addition of triton X. The staining seen is cytoplasmic and not membranous

since the addition of triton X permeabilises the cell membrane. Figure 4.3 shows COS7 cells transfected with Sema4D-Fc without triton X and the Sema4D is not detected indicating Sema4D is cytoplasmic.

*Figure 4.2 Sema4D expression in COS7 cells transfected with Sema4D-Fc (with Triton X). Primary antibody Goat anti-human Fc Ab 1:100, Secondary antibody mouse anti-goat FITC 1:200. When COS7 cells are transfected with Sema4D-Fc, intracytoplasmic Sema4D protein expression is seen. The larger picture is a merged image of the two smaller images (Dapi stained cells and antiFc-FITC stained cells). The cells were viewed using a fluorescent microscope (Nikon, C-SHG1 with epifluorescent attachment).*

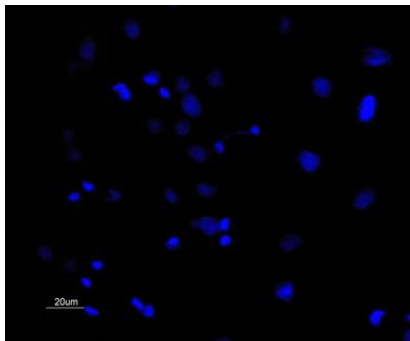
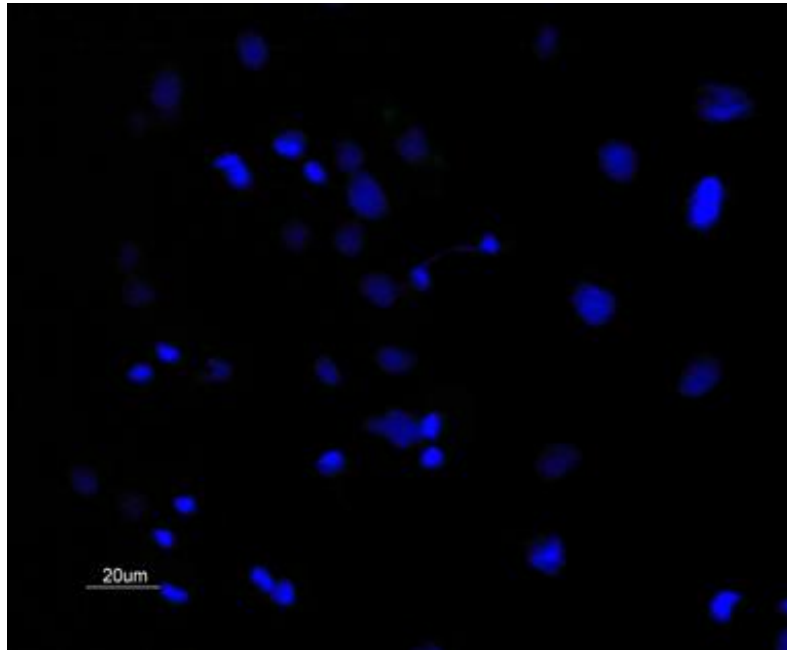


Dapi

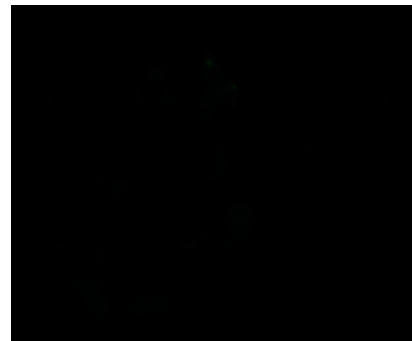


Sema4D-Fc

*Figure 4.3 COS7 cells transfected with Sema4D-Fc (no Triton X). Primary antibody Goat anti-human Fc Ab 1:100, Secondary antibody mouse anti-goat FITC 1:200. When COS7 cells are transfected with Sema4D-Fc and Triton X is not added, Sema4D protein expression is not detected. The larger picture is a merged image of the two smaller images (Dapi stained cells and antiFc-FITC stained cells). The cells were viewed using a fluorescent microscope (Nikon, C-SHG1 with epifluorescent attachment).*



Dapi



Sema4D-Fc

Despite showing intracellular protein expression of Sema4D in COS7 cells transfected with Sema4D-Fc, the addition of Sema4D-Fc protein to COS7 cells transfected with Plexin B1 did not highlight any cells (images not shown). Until this time, an antibody against Plexin B1 was not available and the method described above, of indirectly detecting Plexin B1 using Sema4D-Fc and the Fc antibody had to be abandoned. Therefore this method could not be used in the collapse assay.

An alternative method to identify which cells had been successfully transfected with Plexin B1, was to stain the cells with an antibody to the Plexin B1. The immunofluorescence technique using a rabbit polyclonal antibody against human Plexin B1 extracellular amino acids 771-1070 and a goat anti-rabbit IgG antibody conjugated to TRITC as the secondary antibody (Southern Biotech) was optimised. Using the newly acquired antibody for Plexin B1 (Plexin B1 H300 rabbit polyclonal, Santa Cruz), protein expression of full length Plexin B1 transfected in COS7 cells could be shown.

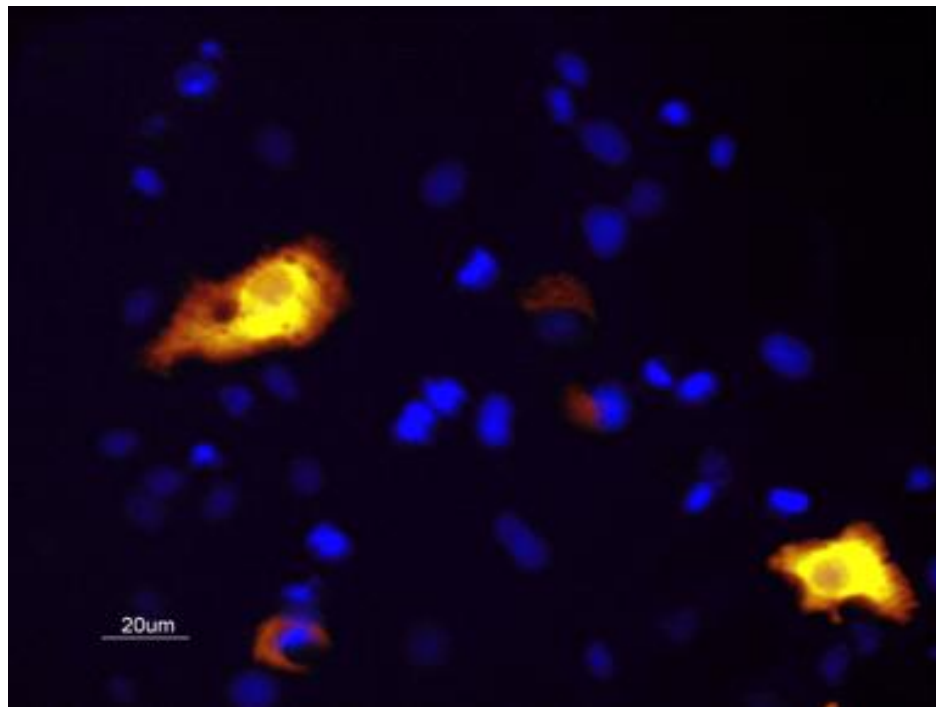
Figure 4.4 shows protein expression, in COS7 cells, of the wild type full length Plexin B1 (1° Ab Santa Cruz Plexin B1 rabbit polyclonal 1/200, 2° Ab Goat anti rabbit TRITC 1/100).

Plexin B1 is a cell surface receptor. In order to determine whether the mutant Plexin B1 was transported to the cell membrane, confocal images were obtained. With the

addition of Triton X, which permeabilises the cell membrane, cell surface expression of Plexin B1 could be seen. These images were generated using a confocal microscope (Zeiss LSM 510W upright confocal microscope).

Figure 4.5-4.6 show the expression of the wild type full length Plexin B1 and the mutant Plexin B1 in transfected COS7 cells. Cytoplasmic staining is seen with the addition of Triton X and membranous staining is seen without the Triton X.

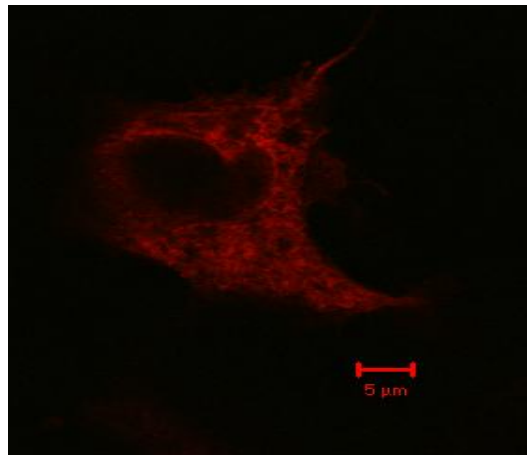
*Figure 4.4 Protein expression of Wild Type Full Length Plexin B1. Primary antibody Santa Cruz Plexin B1 rabbit polyclonal 1/200, secondary antibody Goat anti rabbit TRITC 1/100. Shows expression of wild type Plexin B1 in COS7 that have been transfected with wild type Plexin B1 (Dapi stained cells and anti-Plexin B1 stained cells). The cells were viewed using a fluorescent microscope (Nikon, C-SHG1 with epifluorescence attachment).*



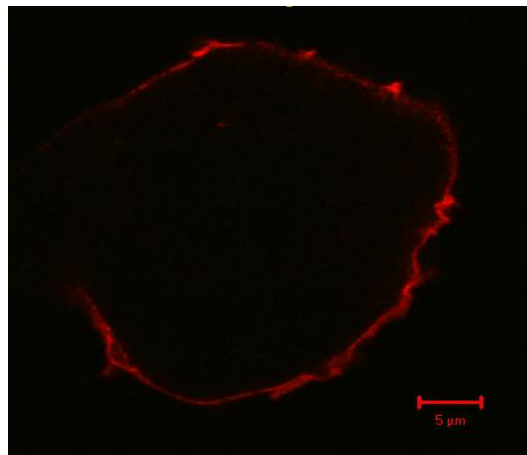


*Figure 4.5 Protein expression of wild type Plexin B1 (Confocal Image) a) with the addition of Triton X b) without Triton X. Primary antibody Santa Cruz Plexin B1 rabbit polyclonal 1/200, secondary antibody Goat anti rabbit TRITC 1/100. COS7 cells transfected with wild type Plexin B1, showing expression of wild type Plexin B1. Cytoplasmic staining is seen with the addition of Triton X. Membranous staining is seen without Triton X (Zeiss LSM 510W).*

a)

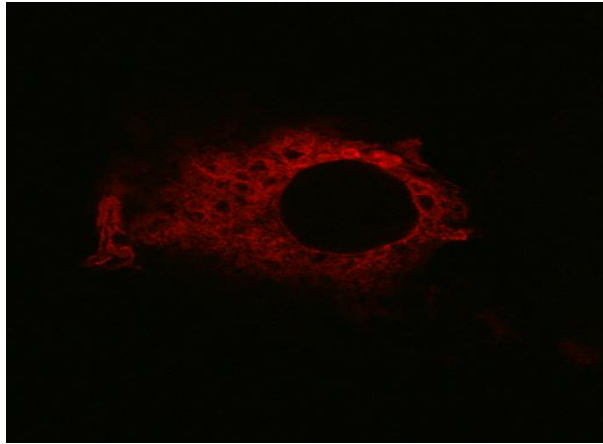


b)

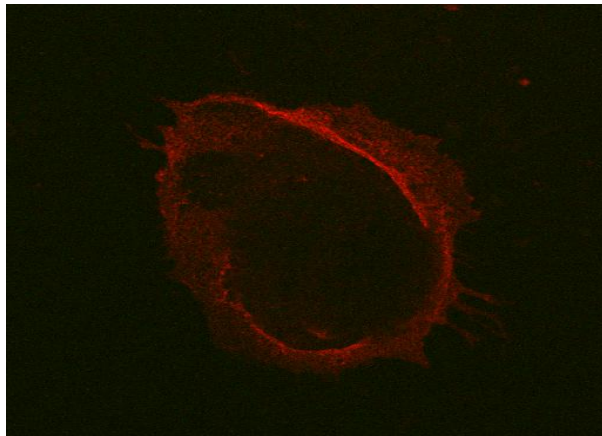


*Figure 4.6 Protein expression of mutant Plexin B1 (Confocal Image) a) with the addition of Triton X b) without Triton X. Primary antibody Santa Cruz Plexin B1 rabbit polyclonal 1/200, secondary antibody Goat anti rabbit TRITC 1/100. COS7 cells transfected with mutant Plexin B1, showing protein expression of mutant Plexin B1. Cytoplasmic staining is seen with the addition of Triton X. Membranous staining is seen without Triton X (Zeiss LSM 510W).*

a)



b)

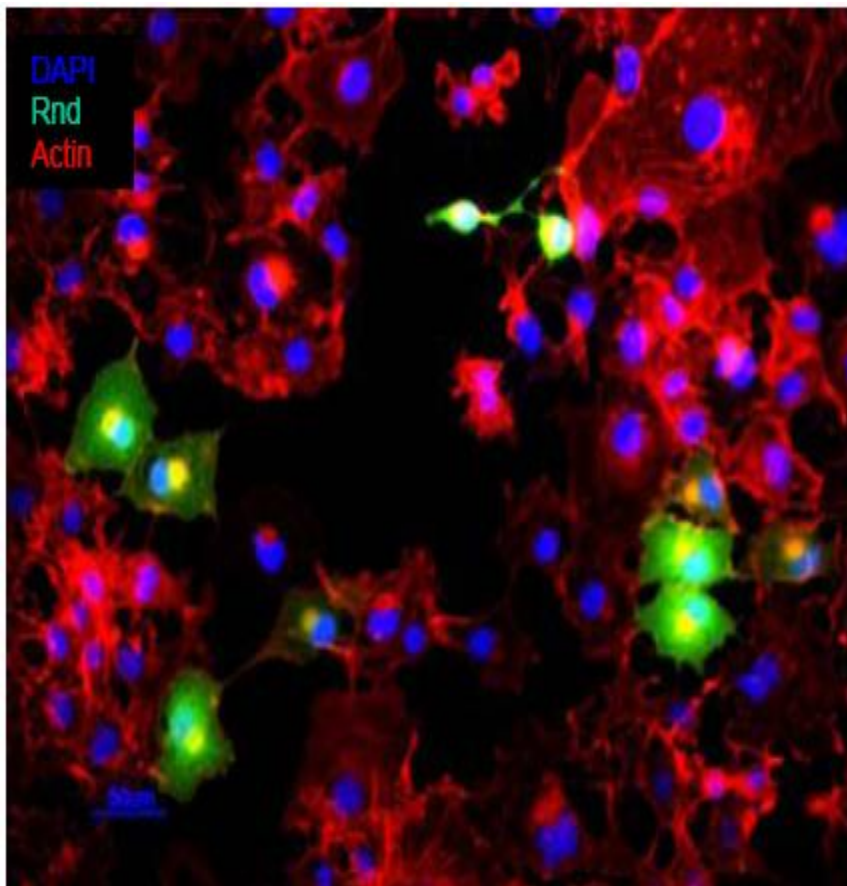


In 2003, Oinuma et al showed that Rnd 1, a member of the Rho family small GTPases, directly interacted with the cytoplasmic domain of Plexin B1 and that coexpression of Rnd1 and Plexin B1 induced cell contraction in COS7 cells in response to Sema4D. Expression of Plexin B1 alone or Rnd1 alone did not result in cell collapse (Oinuma et al. 2003).

To express Rnd1, Myc-Rnd1 was transfected into COS7 cells and using anti-myc antibodies and the appropriate secondary antibody, Rnd1 expression was shown using immunofluorescence. The optimal concentration for the anti-myc mouse monoclonal antibody (Santa Cruz) and for the secondary antibody, goat anti- mouse FITC antibody (Southern Biotech) was 5µg/ ml. Expression of Rnd1 was membranous and perinuclear (Figure 4.7).

The protein expression of the wild type and mutant full length Plexin B1 has now been shown using the newly acquired anti-Plexin B1 antibody. The protein expression of Rnd1 has also been shown in COS7 cells transfected with Myc-Rnd1 and stained using an anti-myc antibody. The next aim was to transfect COS7 cells with the full length Plexin B1 construct and add Sema4D-Fc and stain for Plexin B1 using the Plexin B1 (Santa Cruz) antibody and determine whether the cells collapse. If collapsed cells are seen then a comparison can be made between the wild type and the mutant constructs. The question as to whether Rnd1 is required for cell collapse would also need to be addressed.

*Figure 4.7 COS7 cells transfected with Rnd1 using Immunofluorescence. Anti-Myc 9E10 mouse monoclonal antibody, Santa Cruz (primary antibody), Goat anti-mouse FITC antibody, Southern Biotech (secondary antibody). When Rnd1 was transfected into COS7 cells membranous and perinuclear staining were seen. The cells were viewed using a fluorescent microscope (Nikon, C-SHG1 with epifluorescence attachment).*



### 4.2.3 The Collapse Assay

COS7 cells were transfected with either wild type Plexin B1 (WT) or mutant Plexin B1 (M) and cotransfected with Rnd1 or without Rnd1 and treated with and without Sema4D. The rabbit polyclonal antibody against Plexin B1, Santa Cruz (primary antibody) and goat anti-rabbit IgG antibody conjugated to TRITC (secondary antibody) were used for the immunofluorescence.

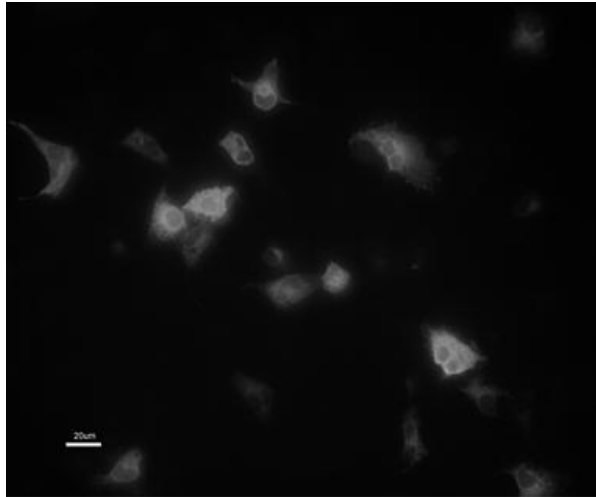
On initial inspection it appeared that cells transfected with Plexin B1 and Rnd1 (figs. 4.9, 4.11) appeared smaller and more rounded than cells transfected with Plexin B1 alone (figs. 4.8, 4.10). This suggested that when Plexin B1 and Rnd1 were cotransfected into COS7 cells, collapse was seen. It also appeared that Rnd1 and Plexin B1 were needed for the cells to collapse regardless of whether Sema4D was present or not.

Does this mean that Rnd1 alone is causing the collapse? According to Oinuma et al, 2003 this should not be the case.

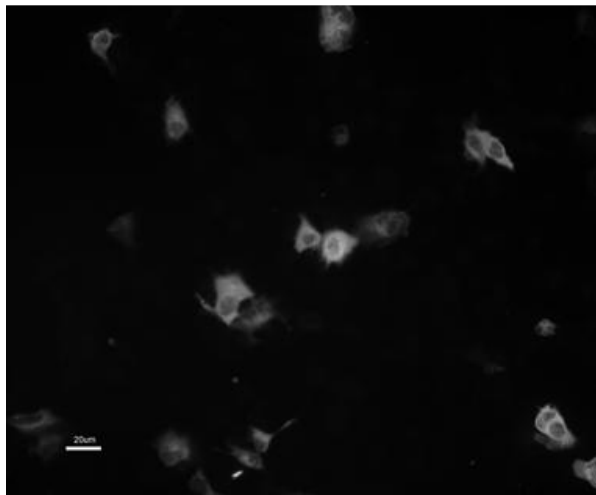
This was tested by transfecting COS7 cells with Rnd1 alone with and without Sema4D. Few cells collapsed, implying that both Rnd1 and Plexin B1 are required for cell collapse (figure 4.12). This data was objectively analysed using image j software that allowed the area of each cell to be calculated (figure 4.13).

*Figure 4.8 COS7 cells transfected with wild type Plexin B1 (without Rnd1) a) without Sema4D-Fc b) with Sema4D. Primary antibody Santa Cruz Plexin B1 rabbit polyclonal 1/200, secondary antibody Goat anti rabbit TRITC 1/100. Collapsed cells were counted as a percentage of the total number of transfected cells and are the mean of three independent experiments, with 50 cells sized per experiment. When COS7 cells were transfected with wild type Plexin B1 (no Rnd1) 15% of cells were collapsed (+/- SEM) when Sema4D was added and 10% (+/- SEM) collapsed without Sema4D.*

a)

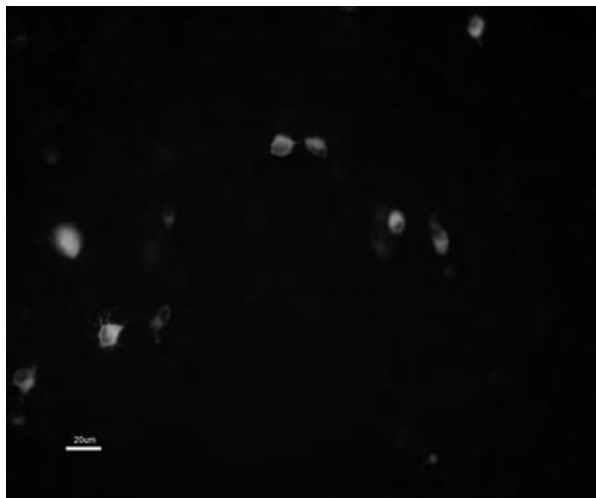


b)

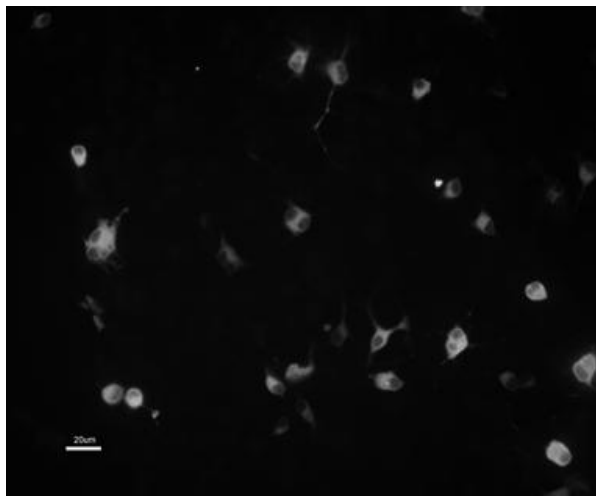


*Figure 4.9 COS7 cells cotransfected with wild type Plexin B1 and Rnd1 a) without Sema4D-Fc b) with Sema4D. Primary antibody santa cruz Plexin B1 rabbit polyclonal 1/200, secondary antibody Goat anti rabbit TRITC 1/100. Collapsed cells were counted as a percentage of the total number of transfected cells and are the mean of three independent experiments, with 50 cells sized per experiment. When COS7 cells were cotransfected with wild type Plexin B1 and Rnd1 82% of cells were collapsed (+/- SEM) when Sema4D was added and 79% (+/-SEM) collapsed without Sema4D.*

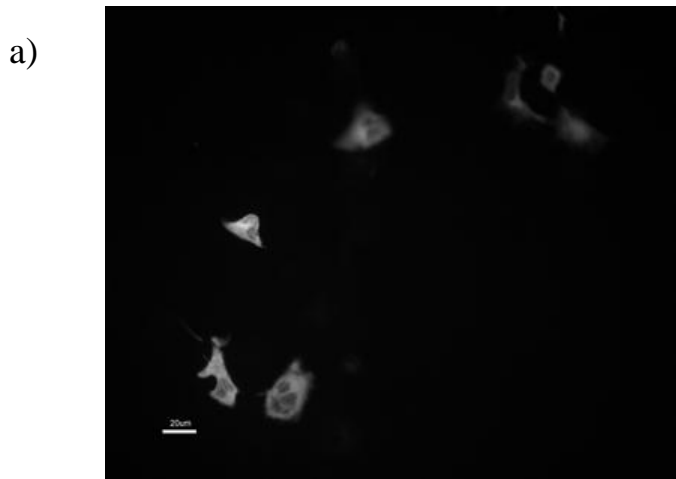
a)



b)

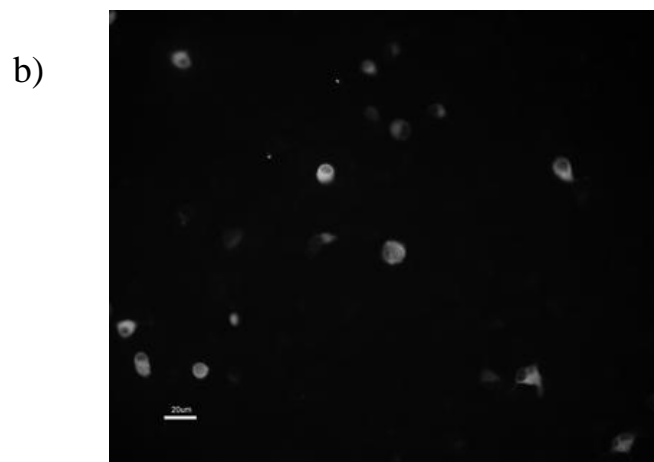
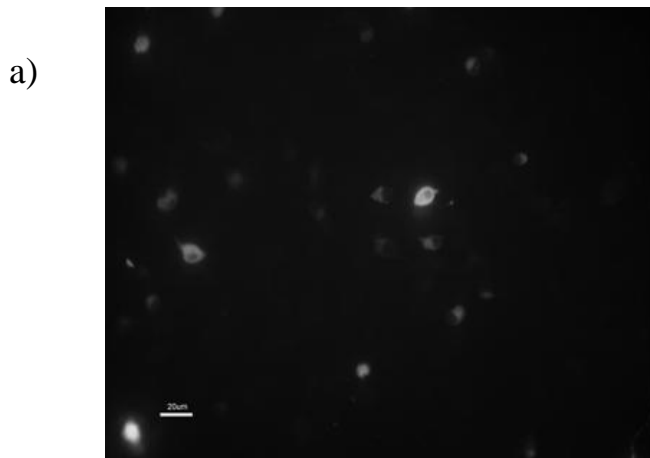


*Figure 4.10 COS7 cells transfected with Mutant Plexin B1 without Rnd1 a) without Sema4D-Fc b) with Sema4D. Primary antibody santa cruz Plexin B1 rabbit polyclonal 1/200, secondary antibody Goat anti rabbit TRITC 1/100. Collapsed cells were counted as a percentage of the total number of transfected cells and are the mean of three independent experiments, with 50 cells sized per experiment. When COS7 cells were transfected with Mutant Plexin B1 (no Rnd1) 21% of cells were collapsed (+/- SEM) when Sema4D was added and 11% (+/-SEM) collapsed without Sema4D.*



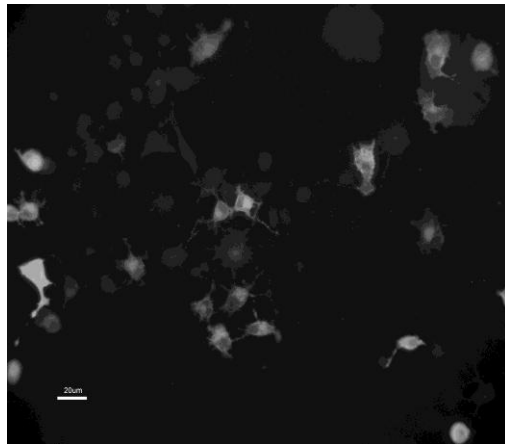


*Figure 4.11 COS7 cells cotransfected with Mutant Plexin B1 and Rnd1 a) without Sema4D-Fc b) with Sema4D. Primary antibody santa cruz Plexin B1 rabbit polyclonal 1/200, secondary antibody Goat anti rabbit TRITC 1/100. Collapsed cells were counted as a percentage of the total number of transfected cells and are the mean of three independent experiments, with 50 cells sized per experiment. When COS7 cells were cotransfected with Mutant Plexin B1 and Rnd1 72% (+/- SEM) were collapsed (+/- SEM) when Sema4D was added and 91% (+/-SEM) collapsed without Sema4D.*

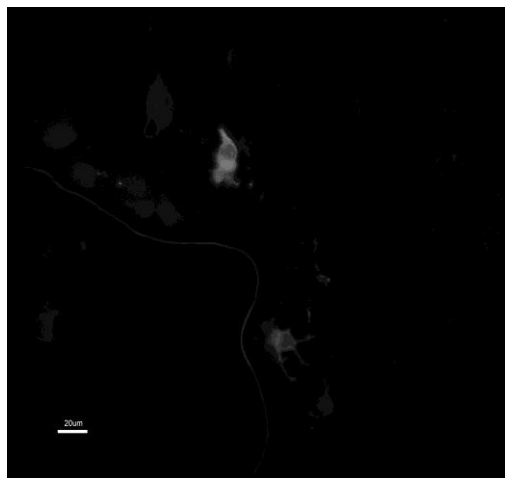


*Figure 4.12 COS7 cells transfected with Rnd1 a) with Sema4D-Fc b) without Sema4D-Fc. Anti-Myc 9E10 mouse monoclonal antibody, Santa Cruz (primary antibody), Goat anti-mouse FITC antibody, Southern Biotech (secondary antibody). Collapsed cells were counted as a percentage of the total number of transfected cells and are the mean of three independent experiments, with 50 cells sized per experiment. When COS7 cells were transfected with Rnd1 alone 18% of cells were collapsed (+/- SEM) when Sema4D was added and 6% (+/-SEM) collapsed without Sema4D.*

a)



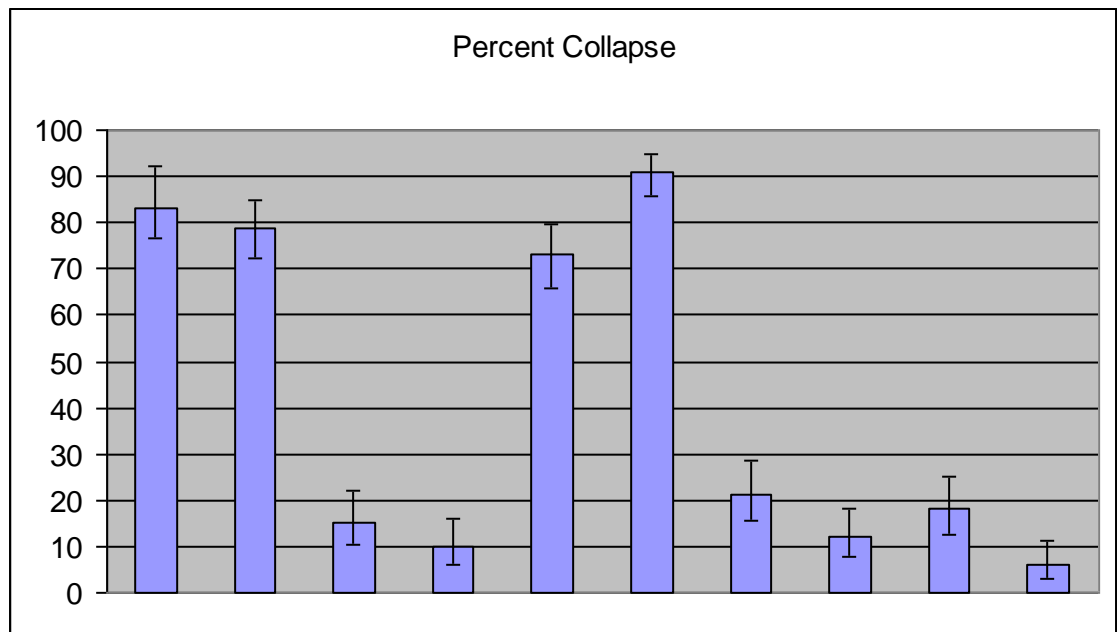
b)



Collapsed cells were defined as those with a surface area of less than  $350\mu\text{m}^2$  (Oinuma et al. 2003). The area of each cell was calculated by using Image J, version 1.38 (Image J\ plugins\Particle counting\Cell\_Area.txt). Using the image tool, transfected cells were drawn around. The area of the cells could then be analysed using the analysis tool, ensuring that the calibration had been controlled (Fig 4.14). Collapsed cells were counted as a percentage of the total number of transfected cells and the results are the mean of three independent experiments, with 50 cells sized per experiment. Figure 4.13 shows the percentage of transfected COS7 cells that were less than  $350\mu\text{m}^2$ . There is a clear increase in the proportion of collapsed cells in the wild type and mutant Plexin B1 constructs that had been cotransfected with Rnd1. The addition of the ligand Sema4D did not change the level of collapse. When COS7 cells were transfected with Rnd1 alone, the proportion of collapsed COS7 cells was small. This rate of collapse is similar to that described by Oinuma et al. 2003, with a background collapse rate of 10-20%.

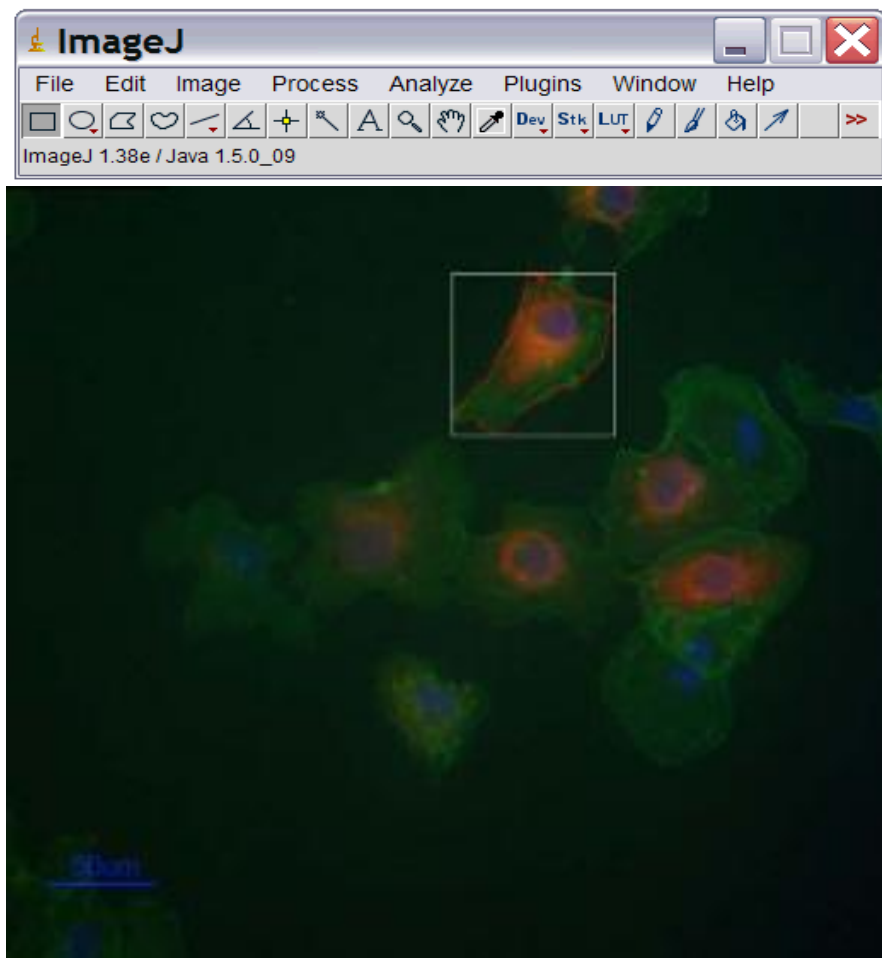
The Fishers exact test was used to analyse the statistical difference in collapse rate between the wild type Plexin B1 and the mutant Plexin B1 (both with Rnd1 and Sema4D). The two tailed 'p' value equals 0.0518, suggesting that the difference between the two is not statistically significant. There was not a significant difference in the collapse rate when comparing the wild type Plexin B1 to the mutant Plexin B1 (C5662T mutation) when the constructs were co-transfected with Rnd1 and treated with Sema4D.

Figure 4.13 Analysis of COS7 cell collapse (%). WT = wild type, M= Mutant. Quantative analysis of COS7 collapse. Collapsed cells (defined as  $<350\mu\text{m}^2$ ) were counted as a percentage of the total number of transfected cells and are the mean of three independent experiments (Error bars indicate standard error of mean, SEM), with 50 cells sized per experiment. There was not a significant difference in the collapse rate when comparing the wild type Plexin B1 to the mutant Plexin B1 (C5662T mutation),  $P=0.0518$  Fishers exact test. Collapse was not dependent on the addition of Semaphorin4D. Both Plexin B1 and Rnd1 are required for cell collapse.



Plexin B1	+(WT)	+(WT)	+(WT)	+(WT)	+(M)	+(M)	+(M)	+(M)	-	-
Rnd 1	+	+	-	-	+	+	-	-	+	+
Sema4D	+	-	+	-	+	-	+	-	+	-

Figure 4.14 COS 7 cells transfected with Plexin B1 and Rnd were sized using image J software. The white bordered area shows the area of interest. The red bordered area drawn around the cell is selected for in the free hand selection tool. This is the area that is calculated. Analyze>Set Scale was used to calibrate the image (using the tool bar below). The image is converted to grayscale (image>type>8-bit). The area of the outlined region is calculated (Analyze>Analyze particles). The Data window gives an area of 2460 $\mu\text{m}^2$ . The area of each cell was calculated individually.



### 4.3 Discussion

Semaphorins have mainly been studied for their ability to induce the retraction of axonal processes ie axonal collapse. This has been attributed to a turnover of actin filaments and microtubules (Kolodkin et al. 1993) and it has been postulated that semaphorins may similarly act to mediate retraction of pseudopodia of a migrating cell and affect its motility. The cellular mechanism mediating this function is not known. However a role for Rho GTPase has been proposed.

In 2003, Oinuma et al had shown that Rnd1, a member of the Rho family GTPases, interacted with the cytoplasmic domain of Plexin B1. In COS7 cells, coexpression of Rnd1 and Plexin B1 induced cell contraction in response to Semaphorin 4D. The association of Plexin B1 and Rnd1 seems to require PDZ Rho-GEF for this morphological effect (Oinuma et al. 2003). In COS7 cells the association of Rnd1 and Plexin B1 promotes the interaction between Plexin B1 and PDZ-RhoGEF. When Plexin B1 is activated, this results in cell contraction/collapse by activating RhoA which causes an increase in the contractile force at the cell surface (Oinuma et al. 2003).

The same authors have also found that the Plexin B1-Rnd1 complex stimulates GTPase activity of R-Ras in hippocampal neurons (Oinuma et al, 2004). R-Ras promotes cell adhesion and neurite outgrowth by activating integrins (Zhang at al.

1996; Ivins et al. 2000). More recently Oinuma et al, 2004 show that Rnd1 opens the two R-Ras GAP domains of Plexin B1, and Sema4D-induced receptor clustering stimulates R-Ras GAP activity and neurite remodelling in hippocampal neurons.

The results presented in these experiments confirm that Plexin B1 and Rnd 1 are required for COS7 cell collapse but this is independent of Sema4D suggesting that collapse in our experiment was ligand independent. This may be due to overexpression of Plexin B1 during transfection leading to clustering of Plexin B1 and activation. Giordano et al, 2002 have shown that liver progenitor cells overexpressing Plexin B1 demonstrate a ligand independent phenotype. It is speculated that overexpression of Plexin B1 causes clustering of the Plexin B1 receptor and this activates downstream regulators, mimicking Sema4D binding.

In contrast to the above experimental work, it is possible that instead of regulating cell migration via cytoskeletal dynamics, that plexins may act by directly impinging on cell adhesion to the extracellular matrix (Barberis et al, 2004). Barberis et al show that semaphorin stimulation rapidly induces disassembly of focal adhesive structures and of F-actin cables in adherent cells. Plexin activation inhibits cell adhesion, lamellipodia extension and cell migration.

It is likely that collapse is the net result of a combination of many pathways including Rho activation resulting in stress fibre formation and loss of adhesion,

resulting from disassembly of focal adhesive structures which include integrins. Loss of adhesion may be via the R-RasGAP activity of Plexin B1 (Ito et al. 2006). R-Ras activates integrins and promotes adhesion via PI3K (Kinbara et al. 2003). Plexin B1 acts as a GTPase-activating protein for R-Ras which inactivates R-Ras resulting in loss of integrin activation and loss of adhesion (Oinuma et al. 2006). Plexin B1 also binds and sequesters Rac thereby inactivating it, leading to loss of lamellipodia (Vikis et al. 2002).

It seems to be clear that semaphorins do regulate many biological events, including guidance of migrating cells, however the mechanisms mediating these have yet to be defined.

To determine whether a mutant form of Plexin B1 would behave differently from the wild type Plexin B1, the cell collapse assay was used. A collapsed COS7 cell in these experiments was defined as a cell with a surface area of less than 350 $\mu\text{m}^2$ . COS7 cells transfected with mutant Plexin B1 did not show any difference in the collapse rate when compared to the wild type Plexin B1. The C5662T mutation may not be functionally significant. The mutation C5662T is predicted to result in a substitution of a proline to a serine at position 1798. Amino acid 1798 is in the RhoGTPase binding domain (residues 1743–1862), this is required for Rac1, Rnd1 and RhoD binding (Tong et al. 2007). Therefore, the mutation would be expected to result in a loss of Rnd1 binding. However, from the results presented, it is speculated that the mutant binds to Rnd as collapse still occurs. It is possible that



Amino Acid 1798, although in the binding region, is not essential for binding. Further functional studies would be required to further evaluate this.

The COS7 cell collapse assay seems to be a useful method of investigating semaphorin function. However it does have its limitations. Semaphorin4D is a transmembrane protein and the recombinant protein used in this assay is a secretable form of the extracellular domain of this protein. Therefore the effects of this may cause a different response to that of the endogenous protein (Turner et al. 2006).

In conclusion, activation of wild-type Plexin B1 causes COS7 cell collapse but this is independent of Sema4D and requires Rnd1. A mutant form of Plexin B1 does not change the rate of COS7 cell collapse.

## **Chapter 5**

### **Discussion and future work**

Initially when the cytoplasmic domain and part of the extracellular domain (exons 1-5) of Plexins A1, A3 and B1 were sequenced using cDNA from the human prostate cancer cell lines PC3, DU145 and LNCaP a single nucleotide change (A5359G) was found in Plexin B1 in LNCaP. LNCaP was derived from a patient of Caucasian origin and the sequence change was absent from the DNA of 60 control individuals (Wong et al. 2007). The rest of the Plexin B1 cDNA was sequenced in PC3, DU145 and LNCAP and no further mutations were found. Quantitative RT-PCR showed high levels of Plexin B1 in LNCaP compared to other prostate cancer cell lines (Personal communication M. Williamson).

The mRNA expression was determined in a number of prostate cell lines. It was shown that Semaphorin 4D and Plexin B1 mRNA were expressed in all normal and prostate cancer cell lines. The expression profile of Plexin B1 was initially shown in the nervous system (Winberg et al. 1998). Although best characterised in the nervous system, plexins are widely expressed in other tissues. Using in situ hybridization, Plexin B1 is expressed in the immature glomeruli and mesenchyme of the developing kidney. In the tooth bud, Plexin B1 is expressed in the oral epithelium, enamel knot and in both the inner and outer enamel epithelium. In the testis, Plexin B1 is expressed in the developing sex chords (Perala et al. 2005). On Northern blot analysis, Semaphorin 4D, is expressed in haematopoietic and nonhaematopoietic tissues. Sema4D transcript is detected in peripheral blood lymphocytes, spleen, thymus and skeletal muscle and is present in testes, brain, kidney, small intestine, prostate, heart, placenta, lung and pancreas, but not in colon

or liver (Delaire et al. 1998). Semaphorin 4D is highly expressed in cell lines derived from head and neck squamous cell carcinomas, a similar result is also seen in prostate, colon, breast and lung cancer tissues (Basile et al. 2006).

To look for further mutations, the study was extended using SSCP analysis of exons 22-29 of the cytoplasmic domain of the Plexin B1 gene in DNA microdissected from eighty nine primary prostate tumours treated by radical prostatectomy, seventeen lymph node metastases and nine prostate cancer bone metastases. Twelve further missense mutations were found. Mutations were present in 89% (8/9) of prostate cancer bone metastases, in 41% (7/17) of lymph node metastases and in 46% (41/89) of primary cancers. Over 40% of prostate cancers contained the same mutation (Wong et al. 2007). The mutations found in Plexin B1 might contribute to the pathogenesis of prostate cancer or they could simply be passenger mutations which occur by chance and are not selected for. The data suggested that cells carrying mutated Plexin B1 are selected for during prostate cancer metastasis. It was therefore hypothesised that the semaphorin signalling pathway might be harnessed by the cancer cell during metastasis.

To determine whether these mutations were functionally significant, one of the mutations was studied in more detail. The aim was to determine if the C5662T mutation altered the function of the protein. The C5662T mutation is predicted to result in a substitution of a proline to a serine at position 1798. This mutation was found in 1/9 prostate cancer metastases. The amino acid, at position 1798 is highly

conserved in evolution. A proline is present in the protein in mouse, *Drosophila* and *C. elegans* and other classes of the Plexin family- A1, A2, B2, B3.

Three objectives were originally set. Using primers containing the point mutation, the altered sequence would be introduced into the wild type gene. The altered construct would be used to transform *E. coli*. and colonies selected, grown up and the identity of the mutation be confirmed by direct sequencing.

The mutation would then be transfected into suitable cells. Transfected cells would be selected in G418 and individual colonies expanded and frozen stocks produced. The presence of the mutation would be confirmed and the level of protein expression measured by western blotting and immunofluorescence.

In vitro assays would be used to assess the effect of the mutation on the behaviour of cells. It was not known which components of the semaphorin signalling pathway would be affected by the mutation.

The work in this thesis has achieved a number of the objectives that were originally set out. An expression vector containing the mutation had been constructed using the full length Plexin B1 and the truncated CD2 Plexin B1. This was done using a process of in-vitro mutagenesis of the wild type Plexin B1.

Before using the vector, the presence of the mutation was confirmed using restriction enzyme analysis and direct sequencing. The mutant, wild type and vector constructs were then transfected into suitable cells using lipofectamine. Transient transfections and stable transfections were used. Transfected cells were selected in G418 and individual colonies were expanded and frozen stocks produced. The presence of the mutation was confirmed again using restriction enzyme analysis and cycle sequencing. The whole of the cytoplasmic domain of Plexin B1 was also sequenced to confirm the presence of the mutation and that no new mutations had been introduced.

The relative expression of Plexin B1 mRNA was measured using clones stored at -80°C. RNA was extracted and cDNA synthesis performed with and without superscript II. This showed that there was strong expression in all of the mutant and most of the wild type clones.

With western blotting, protein expression was not shown and this was likely to be due to a non-specific antibody and therefore attention was turned towards immunofluorescence. This confirmed protein expression in the transiently transfected cells but not in the stable transfections.

To determine the effect of the mutation the collapse assay was used, this has become the standard assay to assess Plexin B1 function. Plexin B1 is the receptor for Semaphorin 4D, and for the functional assays it was necessary to produce

recombinant Semaphorin 4D. Recombinant Sema4D-Fc was produced and purified. It was not known which components of the semaphorin signalling pathway will be affected by the mutation. It was possible to show that Plexin B1 is involved in cell collapse and that Rnd1 is required for this process. Cell collapse was seen in cells expressing the wild type and mutant Plexin B1. I have been unable to show a functional difference between the wild type Plexin B1 and the mutant (C5662T). This suggested that the mutant Plexin B1 does not affect the collapse response and more work in the future will be needed to define whether this is a significant mutation. This work has been continued by scientists in the same lab. Using the collapse assay, the other mutations that were originally found are being assessed and other functional assays are being optimized.

So far, some of the mutations that have been tested have been shown to alter the function of the Plexin B1 protein and result in increased cell motility, adhesion and decrease cell collapse when compared with the wild type (Wong et al. 2007). These results suggest a role for Plexin B1 in prostate cancer progression. The mutations are unlikely to affect the pathways mediated by c-MET and ErbB2, as these proteins interact with the extracellular domain of Plexin B1 and the mutations are in the cytoplasmic domain. The mutations may inhibit Plexin B1 inhibitory pathways via R-Ras and Rac resulting in an increase in adhesion, motility and invasion (Wong et al. 2007).

The mutation, C5662T, may affect one or more of the many signalling pathways downstream of Plexin B1 via Rho, R-Ras or Rac and it may affect cell migration, cell adhesion or cell spread. This could be determined by Rho activity assays, R-Ras GAP activity assays, Rac binding, lamellipodia formation and adhesion experiments using the vector constructed in this work.

An understanding of the role of the Plexin B1 mutations in cancer may provide insight into the role of semaphorin signalling in cancer progression and these studies may facilitate the design of anti-cancer therapies to target this pathway with the aim of delaying or preventing the progression of prostate cancer. Currently, prostate specific antigen (PSA) is used to diagnose and manage prostate cancer. However, the PSA is unable to differentiate the prostate cancers that have a high metastatic potential and therefore are potentially incurable. Identifying a Plexin B1 mutation in patients when they are diagnosed with prostate cancer, may allow us determine those patients that have slow progressing prostate cancer and those that have aggressive disease.

In conclusion, a high frequency of somatic missense mutations in the Plexin B1 gene in localized and metastatic prostate cancer have been found. The C5662T mutation in Plexin B1 does not alter cell collapse, but a number of the mutations have been found to alter the function of the Plexin B1 protein, suggesting that Plexin B1 mutations are functionally significant. The resources that were generated during this research, mutant (C5662T), wild type and vector constructs of truncated



and full-length Plexin B1, recombinant Semaphorin 4D, are being used for further investigations to see if Plexin B1 is a key player in the progression of prostate cancer.

## REFERENCES

Alexander EE, Qian J, Wollan PC, Myers RP, Bostwick DG. Prostatic intraepithelial neoplasia does not appear to raise serum prostate-specific antigen concentration. *Urology* 1996;47(5):693-8.

Antipenko A, Himanen JP, van Leyen K, Nardi-Dei V, Lesniak J, Barton WA et al. Structure of the semaphorin-3A receptor binding module. *Neuron* 2003;39(4):589-598.

Argast GM, Croy CH, Coutts KL, Zhang Z et al. Plexin B1 is repressed by oncogenic B-Raf signaling and functions as a tumor suppressor in melanoma cells. *Oncogene*. 2009;28(30):2697-709.

Artigiani S, Barberis D, Fazzari P, Longati P, Angelini P, van de Loo JW, Comoglio PM, Tamagnone L. Functional regulation of semaphorin receptors by proprotein convertases. *J Biol Chem*. 2003;278:10094-101.

Artigiani S, Comoglio PM, Tamagnone L. Plexins, semaphorins, and scatter factor receptors: a common root for cell guidance signals? *IUBMB Life* 1999;48(5):477-82.

Aurandt J, Vikis HG, Gutkind JS, Ahn N, Guan KL. The semaphorin receptor plexin-B1 signals through a direct interaction with the Rho-specific nucleotide exchange factor, LARG. *Proc Natl Acad Sci U S A* 2002;99(19):12085-90.

Barberis D, Artigiani S, Casazza A, Corso S, Giordano S, Love CA, Jones EY, Comoglio PM, Tamagnone L. Plexin signaling hampers integrin-based adhesion, leading to Rho-kinase independent cell rounding, and inhibiting lamellipodia extension and cell motility. *FASEB J.* 2004;18(3):592-4.

Basile JR, Castilho RM, Williams VP, Gutkind JS. Semaphorin 4D provides a link between axon guidance processes and tumor induced angiogenesis. *Proc Natl Acad Sci USA* 2006;103(24):9017-9022.

Basile JR, Gavard J, Gutkind JS. Plexin-B1 utilizes RHOA and ROK to promote the integrin-dependent activation of AKT and ERK, and endothelial cell motility. *J Biol Chem* 2007;282(48):34888-95.

Behar O, Golden JA, Mashimo H, Schoen FJ, Fishman MC. Semaphorin III is needed for normal patterning and growth of nerves, bones and heart. *Nature* 1996;383(6600):525-8.

Bergers G, Benjamin LE. Tumorigenesis and the angiogenic switch. *Nat Rev Cancer* 2003;3(6):401-10.

Berget S, Moore C, Sharp P. Spliced segments at the 5' terminus of adenovirus 2 late mRNA. *Proc Natl Acad Sci U S A.* 1977;74(8):3171–3175.

Black D. Mechanisms of alternative pre-messenger RNA splicing. *Annual Review of Biochemistry* 2003;72:291-336.

Bork P, Doerks T, Springer TA, Snel B. Domains in plexins: links to integrins and transcription factors. *Trends Biochem Sci.* 1999;24(7):261-3.

Brambilla E, Constantin B, Drabkin H, Roche J. Semaphorin SEMA3F localization in malignant human lung and cell lines: A suggested role in cell adhesion and cell migration. *Am J Pathol.* 2000;156(3):939-50.

Bratt O. Hereditary prostate cancer: clinical aspects. *J of Urology* 2002;168(3):906-913.

Buckwalter JA, Brandser EA. Metastatic disease of the skeleton. *Am Fam Physician* 1997;55(5):1761-8.

Butler TP, Gullino P. Quantitation of cell shedding into efferent blood vessels of mammary adenocarcinoma. *Cancer Res.* 1975;35:512-6.

Cancer research UK. Prostate Cancer statistics, Internet communication.  
www.cancerresearchuk.org

Carter HB, Coffey DS. The prostate: an increasing medical problem. *Prostate* 1990;16(1):39-48.

Chamberlain J, Melia J, Moss S, Brown J. The diagnosis, management, treatment and costs of prostate cancer in England and Wales. *Health Technol Assess.* 1997;1(3):1-53.

Christensen C, Ambartsumian N, Gilestro G, Thomsen B et al. Proteolytic processing converts the repelling signal Sema3E into an inducer of invasive growth and lung metastasis. *Cancer Res.* 2005;65(14):6167-77.

Christensen CR, Klingelhofer J, Tarabykina S, Hulgaard EF, Kramerov D, Lukanidin E. Transcription of a novel mouse semaphorin gene, M-semaH, correlates with the metastatic ability of mouse tumor cell lines. *Cancer Res.* 1998;58(6):1238-44.

Comoglio PM, Trusolino L. Invasive growth: from development to metastasis. *J Clin Invest.* 2002;109(7):857-62.

Conrotto P, Valdembri D, Corso S, Serini G, Tamagnone L, Comoglio PM et al. Sema4D induces angiogenesis through Met recruitment by Plexin B1. *Blood* 2005;105(11):4321-9.

Delaire S, Elhabazi A, Bensussan A, Boumsell L. CD100 is a leukocyte semaphorin. *CMLS, Cell. Mol. Life Sci.* 1998;1265–1276.

Deng S, Hirschberg A, Worzfeld T, Penachioni JY et al. Plexin-B2, but not Plexin-B1, critically modulates neuronal migration and patterning of the developing nervous system in vivo. *J Neurosci.* 2007;27(23):6333-47.

Dickson BJ. Rho GTPases in growth cone guidance. *Curr Opin Neurobiol.* 2001;11(1):103-10.

Driessens MH, Hu H, Nobes CD, Self A, Jordens I, Goodman CS, Hall A. Plexin-B semaphorin receptors interact directly with active Rac and regulate the actin cytoskeleton by activating Rho. *Curr Biol.* 2001;11(5):339-44.

Driessens MH, Olivo C, Nagata K, Inagaki M, Collard JG. B plexins activate Rho through PDZ-RhoGEF. *FEBS Lett.* 2002;529:168-72.

Elhabazi A, Marie-Cardine A, Chabbert-de Ponnat I, Bensussan A, Boumsell L. Structure and function of the immune semaphorin CD100/SEMA4D. *Crit Rev Immunol*. 2003;23:65-81.

Epstein JI, Partin AW, Sauvageot J, Walsh PC. Prediction of progression following radical prostatectomy. A multivariate analysis of 721 men with long-term follow-up. *Am J Surg Pathol*. 1996;20(3):286-92.

Esper P, Redman BG. Supportive care, pain management, and quality of life in advanced prostate cancer. *Urol Clin North Am*. 1999;26(2):375-89.

Etienne-Manneville S, Hall A. Rho GTPases in cell biology. *Nature* 2002;420(6916):629-35.

Ewing, J. Neoplastic diseases; a treatise on tumors. 4<sup>th</sup> ed., rev. and enl. Philadelphia, W.B. Saunders, 1940.

Feiner L, Koppel AM, Kobayashi H, Raper JA. Secreted chick semaphorins bind recombinant neuropilin with similar affinities but bind different subsets of neurons in situ. *Neuron* 1997;19(3):539-45.

Fidler IJ, Nicolson GL. Organ selectivity for implantation survival and growth of B16 melanoma variant tumor lines. *J Natl Cancer Inst*. 1976;57:1199-1202.

Fidler IJ. Modulation of the organ microenvironment for treatment of cancer metastasis. *J Natl Cancer Inst.* 1995;87(21):1588-92.

Franklin MC, Carey KD, Vajdos FF, Leahy DJ, de Vos AM, Sliwkowski MX. Insights into ErbB signaling from the structure of the ErbB2-pertuzumab complex. *Cancer Cell* 2004;5(4):317-28.

Giger RJ, Urquhart ER, Gillespie SK, Levengood DV, Ginty DD, Kolodkin AL. Neuropilin-2 is a receptor for semaphorin IV: insight into the structural basis of receptor function and specificity. *Neuron.* 1998;21(5):1079-92.

Gillenwater JY. *Adult and Pediatric Urology.* 4<sup>th</sup> Edition . Vol. 2; Chapter 33:1477-1479.

Giordano S, Corso S, Conrotto P, Artigiani S, Gilestro G, Barberis D, Tamagnone L, Comoglio PM. The semaphorin 4D receptor controls invasive growth by coupling with Met. *Nat Cell Biol.* 2002;4(9):720-4.

Giordano S, Ponzetto C, Di Renzo MF, Cooper CS, Comoglio PM. Tyrosine kinase receptor indistinguishable from the c-met protein. *Nature* 1989;339(6220):155-6.

Gittes RF. Carcinoma of the prostate. *N Engl J Med.* 1991;324(4):236-45.



Gleason DF, Mellinger GT. Prediction of prognosis for prostate adenocarcinoma by combined histological grading and clinical staging. *J Urol.* 1974;111:58-64.

Gleason DF. Histologic grading of prostate cancer: a perspective. *Hum Pathol.* 1992;23:273-9.

Green GA, Hanlon AL, Al-Saleem T, Hanks GE. A Gleason score of 7 predicts a worse outcome for prostate carcinoma patients treated with radiotherapy. *Cancer.* 1998;83(5):971-6.

Gronberg H. Prostate cancer epidemiology. *Lancet* 2003;361(9360):859-864.

Hage WD, Aboulaflia AJ, Aboulaflia DM. Incidence, location, and diagnostic evaluation of metastatic bone disease. *Orthop Clin North Am.* 2000;31(4):515-28.

Hall A. Rho GTPases and the actin cytoskeleton. *Science.* 1998;279(5350):509- 14.

Hall KT, Boumsell L, Schultze JL, Boussiotis VA, Dorfman DM, Cardoso AA, Bensussan A, Nadler LM, Freeman GJ. Human CD100, a novel leukocyte semaphorin that promotes B-cell aggregation and differentiation. *Proc Natl Acad Sci U S A* 1996;93(21):11780-5.

Hill PB, Wynder EL. Effect of a vegetarian diet and dexamethasone on plasma prolactin, testosterone and dehydroepiandrosterone in men and women. *Cancer Lett.* 1979;7(5):273-82.

Holleb AI, Folkman J. Tumor angiogenesis. *CA Cancer J Clin.* 1972;22(4):226-9.

Horoszewicz JS, Leong SS, Kawinski E, Karr JP, Rosenthal H, Chu TM et al. LNCaP model of human prostatic carcinoma. *Cancer Res* 1983;43(4):1809-1818.

Housseau F, Bright RK, Simonis T, Nishimura MI, Topalian SL. Recognition of a shared human prostate cancer-associated antigen by nonclassical MHC-restricted CD8<sup>+</sup> T cells. *J Immunol* 1999;163(11):6330-6337.

Hsing A, Tsao L, Devesa S. International trends and patterns of prostate cancer incidence and mortality. *International Journal of cancer* 2000;85:60-67.

Hynes RO. Integrins: bidirectional, allosteric signaling machines. *Cell* 2002;110(6):673-87.

Ito Y, Oinuma I, Katoh H, Kaibuchi K, Negishi M. Sema4D/plexin-B1 activates GSK-3 $\beta$  through R-Ras GAP activity, inducing growth cone collapse. *EMBO Rep* 2006; 7(7):704-709.

Ivins JK, Yurchenco PD, Lander AD. Regulation of neurite outgrowth by integrin activation. *J Neurosci.* 2000;20(17):6551-60.

Jainchill JL, Aaronson SA, Todaro GJ. Murine sarcoma and leukemia viruses: assay using clonal lines of contact-inhibited mouse cells. *J Virol* 1969;4(5):549-553.

Jensen FC, Giardi AJ, Gilden RV, Koprowski H. Infection of human and simian tissue cultures with rous sarcoma virus. *PNAS* 1964;52:53-59.

Kaighn ME, Narayan KS, Ohnuki Y, Lechner JF, Jones LW. Establishment and characterization of a human prostatic carcinoma cell line (PC-3). *Invest Urol* 1979;17(1):16-23.

Kamoi K, Troncoso P, Babaian RJ. Strategy for repeat biopsy in patients with high grade prostatic intraepithelial neoplasia. *J Urol.* 2000;163(3):819-23.

Keetch DW, Humphrey P, Stahl D, Smith DS, Catalona WJ. Morphometric analysis and clinical followup of isolated prostatic intraepithelial neoplasia in needle biopsy of the prostate. *J Urol.* 1995;154:347-51.

Kigel B, Varshavsky A, Kessler O, Neufeld G. Successful inhibition of tumor development by specific class-3 semaphorins is associated with expression of appropriate semaphorin receptors by tumor cells. *PLoS One.* 2003;(9):3287.

Kinbara K, Goldfinger LE, Hansen M et al. Ras GTPases: integrins' friends or foes?  
Nat Rev Mol Cell Biol. 2003;4(10):767-76.

Kim KJ, Li B, Winer J, Armanini M, Gillet N, Phillips HS, Ferrara N. Inhibition of  
vascular endothelial growth factor-induced angiogenesis suppresses tumour growth  
in vivo. Nature 1993;362:841-844.

Kolodkin AL, Levensgood DV, Rowe EG, Tai YT, Giger RJ, Ginty DD. Neuropilin  
is a semaphorin III receptor. Cell 1997;90(4):753-62.

Kolodkin AL, Ginty DD. Steering clear of semaphorins: neuropilins sound the  
retreat. Neuron 1997;19(6):1159-62.

Kolodkin AL, Matthes DJ, Goodman CS. The semaphorin genes encode a family of  
transmembrane and secreted growth cone guidance molecules. Cell  
1993;75(7):1389-1399.

Kolodkin AL, Matthes DJ, O'Connor TP, Patel NH, Admon A, Bentley D,  
Goodman CS. Fasciclin IV: sequence, expression, and function during growth cone  
guidance in the grasshopper embryo. Neuron 1992;9(5):831-45.

Kong-Beltran M, Stamos J, Wickramasinghe D. The Sema domain of Met is necessary for receptor dimerization and activation. *Cancer Cell* 2004;6(1):75-84.

Korostylev A, Worzfeld T, Deng S, Friedel RH, Swiercz JM, Vodrazka P et al. A functional role for semaphoring 4D/plexin B1 interactions in epithelial branching morphogenesis during organogenesis. *Development* 2008;135(20):3333-3343.

Kourlas PJ, Strout MP, Becknell B, Veronese ML, Croce CM, Theil KS, Krahe R, Ruutu T, Knuutila S, Bloomfield CD, Caligiuri MA. Identification of a gene at 11q23 encoding a guanine nucleotide exchange factor: evidence for its fusion with MLL in acute myeloid leukemia. *Proc Natl Acad Sci U S A* 2000;97(5):2145-50.

Kruger RP, Aurandt J, Guan KL. Semaphorins command cells to move. *Nat Rev Mol Cell Biol.* 2005;6(10):689-800.

Kumanogoh A, Kikutani H. The CD100-CD72 interaction: a novel mechanism of immune regulation. *Trends Immunol.* 2001;22(12):670-6.

Langer JE, Rovner ES, Coleman BG, Yin D, Arger PH, Malkowicz SB, Nisenbaum HL, Rowling SE, Tomaszewski JE, Wein AJ, Jacobs JE. Strategy for repeat biopsy of patients with prostatic intraepithelial neoplasia detected by prostate needle biopsy. *J Urol.* 1996;155(1):228-31.

Lippman SM, Klein EA, Goodman PJ, Lucia MS, Thompson IM, Ford LG, Parnes HL, Minasian LM et al. Effect of selenium and vitamin E on risk of prostate cancer and other cancers: the Selenium and Vitamin E Prevention Trial. *JAMA* 2009;301(1):39-51.

Liotta LA. An attractive force in metastasis. *Nature* 2001;410(6824):24-5.

Love CA, Harlos K, Mavaddat N, Davis SJ, Stuart DI, Jones EY, Esnouf RM. The ligand-binding face of the semaphorins revealed by the high-resolution crystal structure of SEMA4D. *Nat Struct Biol.* 2003;10(10):843-8.

Luo Y, Raible D, Raper JA. Collapsin: a protein in brain that induces the collapse and paralysis of neuronal growth cones. *Cell* 1993;75(2):217-27.

Mackay DJ, Hall A. Rho GTPases. *J Biol Chem.* 1998;273(33):20685-8.

Maestrini E, Tamagnone L, Longati P, Cremona O, Gulisano M, Bione S, Tamanini F, Neel BG, Toniolo D, Comoglio PM. A family of transmembrane proteins with homology to the MET-hepatocyte growth factor receptor. *Proc Natl Acad Sci U S A* 1996;93(2):674-8.

Majeed A, Babb P, Jones J, Quinn M. Trends in prostate cancer incidence, mortality and survival in England and Wales 1971-1998. *BJU Int.* 2000;85(9):1058-62.

Martin-Satue M, Blanco J. Identification of semaphorin E gene expression in metastatic human lung adenocarcinoma cells by mRNA differential display. *J Surg Oncol.* 1999;72(1):18-23.

Matthes DJ, Sink H, Kolodkin AL, Goodman CS. Semaphorin II can function as a selective inhibitor of specific synaptic arborizations. *Cell* 1995;81(4):631-9.

McNeal JE, Bostwick DG. Intraductal dysplasia: a premalignant lesion of the prostate. *Hum Pathol.* 1986;17(1):64-71.

McNeal JE. Origin and development of carcinoma in the prostate. *Cancer* 1969;23(1):24-34.

McNeal JE, Villers AA, Redwine EA, Freiha FS, Stamey TA. Histologic differentiation, cancer volume, and pelvic lymph node metastasis in adenocarcinoma of the prostate. *Cancer* 1990;66(6):1225-33.

Miao HQ, Lee P, Lin H, Soker S, Klagsbrun M. Neuropilin-1 expression by tumor cells promotes tumor angiogenesis and progression. *FASEB J.* 2000;14(15):2532-9.

Miao HQ, Soker S, Feiner L, Alonso JL, Raper JA, Klagsbrun M. Neuropilin-1 mediates collapsin-1/semaphorin III inhibition of endothelial cell motility:

functional competition of collapsin-1 and vascular endothelial growth factor-165. *J Cell Biol.* 1999;146(1):233-42.

Mostofi FK, Davis CJ, Sesterhenn IA. Pathology of carcinoma of the prostate. *Cancer* 1992;70:235-53.

Muller A, Homey B, Soto H, Ge N, Catron D, Buchanan ME, McClanahan T, Murphy E, Yuan W, Wagner SN, Barrera JL, Mohar A, Verastegui E, Zlotnik A. Involvement of chemokine receptors in breast cancer metastasis. *Nature* 2001;410(6824):50-6.

Jin H, Varner J. Integrins: roles in cancer development and as treatment targets. *Br J Cancer* 2004;90(3):561-565.

Nakamura F, Kalb RG, Strittmatter SM. Molecular basis of semaphorin-mediated axon guidance. *J Neurobiol.* 2000;44(2):219-29.

Nakamura F, Tanaka M, Takahashi T, Kalb RG, Strittmatter SM. Neuropilin-1 extracellular domains mediate semaphorin D/III-induced growth cone collapse. *Neuron* 1998;21(5):1093-100.

Narayan P. Neoplasms of the prostate gland. *Smiths general urology.* 14<sup>th</sup> ed. Norwalk, CT: Appleton & Lange, 1995:238



Negishi M, Katoh H. Rho family GTPases as key regulators for neuronal network formation J. Biochem. 2002;132:157-166.

Nobes CD, Lauritzen I, Mattei MG, Paris S, Hall A, Chardin P. A new member of the Rho family, Rnd1, promotes disassembly of actin filament structures and loss of cell adhesion. J Cell Biol 1998;141(1):187-197.

Nobes CD, Hall A. Rho, rac, and cdc42 GTPases regulate the assembly of multimolecular focal complexes associated with actin stress fibers, lamellipodia, and filopodia. Cell 1995;81(1):53-62.

Office for National Statistics, 2009 Mortality Statistics: Deaths registered in England and Wales.2007.

[http://www.statistics.gov.uk/downloads/theme\\_health/DR2007/DR\\_07\\_2007.pdf](http://www.statistics.gov.uk/downloads/theme_health/DR2007/DR_07_2007.pdf)

Office for National Statistics CSR. Registrations of cancer diagnosed in 2004, England.London:NationalStatistics.1-1-2006.

[http://www.statistics.gov.uk/articles/hsq/HSQ38\\_Cancer\\_trends\\_in\\_UK.pdf](http://www.statistics.gov.uk/articles/hsq/HSQ38_Cancer_trends_in_UK.pdf)

Okamoto T, Ogiu K, Sato M. Primary squamous cell carcinoma of the prostate: a case report. Hinyokika Kiyo 1996;42:67-70.

Oinuma I, Katoh H, Harada A, Negishi M. Direct interaction of Rnd1 with Plexin-B1 regulates PDZ-RhoGEF-mediated Rho activation by Plexin-B1 and induces cell contraction in COS-7 cells. *J Biol Chem.* 2003;278(28):25671-7.

Oinuma I, Katoh H, Negishi M. Semaphorin 4D/Plexin-B1-mediated R-Ras GAP activity inhibits cell migration by regulating beta(1) integrin activity. *J Cell Biol.* 2006;173(4):601-13.

Oinuma I, Ishikawa Y, Katoh H, Negishi M. The Semaphorin 4D receptor Plexin-B1 is a GTPase activating protein for R-Ras. *Science* 2004;305(5685):862-5.

Parkin DM, Whelan SL, Perlay J, Teppo L, Thomas DB. Cancer incidence in five continents. Lyon: IACR Sci Publ, 1997.

Paget S. The distribution of secondary growths in cancer of the breast. *Lancet* 1889;1:99-101.

Pasterkamp RJ, Kolodkin AL. Semaphorin junction: making tracks toward neural connectivity. *Curr Opin Neurobiol.* 2003;13(1):79-89.

Perala NM, Immonen T, Sariola H. The expression of plexins during mouse embryogenesis. *Gene Expression Patterns* 2005;5(3):355-362.

Poste G, Paruch L, Stephen Paget, M.D., F.R.C.S., (1855-1926). A retrospective. *Cancer Metastasis Rev.* 1989;8(2):93-7.

Ramos CG, Carvahal GF, Mager DE, Haberer B, Catalona WJ. The effect of high grade prostatic intraepithelial neoplasia on serum total and percentage of free prostate specific antigen levels. *J Urol.* 1999;162(5):1587-90.

Reese J H, Freiha FS, Gelb AB, Lum BL, Torti FM. Transitional cell carcinoma of the prostate in patients undergoing cystoprostatectomy. *J Urol.* 1992;147:92-5.

Ridley AJ, Hall A. The small GTP-binding protein rho regulates the assembly of focal adhesions and actin stress fibers in response to growth factors. *Cell* 1992;70(3):389-99.

Ridley AJ, Schwartz MA, Burridge K, Firtel RA, Ginsberg MH, Borisy G et al. Cell migration: integrating signals from front to back. *Science* 2003;302(5651):1704-1709.

Ronnett BM, Carmichael MJ, Carter HB, Epstein JI. Does high grade prostatic intraepithelial neoplasia result in elevated serum prostate specific antigen levels? *J Urol.* 1993;150:386-9.

Ross R, Bernstein L, Judd H, Hanisch R, Pike M, Henderson B. Serum testosterone levels in healthy young black and white men. *J Natl Cancer Inst.* 1986;76(1):45-8.

Saiti Y, Oinuma I, Fujimoto S, Negishi M. Plexin B1 is a GTPase activating protein for M-Ras, remodelling dendrite morphology. *EMBO Rep.* 2009;10(6):614-621.

Semaphorin Nomenclature Committee. *Cell* 1999;97(5):551-2.

Serini G, Valdembri D, Zanivan S, Morterra G, Burkhardt C, Caccavari F, Zammataro L, Primo L, Tamagnone L, Logan M, Tessier-Lavigne M, Taniguchi M, Puschel AW, Bussolino F. Class 3 semaphorins control vascular morphogenesis by inhibiting integrin function. *Nature* 2003;424(6947):391-7.

Shepherd D, Keetch DW, Humphrey PA, Smith DS, Stahl D. Repeat biopsy strategy in men with isolated prostatic intraepithelial neoplasia on prostate needle biopsy. *J Urol.* 1996;156:460-2.

Sierra J, Corso S, Caione L, Cepero V, Conrotto P, Cignetti A, Piacibello W et al. Tumor angiogenesis and progression are enhanced by Sema4D produced by tumor-associated macrophages. *J Exp Med.* 2008;205(7):1673-1685.

Souhami RL, Tannock I, Hohenberger P, Horiot JC. *Oxford Textbook of Oncology.* 2<sup>nd</sup> Ed. Vol.1 2002:103-113.

Stone KR, Mickey DD, Wunderli H, Mickey GH, Paulson DF. Isolation of a human prostate carcinoma cell line (DU 145). *Int J Cancer* 1978; 21(3):274-281.

Swiercz JM, Kuner R, Offermanns S. Plexin-B1/RhoGEF-mediated RhoA activation involves the receptor tyrosine kinase ErbB-2. *J Cell Biol.* 2004;165(6):869-80.

Swiercz JM, Worzfeld T, Offermanns S. ERBB-2 and met reciprocally regulate cellular signaling via plexin-B1. *J Biol Chem* 2008;283(4):1893-1901.

Tamagnone L, Artigiani S, Chen H, He Z, Ming GI, Song H, Chedotal A, Winberg ML, Goodman CS, Poo M, Tessier-Lavigne M, Comoglio PM. Plexins are a large family of receptors for transmembrane, secreted, and GPI-anchored semaphorins in vertebrates. *Cell* 1999;99(1):71-80.

Tamagnone L, Comoglio PM. Signalling by semaphorin receptors: cell guidance and beyond. *Trends Cell Biol.* 2000;10(9):377-83.

Takahashi T, Fournier A, Nakamura F, Wang LH, Murakami Y, Kalb RG, Fujisawa H, Strittmatter SM. Plexin-neuropilin-1 complexes form functional semaphorin-3A receptors. *Cell* 1999;99(1):59-69.

Tessier-Lavigne M, Goodman CS. The molecular biology of axon guidance. *Science* 1996;274(5290):1123-33.

Tomizawa Y, Sekido Y, Kondo M, Gao B et al. Inhibition of lung cancer cell growth and induction of apoptosis after reexpression of 3p21.3 candidate tumor suppressor gene SEMA3B. *Proc Natl Acad Sci U S A*. 2001;98(24):13954-9.

Tong Y, Chugha P, Hota PK, Alviani RS, Li M, Tempel W et al. Binding of Rac1, Rnd1 and RhoD to a novel Rho GTPase interaction motif destabilizes dimerization of the plexin-B1 Effector domain. *J Biol Chem* 2007;282(51):37215-24.

Touijer K, Rabbani F, Otero JR, Secin FP et al. Standard versus limited pelvic lymph node dissection for prostate cancer in patients with a predicted probability of nodal metastasis greater than 1%. *J Urol*. 2007;178(1):120-4.

Trusolino L, Comoglio PM. Scatter-factor and semaphorin receptors: cell signalling for invasive growth. *Nat Rev Cancer* 2002;2(4):289-300.

Tse C, Xiang RH, Bracht T, Naylor SL. Human Semaphorin 3B (SEMA3B) located at chromosome 3p21.3 suppresses tumor formation in an adenocarcinoma cell line. *Cancer Res*. 2002;62(2):542-6.

Turner LJ, Hall A. Plexin-induced collapse assay in COS cells. *Methods Enzymol.* 2006;406:665-676.

Turner LJ, Nicholls S, Hall A. The activity of the plexin-A1 receptor is regulated by Rac. *J Biol Chem.* 2004;279(32):33199-205.

Usui H, Taniguchi M, Yokomizo T, Shimizu T. Plexin-A1 and plexin-B1 specifically interact at their cytoplasmic domains. *Biochem Biophys Res Commun* 2003;300(4):927-31.

Vikis HG, Li W, Guan KL. The plexin-B1/Rac interaction inhibits PAK activation and enhances Sema4D ligand binding. *Genes Dev.* 2002;16(7):836-45.

Vikis HG, Li W, He Z, Guan KL. The semaphorin receptor plexin-B1 specifically interacts with active Rac in a ligand-dependent manner. *Proc Natl Acad Sci U S A* 2000;97(23):12457-62.

Webcutter. 2004. <http://www.firstmarket.com/cutter/cut2.html> Ref Type: Internet Communication.

Welch DR, Rinker-Schaeffer CW. What defines a useful marker of metastasis in human cancer? *J Natl Cancer Inst* 1999;91:1351-1353.

Weiss L, Grundmann E, Torhorst J, Hartveit F, Moberg I, Eder M, Fenoglio-Preiser CM, Napier J, Horne CH, Lopez MJ, et al. Haematogenous metastatic patterns in colonic carcinoma: an analysis of 1541 necropsies. *J Pathol.* 1986;150(3):195-203.

Weiss L, Harlos JP. The validity of negative necropsy reports for metastases in solid organs. *J Pathol.* 1986;148(3):203-6.

Weiss L, Harlos JP, Torhorst J, Gunthard B, Hartveit F, Svendsen E, Huang WL, Grundmann E, Eder M, Zwicknagl M, et al. Metastatic patterns of renal carcinoma: an analysis of 687 necropsies. *J Cancer Res Clin Oncol.* 1988;114(6):605-12.

Winberg ML, Noordermeer JN, Tamagnone L, Comoglio PM, Spriggs MK, Tessier-Lavigne M, Goodman CS. Plexin A is a neuronal semaphorin receptor that controls axon guidance. *Cell* 1998;95(7):903-16.

Winter H, Cheng KK, Cummins C, Maric R, Silcocks P, Varghese C. Cancer incidence in the south Asian population of England (1990-92). *Br J Cancer* 1999;79(3-4):645-54.

Wong OGW, Nitkunan T, Oinuma I, Zhou C, Blanc V, Brown R, Bott SRJ, Nariculum J, Box G, Munson P, Constantinou J et al. Plexin B1 Mutations in Prostate Cancer. *PNAS* 2007;104(48):19040-19045.



Woodhouse EC, Fisher A, Bandle RW, Bryant-Greenwood B, Charboneau L, Petricoin EF 3rd, Liotta LA. Drosophila screening model for metastasis: Semaphorin 5c is required for l(2)gl cancer phenotype. Proc Natl Acad Sci U S A 2003;100(20):11463-8.

Worzfeld T, Püschel AW, Offermanns S, Kuner R. Plexin-B family members demonstrate non-redundant expression patterns in the developing mouse nervous system: an anatomical basis for morphogenetic effects of Sema4D during development. Eur J Neurosci. 2004;19(10):2622-32.

Xiang R, Davalos AR, Hensel CH, Zhou XJ, Tse C, Naylor SL. Semaphorin 3F gene from human 3p21.3 suppresses tumor formation in nude mice. Cancer Res. 2002;62(9):2637-43.

Yamada T, Endo R, Gotoh M, Hirohashi S. Identification of semaphorin E as a non-MDR drug resistance gene of human cancers. Proc Natl Acad Sci U S A 1997;94(26):14713-8.

Zhang Z, Vuori K, Wang H, Reed JC, Ruoslahti E. Integrin activation by R-ras. Cell 1996;85(1):61-9.

## Appendix

### Plexin B1 sequence

[NM\\_002673](#) [gi:6631105]

#### Protein sequence:

MPALGPALLQALWAGWVLTQLPPTAFTPNGTYLQHLARDPTSGTLYLG  
ATNFLFQLSPGLQLEATVSTGPNLDSRDCLPPVMPDECPQAQPTNNPNQLLL  
VSPGALVVCVSVHQGVCEQRRLGQLEQLLLRPERPGDTQYVAANDPAVST  
VGLVAQGLAGEPLLFVGRGYTSRGVGGGIPPITRALWPPDPQAAFSYEET  
AKLAVGRLSEYSHHFVSAFARGASAYFLFLRRDLQAQSRAFRAYVSRVCLR  
DQHYYSYVELPLACEGGRYGLIQAAAVATSREVAHGEVLFAAFSSAAPPTV  
GRPPSAAAGASGASALCAFPDLDVDRLANRTRDACYTREGRAEDGTEVAYI  
EYDVNSDCAQLPVDTLDAYPCGSDHTPSPMASRVPLEATPILEWPGIQLTA  
VAVTMEDGHTIAFLGDSQGQLHRVYLGPGSDGHPYSTQSIQQGSAVSRDLT  
FDGTFEHLVYVMTQSTLLKVPVASCAQHLDACSLAHRDPYCGWCVLLGRC  
SRRSECSRQGPEQWLWSFQPELGCLQVAAMSPANISREETREVFSLVDPDL  
PLWPGESYSCHFGEHQSPALLTGSGVMCPSPDPSEAPVLPRGADYVSVSVE  
LRFGAVVIAKTSLSFYDCVAVTELRPSAQCQACVSSRWGCNWCVWQHLCT  
HKASCDAGPMVASHQSPLVSPDPPARGGSPSPPTAPKALATPAPDTLPVEP  
GAPSTATASDISPGASPSLLSPWGPWAGSGSISPGSTGSPLHEEPSPPSPQNG  
PGTAVPAPTDFRPSATPEDLLASPLSPSEVAAVPPADPGPEALHPTVPLDLPP  
ATVPATTFPGAMGSVKPALDWLTREGGELPEADEWTGGDAPAFSTSTLLS  
GDGDSAELEGPPAPLILPSSLDYQYDTPGLWELEEATLGASSCPCVESVQGS  
TLMPVHVEREIRLLGRNLHLFQDGGPDNECVMELEGLEVVEARVECEPPP

DTQCHVTCQQHQLSYEALQPELRVGLFLRRAGRLRVDSAEGLVVLYDCS  
VGHGDCSRCQTAMPQYGCVWCEGERPRCVTREACGEAEAVATQCPAPLIH  
SVEPLTGPVDGGTRVTIRGSNLGQHVQDVLGMVTVAGVPCAVDAQEYEVS  
SSLVCITGASGEEVAGATAVEVPGRGRGVSEHDFAYQDPK VHSIFPARGPR  
AGGTRLTLNGSKLLTGRLEDIRVVVGDPCHLLPEQQSEQLRCETSPRPTPA  
TLPVAVWFGATERRLQRGQFKYTLDPNITSAGPTKSFLSGGREICVRGQNL  
DVVQTPRIRVTVVSRLQPNQGLGRRRRVVPETACSLGPSCSSQQFEETCH  
VNSSLITCRTPALPGLPEDPWVRVEFILDNLVDFATLNPTPFSYEADPTLQ  
PLNPEDPTMPFRHKPGSVFSVEGENLDLAMSKEEVVAMIGDGPCVVKTLTR  
HHLyceppveqplprhhalreapdslpeftvqmgnlrfsLGHVQYDGESPG  
AFPVAAQVGLGVGTSLLALGVIIIIVLMYRRKSKQALRDYKKVQIQLENLES  
SVRDRCKKEFTDLMTEMTDLTSDLLGSGIPFLDYKVYAERIFFPGHRESPLH  
RDLGVPEARRPTVEQGLGQLSNLLNSKLFLTKFIHTLETQRTFSARDRAYVA  
SLLTVALHGKLEYFTDILRTLSDLVAQYVAKNPKLMLRRTETVVEKLLTN  
WMSICLYTFVRDSVGEPLYMLFRGIKHQVDKGPVDSVTGKAKYTLNDNRL  
LREDVEYRPLTLNALLAVGPGAGEAQGVVVKVLDCTISQAKEKMLDQLY  
KGVPLTQRDPRTLDVEWRSGVAGHLILSDEDVTSEVQGLWRRNLTLQHY  
KVPDGATVALVPCLTKHVLRENQDYVPGERTPMLEDVDEGGIRPWHLVKP  
SDEPEPPRRRGLRGGGERERAKAIPeiYLTRLLSMKGTlQKFVDDLfQVILS  
TSRPVPLAVKYFFDLLDEQAQQHGISDQDTIHIWKTNSLPLRFWINIKNPQF  
VFDVQTSNMDAVLLVIAQTFMDACTLADHKLGRDSPINKLLYARDIPRY  
KRMVERYYADIRQTVPASDQEMNSVLAELSWNYSGDLGARVALHELYKYI  
NKYYDQIITALEEDGTAQKMQLGYRLQQIAAAVENKVTD

## Nucleic acid sequence:

1 atgctgtctc tgggccagc tcttctccag gctctctggg ccgggtgggt cctcacctc  
61 cagccccttc caccaactgc attactccc aatggcacgt atctgcagca cctggcaagg  
121 gacccacct caggcacctt ctacctgggg gctaccaact tctgttcca gctgagcct  
181 gggctgcagc tggaggccac agtgtccacc ggcctgtgc tagacagcag ggactgcctg  
241 ccacctgtga tgctgatga gtgccccag gccagccta ccaacaacc gaatcagctg  
301 ctctgggta gccaggggc cctgggtgta tgcgggagcg tgcaccaggg ggtctgtgaa  
361 cagcgggcc tggggcagct cgagcagctg ctgctgccc cagagcggcc tggggacaca  
421 caatatgtg ctccaatga tctgcccgc agcacggtg ggctggtag ccagggttg  
481 gcaggggagc ccctctgtt tgtggggcga ggatacaca gcaggggtg ggggggtggc  
541 attcaccca tcacaaccg ggcctgtgg ccggccgacc ccaagctgc ctctcctat  
601 gaggagacag ccaagctggc agtgggccc ctctccgagt acagccacca ctctgtgagt  
661 gccttgcaac gtggggccag cgctacttc ctgtcctgc ggcgggacct gcaggctcag  
721 tctagagctt ttcgtgcta tgtatctga gtgtgtctcc gggaccagca ctactactcc  
781 tatgtggagt tgcctctggc ctgcaaggt ggccgctac ggctgatcca ggctgcagct  
841 gtggccacgt ccaggaggt ggcgatggg gaggtgtct tgcagcttt ctctcggct  
901 gcacccccca ctgtggccg gcccacatc gcggtgctg gggcatctg agcctctgcc  
961 ctctgtcct tcccctgga tgagggtgac cggcttgta atcgacgcg agatgcctgc  
1021 tacaccggg agggctgtg tgaggatgg accgaggtg cctacatcga gtagatgtc  
1081 aattctgact gtgcacagct gccagtggc accctggatg ctatccctg tggtcagac  
1141 cacacgcca gcccatggc cagccgggc ccgctggaag ccacaccaat tctggagtgg  
1201 ccagggattc agtaacagc tgtggcagtc accatggaag atggacacac catcgcttc  
1261 ctgggtgata gtcaaggca gctgcacagg gtctacttg gccagggag cgatggccac  
1321 ccatactcca cacagagcat ccagcaggg tctgcagtga gcagagacct caccttgat  
1381 gggaccttg agcacctgta tgtcatgacc cagagcacac ttctgaaggt tctgtggct  
1441 tctgtgctc agcacctgga ctgtcatct tgcctgctc acagggacc atactgtgg

1501 tgggtcgtgc tcctggcag gtcagtcgc cgttctgagt gctcgagggg ccagggccca  
1561 gagcagtggc tatggagctt ccagcctgag ctgggctgtc tgcaagtggc agccatgagt  
1621 cctgccaaca tcagccgaga ggagacgagg gaggtttcc tatcagtgcc agacctgcca  
1681 cccctgtggc caggggagtc atattcctgc cactttgggg aacatcagag tctgcccctg  
1741 ctgactgggt ctggtgtgat gtgcccctcc ccagacccta gtgaggcccc agtgctgccg  
1801 agaggagccg actacgtatc cgtgagcgtg gagctcagat ttggcgtgtg tgtgatgcc  
1861 aaaactccc tctcttcta tgactgtgtg gcggtcactg aactccgcc atctgcgag  
1921 tgccaggcct gtgtgagcag ccgctggggg tgtaactggt gtgtctggca gcacctgtc  
1981 acccacaagg cctcgtgtga tgctgggcc atggttcaa gccatcagag cccgctgtc  
2041 tcccagacc ctctgcaag aggtggacc agcccctccc caccacagc ccccaaagcc  
2101 ctggccacc ctgctcctga caccctccc gtggagcctg gggctccctc cacagccaca  
2161 gcttcggaca tctcacctgg ggctagtctt tcctgtca gccctgggg gccatggga  
2221 ggttctggct ccatatctt cctggctcc acaggtcgc ctctcatga ggagccctc  
2281 cctcccagc cccaaaatgg acctggaacc gctgtccctg cccactga ctacagacc  
2341 tcagccacac ctgaggacct ctggcctcc ccgctgtcac cctcagaggt agcagcagt  
2401 cccctgcag accctggccc cgaggctctt catccacag tgcccctgga cctgcccct  
2461 gccactgtc ctgccaccac ttcccaggg gccatgggt ccgtgaagcc cgcctggac  
2521 tggctcacga gagaaggcgg cgagctgcc gaggcggacg agtggacggg gggtgacgca  
2581 cccgcttct cactccac cctctca ggtgatggag actcagcaga gcttgagggc  
2641 cctccgcc cctcatct cccgtccagc ctgactacc agtatgacac cccgggctc  
2701 tgggagctg aagaggcag ctgggggca agctcctgcc cctgtgtgga gagcgttca  
2761 ggctccactg tatgcccgt ccatgtggag cgggaaatcc ggctgctagg caggaacctg  
2821 caccttcc aggatggccc aggagacaat gagtgtgtga tggagctgga gggcctcag  
2881 gtggtggtg agggccggg cgagtgtgag ccacctccag ataccagtg ccatgtcacc  
2941 tgccagcag accagctcag ctatgaggct ctgcagccgg agctccgtg ggggctggtt  
3001 ctgcgtcgg cggccgtct gcgtgtggac agtgctgagg ggctcatgt ggtactgtat  
3061 gactgttccg tgggacatgg agactgcagc cgctgcaaaa ctgcatgcc ccagtatggc  
3121 tgtgtgtgtg gtgaggggga gcgtccactg tgtgtgacct gggaggcctg tggtaggct


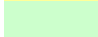

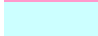

3181 gaggtgtgg ccaccagtg cccagcgccc ctcatccact cggaggagcc actgactggg  
3241 cctgtagacg gaggcacccg tgtaccatc aggggtcca acctgggcca gcatgtgac  
3301 gatgtgctgg gcatggtcac ggtggctgga gtgccctgtg ctgtggatgc ccaggagtac  
3361 gaggtctcca gcagcctcgt gtgcatcacc ggggccagtg gggaggaggt ggccggcgcc  
3421 acagcggtag aggtgccggg aagaggacgt ggtgtctcag aacacgactt tgcctaccag  
3481 gatccgaagg tccattccat cttccggcc cgcggcccca gagctggggg cacccgtctc  
3541 acctgaatg gctccaagct cctgactggg cggctggagg acatccgagt ggtggttga  
3601 gaccagcctt gtcactgct gccggagcag cagtcagaac aactcggtg tgagaccagc  
3661 ccacgcccc cgcctgccac gctccctgtg gctgtgtgtg ttggggccac ggagcggagg  
3721 cttcaacgcg gacagttcaa gtatacctg gacccaaca tcacctctgc tggccccacc  
3781 aagagcttcc tcagtggagg acgtgagata tgcgtccgtg gccagaatct ggacgtgta  
3841 cagacgcaa gaatccgggt gaccgtggtc tcgagaatgc tcagcccaa ccaggggctt  
3901 ggacggaggc gtcgctggt cccggagacg gcatgttccc ttggaccctc ctgcagtagc  
3961 cagcaattg aggagccgtg ccatgtcaac tctcccagc tcatcagtg ccgacacct  
4021 gccctcccag gcctgcctga ggaccctgg gtccgggtgg aattatct tgacaacctg  
4081 gtcttgact ttgaacct gaacccaca ctttctct atgaggccga cccaccctg  
4141 cagccactca acctgagga cccaccatg ccattccggc acaagcctgg gagtgtgtc  
4201 tccgtggagg gggagaacct ggacctgca atgtccaagg aggaggtgtt ggctatgata  
4261 ggggatggcc cctgtgtgtg gaagacgctg acgcgccacc acctgtactg cgagcccccc  
4321 gtggagcagc ccctgccacg gcaccatgcc ctccgagagg cacctgactc tttgctgag  
4381 ttcacggtgc agatgggaa cttgcgttc tccctgggtc acgtgcagta tgacggcgag  
4441 agccctgggg ctttctctg ggagccag gtgggcttg ggtgggac ctctctctg  
4501 gctctgggtg tcatcatcat tgcctcatg tacaggagga agagcaagca ggcctgagg  
4561 gactataaga aggtcagat ccagctggag aatctggaga gcagtgtgcg ggaccgctgc  
4621 aagaaggaat tcacagacct catgactgag atgaccgatc tcaccagtg cctcctggg  
4681 agcggcatcc cttcctcga ctacaaggtg tatgcggaga ggatcttct cctgggac  
4741 cgcgagtcgc cttgcaccg ggacctgggt gtgcctgaga gcagacggcc cactgtagag  
4801 caagggtgg ggcagctctc taacctgctc aacagcaagc tottctcac caagttcatc

4861 cacacgctgg agaccagcg cacctttca gctcgggacc gtcctacgt ggcattctg  
4921 **ctcaccgtgg cactgcatgg** gaagctgag tatttcaactg acatcctccg cactctgctc  
4981 **agtgacctgg ttgccagta** tgtggccaag aacccaagc tgatgctgcg caggacagag  
5041 actgtggtgg agaagctgct caccaactgg atgtccatct gtctgtatac ctctgtgagg  
5101 gactccgtag gggagcctct gtacatgctc ttctgagggg ttaagcacca agtgataag  
5161 gggccagtgg acagtgtgac aggcaaggcc aaatacacct tgaacgacaa ccgctgctc  
5221 agagaggatg tggagtaccg tcccctgacc ttgaatgcac tattggctgt ggggctggg  
5281 gcaggagagg cccagggcgt gcccgtaag gtcctagact gtgacacat ctcccaggca  
5341 aaggagaaga tgctggacca gctttataa **ggagtgcctc tcaccagcg** gccagacct  
5401 cgcacccttg **atgtgagtg gcggtctggg** gtggccgggc acctattct ttctgacgag  
5461 gatgtcactt ctgaggcca gggctctgg aggcgcctga acacactgca gcattacaag  
5521 gtcccagatg gagcaactgt ggccctgctc cctgcctca ccaagcatgt gctccgggaa  
5581 aaccaggatt atgtccctgg agagcggacc ccaatgctgg aggatgtaga tgaggggggc  
5641 atccggcctt ggcacctggt gaagccaagt gatgagccgg agccgccag gcctcggagg  
5701 ggcagcctc ggggcgggga gctgagcgc gccaggcca tcctgagat ctacctgacc  
5761 cgctctgt ccatgaagg caccctgag aagtctggt atgacctgt ccaggatgatt  
5821 ctacgacca gccgccccg **gccgctgct** gtgaagtact tcttgacct **gctggatgag**  
5881 **caggc**ccagc agcatggcat ctccgaccag gacacatcc acatctggaa gaccaacagc  
5941 ttgcctctga gttctggat caatataata aaaaaccgc agttgtgtt cgacgtgcaa  
6001 acatctgata acatggatgc ggtgctcctt gtcattgcac agacctcat ggagcctgc  
6061 accctggccg accacaagct gggccgggac tcccgatca acaaacttct gtatgcagg  
6121 gacattcccc ggtacaagcg gatggtggaa aggtactatg cagacatcag acagactgtc  
6181 ccagccagcg accaagagat gaactctgtc ctggtgaac tgtctggaa ctactccgga  
6241 gacctcgggg cgcgagtgcc **cctgcatgaa ctctacaagt** acatcaacaa gtactatgac  
6301 cagatcatca ctgccctgga ggaggatggc acggcccaga agatgcagct gggctatcgg  
6361 ctccagcaga **ttgcagctgc** tgtggaaaac aaggtcacag atctatagga acccaggagc  
6421 cacggcctgc tgttgctca gcctggcctg ggcagccctg gaagctcggg ggagaggcca  
6481 ccttcttagg tgctgtagt gactgacaag cagagttagt ggaaggtgac tcccagctc

6541 ctggtggctc tggcctcggc cctgctggat ccacctcta gaccgggggc ctcaaggctc

6601 atgggtagt acccagcctg ctccccgagt ccagcgacct tgt

Key – Primers

Plexin B1-52	
Plexin B1-2	
Plexin B1-3	
Plexin B1-4	
Sp6	

Ref: <http://www.ncbi.nlm.nih.gov/nuccore/6631105?report=genbank>



**Published work**

# Plexin-B1 mutations in prostate cancer

Oscar Gee-Wan Wong<sup>\*</sup>, Tharanl Nitkunan<sup>\*</sup>, Izumi Oinuma<sup>†</sup>, Chun Zhou<sup>\*</sup>, Veronique Blanc<sup>\*</sup>, Richard S. D. Brown<sup>\*</sup>, Simon R. J. Bott<sup>\*</sup>, Joseph Nariculam<sup>\*</sup>, Gary Box<sup>‡</sup>, Phillipa Munson<sup>§</sup>, Jason Constantinou<sup>\*</sup>, Mark R. Feneley<sup>\*</sup>, Helmut Klocker<sup>¶</sup>, Suzanne A. Eccles<sup>\*</sup>, Manabu Negishi<sup>†</sup>, Alex Freeman<sup>§</sup>, John R. Masters<sup>\*</sup>, and Magali Williamson<sup>\*¶</sup>

<sup>\*</sup>Prostate Cancer Research Centre, Institute of Urology, University College London, 67 Riding House Street, London W1W 7EJ, United Kingdom; <sup>†</sup>Laboratory of Molecular Neurobiology, Graduate School of Biostudies, Kyoto University, Kyoto 606-8501, Japan; <sup>‡</sup>Institute of Cancer Research, Cotswold Road, Sutton, Surrey SM2 5NG, United Kingdom; <sup>§</sup>Department of Histopathology, University College London, London WC1E 6BT, United Kingdom; and <sup>¶</sup>Department of Urology, University of Innsbruck, 6020 Innsbruck, Austria

Edited by Stanley M. Gartler, University of Washington, Seattle, WA, and approved September 28, 2007 (received for review March 19, 2007)

Semaphorins are a large class of secreted or membrane-associated proteins that act as chemotactic cues for cell movement via their transmembrane receptors, plexins. We hypothesized that the function of the semaphorin signaling pathway in the control of cell migration could be harnessed by cancer cells during invasion and metastasis. We now report 13 somatic missense mutations in the cytoplasmic domain of the Plexin-B1 gene. Mutations were found in 89% (8 of 9) of prostate cancer bone metastases, in 41% (7 of 17) of lymph node metastases, and in 46% (41 of 89) of primary cancers. Forty percent of prostate cancers contained the same mutation. Overexpression of the Plexin-B1 protein was found in the majority of primary tumors. The mutations hinder Rac and R-Ras binding and R-RasGAP activity, resulting in an increase in cell motility, invasion, adhesion, and lamellipodia extension. These results identify a key role for Plexin-B1 and the semaphorin signaling pathway it mediates in prostate cancer.

adhesion | migration | R-Ras | Rac | semaphorin

**S**emaphorins are a large class of secreted or membrane-associated proteins that act as chemotactic cues for cell migration and axon guidance (1). Although best characterized in the nervous system, they are widely expressed in other tissues where they have a role in angiogenesis, organogenesis, and immune cell regulation (2, 3). Semaphorins inhibit integrin-mediated adhesion (4) and act as chemorepellants, although some also act as chemoattractants.

Plexins are single-pass transmembrane receptors for semaphorins (5, 6). Nine vertebrate plexins have been identified, grouped into four subfamilies, Plexin-A to Plexin-D, according to structure (5–7). Semaphorin 4D (Sema4D) is the ligand for Plexin-B1 and is expressed in both membrane-bound and secreted forms (6, 8). The cytoplasmic domain of plexins is conserved between plexin family members but has low homology to other receptor proteins (5) and lacks intrinsic tyrosine kinase activity. Plexins have a role in the regulation of the actin cytoskeleton, controlling the activity of the small GTPases, Rnd1, R-Ras, Rac, and Rho (9–12). Plexins also interact with and activate the receptor tyrosine kinases, ErbB2 (13) and c-Met (14). Plexins activate many characteristics of the invasive phenotype seen in cancer progression, inducing changes in extracellular matrix (ECM) adhesion, motility, scatter, and branching morphogenesis (15, 16). Prostate cancer is the second leading cause of cancer-related death in men in the U.S. and U.K.

We hypothesized that the function of the semaphorin-signaling pathway in control of cell migration could be harnessed by the cancer cell during invasion and metastasis. Our findings suggest that mutation or overexpression of the Plexin-B1 gene contributes to prostate cancer progression.

## Results

**Mutation of Plexin-B1 in Prostate Cancer Cell Lines.** We hypothesized that mutations in the cytoplasmic domain of the semaphorin receptors, plexins, would be most likely to affect semaphorin signaling. We therefore focused our screen for mutations on stretches of the receptor genes encoding the cytoplasmic domain.

The cytoplasmic domain and part of the extracellular domain (exons 1–5) of plexins A1, A3, and B1 were sequenced using cDNA from the human prostate cancer cell lines PC3, DU145, and LNCaP. A single nucleotide change (A5359G) was found in Plexin-B1 in LNCaP, which potentially changes threonine 1697 to an alanine. The A5359G mutation alters a BstZ171 site, and estimation of the relative intensities of the mutant and WT restriction digest products (Fig. 1*a* and *b*), as well as the genomic DNA sequence, suggests that the mutation is present in two of the three copies of chromosome 3p in LNCaP cells. LNCaP was derived from a patient of Caucasian origin, and the sequence change was absent from the DNA of 60 control individuals of a similar genetic background. The rest of the Plexin-B1 cDNA was sequenced in PC3, DU145, and LNCaP, and no further mutations were found. Quantitative RT-PCR showed high levels of Plexin-B1 in LNCaP (Fig. 1*c*) relative to the other prostate cancer cell lines lacking a mutation.

**Mutation of Plexin-B1 in Clinical Samples of Prostate Cancer.** SSCP analysis was used to screen exons 22–29 of the cytoplasmic domain of the Plexin-B1 gene in DNA microdissected from tumor tissue. Aberrant bands were excised from the gel and sequenced (Fig. 2). Nine prostate cancer bone metastases were screened, and 17 further missense mutations were found in eight (89%) of the samples. The mutations were absent from uninvolved tissue of the same patient where available (seven cases) and are therefore somatic [Table 1 and supporting information (SI) Fig. 7]. Seventeen lymph node metastases contained nine missense mutations in 7 of 17 (41%) of the samples (Table 1 and SI Fig. 7). Eighty-nine primary prostate tumors treated by radical prostatectomy were screened, including DNA from 9 samples of fresh tissue, and mutations were found in 41 of 89 (46%) samples (Table 1 and SI Fig. 7), including 5 of 9 samples of fresh tissue (Fig. 2*a*).

DNA was also extracted from eight samples of adjacent morphologically normal fresh tissue from the same patients as the fresh primary tumor samples. Two of eight apparently normal tissue samples contained a mutation. In both cases, the same mutation was present in the tumor and the adjacent histopathologically defined normal tissue. These findings suggest that, although retaining a normal morphology, the tissue may contain early changes associated with the development of prostate cancer or that contaminating tumor cells are present, as observed in other studies (17).

Mutations were confirmed by direct sequencing [i.e., amplifica-

Author contributions: O.G.-W.W. and T.N. contributed equally to this work; O.G.-W.W., T.N., I.O., C.Z., V.B., J.N., G.B., P.M., J.C., and M.W. performed research; R.S.D.B., S.R.B., M.F., and H.K. contributed new reagents/analytic tools; S.E., M.N., A.F., and J.R.M. analyzed data; J.R.M. and M.W. designed research; M.W. and J.R.M. wrote the paper.

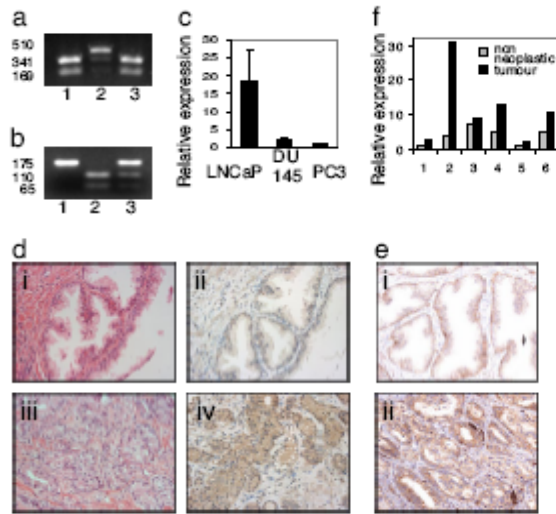
Conflict of interest statement: A patent has been filed by M.W. and J.R.M. for mutations.

This article is a PNAS Direct Submission.

To whom correspondence should be addressed. E-mail: magali.williamson@ucl.ac.uk.

This article contains supporting information online at [www.pnas.org/cgi/content/full/0702544104.DCI](http://www.pnas.org/cgi/content/full/0702544104.DCI).

© 2007 by The National Academy of Sciences of the USA

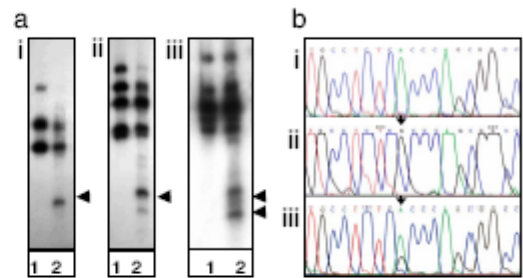


**Fig. 1.** Plexin-B1 expression in prostate cancer. (a) RT-PCR and BstZ171 restriction enzyme digestion of RNA from PC3 (lane 1), LNCaP (lane 2), and DU145 (lane 3). The A5359G mutation in LNCaP destroys a BstZ171 site. Band sizes in base pairs are shown. (b) PCR of genomic DNA and BstZ171 restriction enzyme digestion. Shown are undigested DNA (lane 1), PC3 DNA digested with BstZ171 (lane 2), and LNCaP DNA digested with BstZ171 (lane 3). The A5359G mutation in LNCaP destroys a BstZ171 site. (c) Quantitative RT-PCR of RNA from LNCaP, DU145, and PC3 cells. Results are the average of three independent RNA extractions normalized to PC3 expression. (d) Nonneoplastic (i and ii) and primary cancer (iii and iv) tissue stained with H&E (i and iii) or antibody to Plexin-B1 (ii and iv). (Magnification,  $\times 400$ .) (e) Nonneoplastic (i) and primary cancer (ii) tissue stained with antibody to Sema4D. (Magnification,  $\times 400$ .) (f) Quantitative RT-PCR of RNA from paired samples of nonneoplastic tissue and primary cancer from the same patient (patients 1–6) normalized to nonneoplastic tissue from patient 1.

tion and sequencing of genomic DNA without isolation from a single-stranded conformation polymorphism (SSCP) gel or subcloning] for the metastases (Fig. 2) and fresh primary tissue and by restriction enzyme digestion followed by sequencing for primary paraffin-embedded tissue (SI Fig. 8).

Some of the mutations were present in many tumors (Table 1). One mutation, A5653G (Thr1795Ala), was found in 9 of 26 (35%) metastases and 38 of 89 (43%) primary cancers. This mutation is predicted to result in the loss of a conserved predicted serine/threonine kinase phosphorylation site. C5060T (Pro1597Leu) was found in five metastases and in four primary cancers, and mutation of the adjacent nucleotide (C5059T), which changes the same amino acid to serine, was found in three metastases and one primary cancer. T5714C (Leu1815Pro) was found in three metastases and in two primary tumors. Some of tumor samples analyzed contained more than one mutation, as has been observed previously for other genes in prostate cancer (18, 19). The sequence changes were absent from the DNA of at least 60 control individuals of a similar genetic background in all cases. Many of the mutations found in prostate cancer are at sites conserved during evolution, suggesting functional significance (SI Table 2).

**Expression of Plexin-B1 in Prostate Cancer.** To investigate the levels of expression of Plexin-B1 in prostate cancer, four replicate tissue microarrays (TMAs) of 85 samples of primary prostate cancer and 85 samples of nonneoplastic prostate tissue from the same radical prostatectomy specimens were stained for Plexin-B1 (Fig. 1d). A significantly higher proportion of cores stained positive for Plexin-B1 protein compared with the corresponding nonneoplastic



**Fig. 2.** Plexin-B1 mutations detected by SSCP analysis in prostate cancer. (a) (i) SSCP analysis of nonmalignant DNA (lane 1) and DNA from a primary prostate cancer from fresh-frozen tissue (lane 2). The band marked with an arrow contains the C5060T sequence change. (ii) SSCP analysis of nonmalignant DNA (lane 1) and DNA from a primary prostate cancer from fresh-frozen tissue (lane 2). The band marked with arrows contains the A5653G mutation. (iii) SSCP analysis of nonmalignant DNA (lane 1) and DNA from a prostate cancer lymph node metastasis (lane 2). The bands marked with arrows contain the A5653G mutation. (b) Mutations in the Plexin-B1 gene. (i) Normal DNA sequence. (ii) Sequence of a SSCP band showing the A5653G mutation. (iii) Direct sequence of DNA from a metastasis in the same patient as in *bii*, showing the A5653G mutation.

tissues ( $P < 0.001$ , Mann-Whitney tumor vs. nonneoplastic, for both extent and intensity). Expression of Plexin-B1 was found in 77% (65 of 84) of prostate tumors and 6% (5 of 83) of nonneoplastic tissue from the same patients. All nonneoplastic cores were from patients diagnosed with prostate cancer. Consequently, the five cases of nonneoplastic tissue that did stain for Plexin-B1 may have had early changes associated with prostate cancer, although retaining normal morphology as has been described in other studies (20). Quantitative RT-PCR performed on paired samples of nonneoplastic and primary cancer showed increased expression of Plexin-B1 in the cancer samples relative to nonneoplastic tissue from the same patient (Fig. 1f). These results suggest that the increased protein staining observed in the primary cancers results from increased RNA levels and not from altered protein stability.

The same prostate cancer TMAs were also screened for protein expression of Sema4D, the ligand of Plexin-B1, by immunohistochemistry (Fig. 1e). Cell-surface expression of Sema4D was found in the basal epithelial cells of nonmalignant prostate tissue but was absent from the luminal cells. High levels of Sema4D cell surface staining were seen in prostate cancer cells, demonstrating a cancer-cell-associated overexpression of Sema4D ( $P < 0.001$ , Mann-Whitney, tumor vs. nonneoplastic, for both extent and intensity). Positive staining was found in 58% (49 of 84) of prostate cancers and 3.5% (3 of 84) of nonneoplastic tissues. A significant correlation was also seen between Plexin-B1 and Sema4D staining in the tumor samples ( $P < 0.001$ , Mann-Whitney). The same tumor cores also showed high levels of c-Met expression (data not shown).

**Functional Significance of Mutations in Plexin-B1.** To determine whether the mutations in Plexin-B1 found in prostate cancer metastases have an effect on cell function, cDNA constructs were made encoding WT Plexin-B1 and four mutant versions of the protein. The mutants investigated were the three most frequently found in prostate cancer metastasis, (C5060T, A5653G, and T5714C) and that found in LNCaP (A5359G).

**Mutation of Plexin-B1 Decreases Cell Collapse.** In the presence of Rnd, stimulation of Plexin-B1 with Sema4D results in a transient cell shrinkage or collapse of COS-7 cells (10). To determine the effect of Plexin-B1 mutations on this standard test of plexin function (21), COS-7 cells were transiently transfected with Rnd1 and WT or mutant Plexin-B1, and the cells were stimulated with

**Table 1. Mutations in prostate cancer**

Nucleotide	Amino acid	Bone metastases (total of 9)								LN metastases (total of 17)							1* (total of 89)	Total
		1	2	3	4	5	6	7	8	1	2	3	4	5	6	7		
C5069T	P1597S											x	x	x			1	4
C5060T*	P1597L	x	x			x					x					x	4 <sup>†</sup>	9
G5074A*	G1602R															x	1	1
T5401A	F1711I																1	1
C5468T*	T1733I							x									1	1
A5474G*	N1735S							x									1	1
A5596G	T1776A																1	1
A5653G*	T1795A	x	x	x	x	x		x	x				x	x		38 <sup>†</sup>	47	
C5662T	P1798S								x								1	1
A5674G*	T1802A			x													1	1
T5714C*	L1815P	x															2 <sup>†</sup>	5
C5980T	R1904W					x				x							1	1
Total						8 of 9 (89%)							7 of 17 (41%)				41 of 89	73

\*Mutation absent from noncancer tissue from the same patient in at least one case; the rest are not determined.

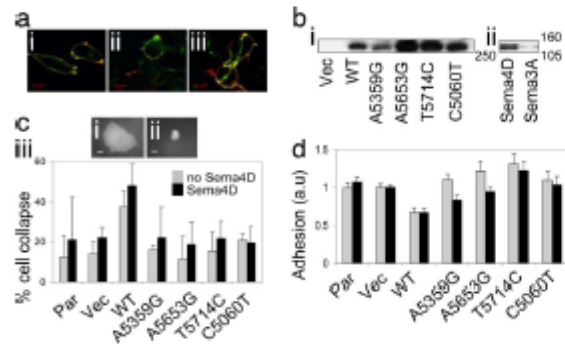
<sup>†</sup>DNA from frozen tissue.

<sup>‡</sup>Includes five samples of DNA from frozen tissue.

Sema4D. Coexpression of Rnd1 and WT Plexin-B1 and treatment with Sema4D for 5 min resulted in an increase in cell collapse as expected (Fig. 3c). In contrast, transient expression of all four Plexin-B1 mutants significantly reduced the percentage of cell collapse relative to expression of WT Plexin-B1 ( $P \leq 0.05$ , Fig. 3c).

**Mutation of Plexin-B1 Increases Cell Adhesion.** Expression of Plexin-B1 in fibroblasts inhibits integrin-dependent cell adhesion to the ECM protein fibronectin (22). This inhibition is due to activation of the intrinsic GTPase activity of R-Ras by Plexin-B1, resulting in R-Ras inactivation and a decrease in integrin-based cell

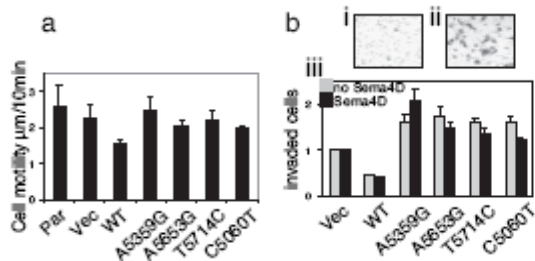
adhesion (9). To assess the effect of four of the mutations found in Plexin-B1 on cell adhesion, stable cell lines expressing WT or mutant Plexin-B1 were made in HEK293 cells by lentiviral transduction. The cell lines expressed similar levels of Plexin-B1 protein, and cell surface expression of WT and mutant Plexin-B1 was observed (Fig. 3a and b). Expression of WT Plexin-B1 reduced adhesion of HEK293 cells to fibronectin relative to a vector control 10 and 30 min after plating (Fig. 3d and SI Fig. 9a). Binding of Plexin-B1 by its ligand, Sema4D (6), results in clustering of the receptor (23), and expression of high levels of Plexin-B1 mimics ligand binding (14) (SI Fig. 9c). Probably for this reason, the addition of Sema4D had little additional effect on adhesion. Expression of all four mutants significantly increased adhesion relative to WT Plexin-B1 after 10 ( $P \leq 0.005$ ) and 30 min ( $P \leq 0.05$ ) (Fig. 3d and SI Fig. 9a). The addition of Sema4D reduced adhesion for all four mutants, but levels remained significantly above WT ( $P < 0.05$ ). Integrin-independent adhesion to poly-L-lysine was negligible and was not affected by expression of any of the constructs (SI Fig. 9b).



**Fig. 3. Mutations in the Plexin-B1 gene inhibit cell collapse and increase cell adhesion.** (a) Lentiviral-transduced HEK293 cells expressing WT Plexin-B1 (i), T5714C (ii), or C5060T mutants (iii), showing cell-surface expression. Cells were stained for Plexin-B1 (TRITC) and actin (FITC-phalloidin). (Scale bar, 10  $\mu$ m.) (b) Western blot of lentiviral-transduced HEK293 cells infected with vector (Vec), WT, or mutant Plexin-B1, selected using blasticidin, and detected by anti-Plexin-B1. (ii) Western blot of purified Sema4D-Fc and Sema3A-Fc. (c) (i and ii) Mutations in Plexin-B1 inhibit cell collapse. COS-7 cells transfected with Rnd-myc and mutant (A5359G) (i) or WT Plexin-B1 (ii) and treated with Sema4D. Cells were stained for myc (FITC) and Plexin-B1 (TRITC). (Scale bar, 10  $\mu$ m.) (iii) Percentage of cell collapse of cells transfected with Rnd and Plexin-B1 (WT or mutant) and treated with Sema4D for 5 min. The size of cells transfected with both constructs was measured, and the percentage of cells  $< 500 \mu\text{m}^2$  was calculated using Andor software. The results are the mean of three independent experiments, with 50 cells sized per experiment.  $P \leq 0.05$  (all mutants vs. WT). Error bars indicate SEM. (d) Mutations in Plexin-B1 increase adhesion. Shown is adhesion of lentiviral-transduced HEK293 cells expressing WT or mutant Plexin-B1 to fibronectin for 10 min. No Sema4D,  $P \leq 0.005$  (all mutants vs. WT); with Sema4D,  $P \leq 0.01$  (C5060T, A5653G, and T5714C) and  $P \leq 0.05$  (A5359G) vs. WT.

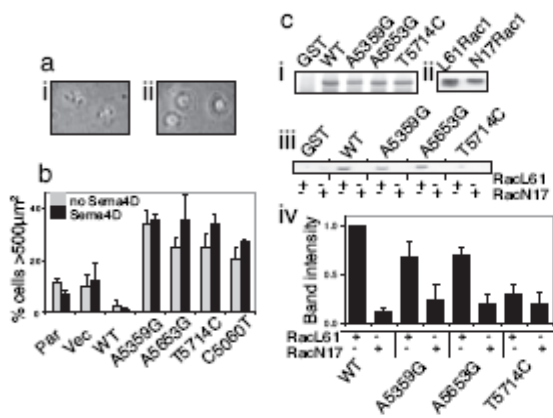
**Mutation of Plexin-B1 Increases Cell Motility and Invasion.** Plexin-B1 expression reduces cell motility in NIH 3T3 and COS7 cells (22, 24) and increases cell motility in cells expressing c-Met (14). To assess the effect of mutation of Plexin-B1 on cell motility, the rate of migration of HEK293 cells expressing WT or mutant Plexin-B1 was measured by time-lapse video microscopy. Expression of WT Plexin-B1 reduced cell motility relative to vector controls (Fig. 4a). Expression of all four mutants of Plexin-B1 significantly increased the rate of migration relative to WT Plexin-B1 ( $P \leq 0.05$ , Fig. 4a). Mutation of Plexin-B1 also increased cell motility in transwell assays ( $P \leq 0.05$ ) (SI Fig. 10a). Expression of WT Plexin-B1 reduced the invasive capacity of HEK293 cells in invasion assays through matrigel (Fig. 4b). In contrast, expression of four mutant versions of the gene increased the invasive capacity of the cells relative to expression of both WT and vector controls. ( $P \leq 0.05$  vs. WT).

**Mutation of Plexin-B1 Increases Cell Spreading.** Expression of Plexin-B1 also blocks extension of lamellipodia after the plating of fibroblasts on fibronectin, as assessed by the percentage of cell spreading (22). Expression of WT Plexin-B1 in HEK293 cells reduced both the percentage of cell spreading (defined as the percentage of cells  $\geq 500 \mu\text{m}^2$ ) and the average cell size 10 min after plating on fibronectin in the presence and absence of Sema4D, relative to a vector control, as expected (Fig. 5a and b and SI Fig. 10b). Conversely, expression of



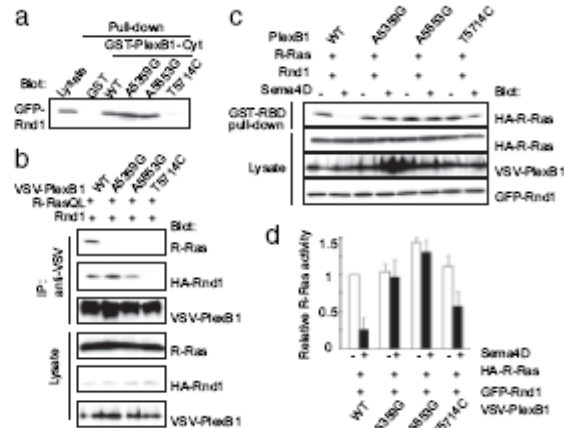
**Fig. 4.** Mutations in Plexin-B1 increase cell motility and invasion. (a) Rate of cell migration of lentiviral-transduced HEK293 cells expressing WT or mutant Plexin-B1 or transduced with control vector, measured by time-lapse video microscopy. Twenty cells were tracked per experiment, and the numbers represent the average of three independent experiments. The experiment was repeated with an independent lentiviral infection and gave similar results.  $P \leq 0.05$ , for all mutants vs. WT. (b) (i and ii) Photomicrographs of lentiviral-transduced HEK293 cells expressing WT (i) or mutant (A5359G) (ii) Plexin-B1 after invasion through matrigel. (Magnification,  $\times 250$ .) (iii) Relative number of HEK293 cells expressing mutant or WT Plexin-B1 to invade through matrigel-coated invasion chambers after 24 h. Expression of four mutant versions of the gene increased the invasive capacity of the cells relative to expression of WT Plexin-B1 ( $P \leq 0.05$ ). The results are the means of the independent experiments performed in duplicate.

similar levels of mutant Plexin-B1 significantly increased the percentage of cell spreading ( $P \leq 0.01$ ) and average cell size ( $P \leq 0.0001$ ) relative to cells expressing WT Plexin-B1 (Fig. 5*a* and *b* and SI Fig. 10*b*). Addition of Sema4D further increased



**Fig. 5.** Mutations in Plexin-B1 increase cell spreading and decrease RacGTP binding. (a) Photomicrographs of lentiviral-transduced HEK293 cells expressing WT (i) or mutant (T5714C) (ii) Plexin-B1 10 min after plating on fibronectin. (Magnification,  $\times 400$ .) (b) Cell spreading. Shown is the percentage of cells  $> 500 \mu\text{m}^2$  in area, 10 min after plating on fibronectin.  $P \leq 0.01$  (for all mutants vs. WT, with and without Sema4D). Numbers represent the mean of four independent experiments performed in triplicate from two independent lentiviral infections from two different virus preps. A minimum of 320 cells were sized per data point. (c) (i and ii) RacGTP binding to Plexin-B1. Shown are the input proteins for GST-pull-down assay. (i) Coomassie blue staining of GST fusion proteins. (ii) Western blot analysis of cell lysate transfected with the indicated Rac1 proteins and detected by anti-myc. (iii) Lysates of HEK293T cells expressing myc-RacL61 or myc-RacN17 were used in a pull-down assay with GST-Plexin-B1 cytoplasmic domain (mutant or WT). Bound proteins were analyzed by immunoblotting with anti-myc antibody. (iv) Band intensities of GST-Plexin-B1 pull-down assays. The results are the average of five experiments  $\pm$  SEM normalized to WT with RacL61;  $P \leq 0.005$  (A5653G and T5714C) and  $P \leq 0.05$  (A5359G) vs. WT.

Wong et al.



**Fig. 6.** Mutations in Plexin-B1 inhibit Rnd1, R-Ras binding, and R-Ras GAP activity. (a) Interaction between Plexin-B1 mutants and Rnd1. Lysates from COS-7 cells expressing GFP-tagged Rnd1 were used in a pull-down assay with GST or GST-Plexin-B1-Cyt mutants. Bound proteins and total-cell lysates were analyzed by immunoblotting with an antibody against GFP. (b) Interaction between Plexin-B1 mutants and R-Ras. Lysates from COS-7 cells expressing the indicated plasmids were immunoprecipitated with an antibody against VSV-G, and bound proteins were analyzed with antibodies against R-Ras, HA, and VSV-G. (c and d). R-Ras GAP activity. COS-7 cells transfected with the indicated plasmids were stimulated with Sema4D for 5 min. The cell lysates were incubated with GST-RBD, and bound R-Ras and total-cell lysates were analyzed by immunoblotting. Relative R-Ras activity was determined by the amount of R-Ras bound to GST-RBD normalized to the amount of R-Ras in cell lysates analyzed by NIH Image software. Results are the means  $\pm$  SEM of three independent experiments.

lamellipodia extension and average cell size vs. WT ( $P \leq 0.01$  and  $P \leq 0.0001$ , respectively).

**Mutation of Plexin-B1 Inhibits Rac Binding.** The increase in cell spreading and extension of lamellipodia observed in cells expressing the mutant versions of the protein is a phenotype characteristic of Rac1 activation. WT Plexin-B1 binds to RacGTP (11) and sequesters it from downstream effectors such as PAK (25). Most of the mutations found in prostate cancer fall within the Rac-binding region of Plexin-B1. We therefore tested the binding of three mutant versions of Plexin-B1 to RacGTP. We found that the T5714C mutation inhibited binding of RacGTP to Plexin-B1, and the other two mutations tested, A5359G and A5653G, showed reduced binding, consistent with the cell-spreading data (Fig. 5*c*).

**The T5714C Mutation Inhibits Rnd1 Binding.** The small GTPase Rnd1 binds to the cytoplasmic domain of Plexin-B1 and is thought to open up the closed inactive conformation of the cytoplasmic domain of Plexin-B1 (23). To determine whether mutation of Plexin-B1 affects Rnd1 binding, immunoprecipitation assays were performed. The Plexin-B1 mutants A5359G and A5653G were found to bind to Rnd1 to a similar extent as WT. In contrast, the mutant T5714C did not bind Rnd1 (Fig. 6*a*).

**Mutation of Plexin-B1 Inhibits R-Ras Binding and R-Ras GTPase-Activating Protein (GAP) Activity.** We speculated that the increase in adhesion and loss of cell collapse seen in cells expressing mutant Plexin-B1 may result from a change in signaling through R-Ras. We therefore tested the effect of mutations in Plexin-B1 on R-Ras binding and R-Ras GAP activity.

Using immunoprecipitation assays, we found that the mutants A5359G, A5653G, and T5714C do not bind R-RasGTP (Fig. 6*b*). Consistent with the lack of R-Ras binding, the A5359G and

A5653G mutants did not show R-RasGAP activity, and R-RasGAP activity was considerably reduced for the T5714C mutant (Fig. 6 *c* and *d*).

These results show that the three mutants tested have lost or considerably reduced their ability to bind R-Ras and inactivate it. Cells expressing mutant Plexin-B1 will therefore have an increased ratio of active/inactive R-Ras relative to cells expressing WT Plexin-B1. Activated R-Ras activates integrins resulting in an increase in cell adhesion and motility. The finding of a loss of R-RasGAP activity for mutant Plexin-B1 is therefore consistent with our *in vitro* assays.

## Discussion

We have found a high frequency of somatic missense mutations in the Plexin-B1 gene in localized and metastatic prostate cancer. The high proportion of nonsynonymous sequence changes found implies that these changes contribute to tumor progression and are not incidental passenger mutations. Furthermore, the mutations tested altered the function of the Plexin-B1 protein, increasing cell motility, invasion, adhesion, and lamellipodia extension and decreasing collapse relative to WT Plexin-B1. The mutations inhibit or hinder Rac1 and R-RasGTP binding and R-RasGAP activity. Overexpression of Plexin-B1 protein in primary prostate cancers was also seen. Together these results suggest that Plexin-B1 has a role in prostate cancer progression.

A standard method of identifying oncogenes is to transfect the gene construct into NIH 3T3 cells and measure tumorigenicity *in vivo*. However, such *in vivo* studies have not been feasible because of an inability to maintain exogenous expression of Plexin-B1 over time and will require the use of inducible vectors.

Plexin-B1 activates the oncogenes c-Met and ErbB2 (13, 14), resulting in an increase in cell motility and promotion of the invasive phenotype (14). High levels of c-Met and ErbB2 protein have been observed in prostate cancer (26, 27), and we have now found that Plexin-B1 and Sema4D are also overexpressed. Overexpression of WT Plexin-B1 in prostate tumor cells may promote the invasive phenotype through activation of c-Met and ErbB2. The mutations are less likely to affect the activating pathways mediated by Plexin-B1 via c-Met and ErbB2, because these proteins interact with the extracellular domain of Plexin-B1, whereas the mutations are in the cytoplasmic domain. The mutations may therefore selectively inhibit Plexin-B1 inhibitory pathways (via R-Ras and Rac) while retaining activation of c-Met and ErbB2, resulting in an increase in adhesion, motility, and invasion. In addition, a significant increase in cell spread was observed in cells expressing mutant Plexin-B1 relative to vector controls. This finding indicates that the mutations may confer a gain of function to the cell in addition to inactivating inhibitory pathways.

Some of the mutations were present in many tumors. The high frequency of mutations at specific sites suggests specific roles for the mutated regions or specific residues in the neoplastic process. Mutational hotspots occur in several other oncogenes such as TP53, RAS, and BRAF (28–30). Some of the tumor samples had up to three mutations in the Plexin-B1 gene. Different mutations may occur in distinct groups of cells or foci. Prostate cancer is genetically heterogeneous with many overlapping foci, each with a distinct genotype, in one tumor. Up to three different mutations were found in the KLF6 gene in single foci of prostate cancer (18), and up to four mutations were found in the androgen receptor gene (19). If present in the same cell, the mutations may destabilize the inactive closed conformation formed between the C1 and C2 regions of the cytoplasmic domain of Plexin-B1 (23). Increasing numbers of mutations would have a cumulative effect on the protein, further destabilizing the closed conformation and offering a greater selective advantage to the cell. The frequency of mutations in Plexin-B1 in primary tumors exceeds the clinical risk of prostate cancer metastasis, suggesting that other factors are important in addition to promote metastasis.

Because prostate tumors often contain overlapping foci of different genotypes and many nonneoplastic cells, the method used to isolate tumor cells for mutation detection is important. Prostate cancer tissue isolated by laser capture microdissection (LCM) provided DNA of sufficient purity for mutation detection by direct sequencing. In contrast, tissue isolated by manual microdissection provided DNA of lesser purity, and mutations were only detected by SSCP analysis and restriction-enzyme digestion. It is likely that mutation detection in DNA from nonmicrodissected prostate cancer tissue will prove more problematic.

Our data indicate that Plexin-B1 is one of the most frequently mutated genes thus far found in prostate cancer. Plexin-B1 is likely to be a key player in cancer invasion and metastasis and is a potential target for anticancer therapy.

## Methods

**Tumor Tissue.** Tissue was obtained by LCM for the metastases and for fresh frozen prostate tissue and by manual microdissection for the paraffin-embedded tissue from primary cancers. Areas of cancer were identified by a consultant histopathologist (A. Freeman, University College London). Samples were collected with local ethical board approval.

**Immunohistochemistry.** Sections from four replicate TMA blocks of 85 primary prostate cancers and 85 samples of nonneoplastic prostate tissue from the same radical prostatectomies were stained with antibodies to Plexin-B1 (H300; SantaCruz), Sema4D (610671; BD Biosciences), c-Met (c-28; Santa Cruz), or with haematoxylin and eosin. The sections were scored blind by a consultant histopathologist according to the extent and intensity of staining. Positive staining was defined as unequivocal staining of at least 75% of epithelial or cancer cells in at least one of the four cores.

**Screening for Mutations.** SSCP analysis was carried out as described in ref. 31; see *SI Methods* for details. Numbering for the mutations is according to GenBank accession no. AB007867. Control DNA from unrelated individuals of Caucasian origin was screened for the presence of each identified mutation by PCR and restriction enzyme digestion (31). See *SI Methods* for details.

**RT-PCR.** Real time RT-PCR was performed on an ABI PRISM 7700 (Applied Biosystems) by using  $\beta$ -actin as control and primers and probe spanning exons 31 and 32 of the Plexin-B1 gene.

**In Vitro Mutagenesis.** Plexin-B1 in pcDNA3 was kindly provided by A. Hall (A. Hall, Memorial Sloan-Kettering Cancer Center, New York, NY). The A5359G, A5653G, T5714C, and C5060T sequence changes were introduced using the QuikChange kit (Stratagene). See *SI Methods* for primer sequences. The sequence was checked by DNA sequencing, and protein expression was confirmed by Western blot analysis and immunocytochemistry.

**Lentiviral Transduction.** WT Plexin-B1 and the four mutant constructs were cloned into pLentiV5-D-TOPO, and the sequence was verified. Virus, produced in 293FT cells, was transduced into HEK293 cells with polybrene (8  $\mu$ g/ml). Infected cells were selected with blasticidin. Protein expression was confirmed by Western blotting and immunocytochemistry.

**Cell Culture.** LNCaP, PC3, and DU145 cells were grown in RPMI medium 1640 with 10% FCS. HEK293 and COS-7 cells were grown in DMEM with 10% FCS.

**Preparation of Recombinant Sema4D-Fc.** The Sema4D-Fc construct was kindly provided by Hitoshi Kikutani (Osaka University, Osaka, Japan) in vector pEFBos. Recombinant Sema4D-Fc was purified from conditioned medium of COS-7 cells transfected with pEFBos (Sema4D-Fc) by using proteinA Sepharose CL-4B beads and was

concentrated using Centricon columns (Amicon). The protein concentration and purity were assessed by Western blotting compared with known concentrations of Sema3A-Fc (R & D Systems).

**Cell-Substrate-Adhesion and Cell-Spreading Assays.** Cells were plated onto the lids of 96-well plates ( $1 \times 10^4$  cells per well) coated with 20  $\mu\text{g}/\text{ml}$  fibronectin or poly-L-lysine with or without Sema4D (100 ng/ml), incubated at 37°C for 10 or 30 min, washed with PBS, fixed, and stained with 0.5% crystal violet. Staining was measured on a plate reader at 595 nm. Results shown are the mean of four independent experiments performed in triplicate with two different lentiviral transductions  $\pm$  SEM.

For the cell-spread assays, cells were plated on 20  $\mu\text{g}/\text{ml}$  fibronectin with or without Sema4D (100 ng/ml), incubated at 37°C for 10 min, washed, fixed, and stained with 0.5% crystal violet. Photomicrographs of cells were sized using Andor imaging systems. A minimum of 320 cells were sized per data point. Results shown are the mean of four independent experiments performed in triplicate with two different lentiviral transductions  $\pm$  SEM.

**Cell-Collapse Assay.** COS-7 cells were transiently transfected with Plexin-B1 and Rnd1-myc and stimulated with Sema4D (100 ng/ml) for 5 min, 16 h after transfection. Cells were fixed in 4% paraformaldehyde and stained by immunofluorescence with Plexin-B1 (H300; Santa Cruz) and anti-myc (9E10; Santa Cruz) antibodies and phalloidin-TRITC (Sigma-Aldrich). The degree of collapse (percentage of cells  $<500 \mu\text{m}^2$ ) was determined by sizing transfected cells using Andor imaging. Fifty cells were counted per experiment. Results are the mean of three independent experiments  $\pm$  SEM.

**Cell-Motility Assays.** Time-lapse video microscopy was performed 24 h after plating the cells in a humidified, 5%  $\text{CO}_2$  atmosphere at 37°C. Images were captured at 10-min intervals over 16 h for each cell type. The experiment was independently repeated three times, and 20 cells were tracked in each experiment by using Motion Analysis (Kinetic Imaging). The average rate of cell migration was determined with Mathematica software (Wolfram Research).

**Invasion Assays.** Serum-starved lentiviral-transduced HEK293 cells ( $6 \times 10^4$  cells per insert) in DMEM were placed in the upper chamber of 24-well, 0.8- $\mu\text{m}$  BD Biocoat matrigel invasion chambers (BD Biosciences) with or without purified Sema4D (100 ng/ml). DMEM with 10% serum was placed in the lower chamber. The chambers were incubated at 37°C for 24 h. Cells on the upper side were removed, and those on the underside were fixed, stained with crystal violet, and counted by using a microscope. Five independent experiments were performed in duplicate.

**GST-B1cyto Purification.** The region of Plexin-B1 cDNA encoding the intracellular domain (amino acids 1,512–2,135; GenPept accession no. NP\_002664) was amplified by PCR (see primer sequences in *SI Methods*). The PCR product was cloned into pGEX-4T-3 (Amersham) by SalI and XhoI sites to produce pGEXB1cytoWT. Mutations were introduced into pGEXB1cytoWT using QuikChange II XL *in vitro* mutagenesis kit (Stratagene). GST-B1cyto fusion proteins were produced in *E. Coli* BL21 and purified with glutathione Sepharose 4B (Amersham). The bound proteins were analyzed by Commassie blue staining in SDS/8% PAGE gel.

**Rac-Binding Assays.** GST-Plexin-B1-coated Sepharose beads were incubated with HEK293T cell lysate expressing constitutively active RacL61 or dominant negative RacN17. The bound protein was analyzed by Western blot analysis.

**Rnd1-Binding Assays.** GST-Plexin-B1-coated Sepharose beads were incubated with COS-7 cell lysate expressing Rnd1. The bound protein was analyzed by Western blot analysis.

**R-Ras-Binding Assays.** COS-7 cells transiently transfected with VSV-Plexin-B1, HA-Rnd1 and R-RasQL were lysed in cell lysis buffer [20 mM Tris-HCl (pH 8.0), 150 mM NaCl, 4 mM  $\text{MgCl}_2$ , 1% Nonidet P-40, 10% glycerol, 1 mM PMSF, 10  $\mu\text{g}/\text{ml}$  aprotinin, 10  $\mu\text{g}/\text{ml}$  leupeptin, and 1 mM DTT]. The lysate was incubated with 4  $\mu\text{g}/\text{ml}$  of monoclonal antibody against VSV (P5D4; Sigma) for 2 h and subsequently incubated with protein G-Sepharose beads (GE Healthcare) for 1 h. The bound protein was analyzed by Western blot analysis.

**R-RasGAP Activity.** Transiently transfected COS-7 cells were stimulated with Sema4D for 5 min, and lysed in cell lysis buffer [25 mM Hepes-NaOH (pH 7.5), 150 mM NaCl, 1% Nonidet P-40, 0.25% Na-deoxycholate, 10% glycerol, 10 mM  $\text{MgCl}_2$ , 10  $\mu\text{g}/\text{ml}$  aprotinin, and 10  $\mu\text{g}/\text{ml}$  leupeptin]. Lysates were incubated with 75  $\mu\text{g}$  of GST-fused Ras-binding domain of c-Raf-1 and analyzed by immunoblotting.

**Statistical Analysis.** For cell-function assays, *P* values were calculated using a two-tailed Student's *t* test, except for Rac binding assays, for which a one-tailed test was used. The Mann-Whitney test (two-tailed) was used for the immunohistochemistry results.

We thank Drs. Constance Parkinson, Athena Nikitopoulou, and Sandra Strautnieks for their help. We also thank the Prostate Cancer Research Centre, Smith's Charity, the Rosettes Trust, the Barcapel Foundation, the McAlpine Foundation, the Orchid Appeal, and the Cecil Pilkington Charitable Trust for funding.

- Kruger RP, Aurandt J, Guan KL (2005) *Nat Rev Mol Cell Biol* 6:789–800.
- Kolodkin AL, Matthes DJ, Goodman CS (1993) *Cell* 75:1389–1399.
- Eklholt BJ, Mackenzie SL, Graham A, Walsh FS, Doherty P (1999) *Development (Cambridge, UK)* 126:2181–2189.
- Serini G, Valdemir D, Zanivan S, Morra G, Burkhardt C, Caccavari F, Zambataro L, Primo L, Tamagnone L, Logan M, et al. (2003) *Nature* 424:391–397.
- Takahashi T, Fournier A, Nakamura F, Wang LH, Murakami Y, Kalb RG, Fujisawa H, Strimatter SM (1999) *Cell* 99:59–69.
- Tamagnone L, Antignani S, Chen H, He Z, Ming G, Song H, Chedoui A, Winberg ML, Goodman CS, Poo M, et al. (1999) *Cell* 99:71–80.
- Mastrini E, Tamagnone L, Longati P, Cremona C, Gulisano M, Bione S, Tamagnini F, Ned BG, Toniolo D, Comoglio PM (1996) *Proc Natl Acad Sci USA* 93:674–678.
- Kumanogoh A, Kitayama H (2004) *Cell Mol Life Sci* 61:292–300.
- Oinuma I, Ishikawa Y, Katoh H, Negishi M (2004) *Science* 305:862–865.
- Oinuma I, Katoh H, Harada A, Negishi M (2003) *J Biol Chem* 278:25671–25677.
- Vakis HG, Li W, He Z, Guan KL (2000) *Proc Natl Acad Sci USA* 97:12457–12462.
- Swienz JM, Kuner R, Behrens J, Offermanns S (2002) *Nature* 35:51–63.
- Swienz JM, Kuner R, Offermanns S (2004) *J Cell Biol* 165:869–880.
- Giordano S, Corso S, Conrotto P, Arigliani S, Galestro G, Barbieri D, Tamagnone L, Comoglio PM (2002) *Nat Cell Biol* 4:720–724.
- Tusolino L, Comoglio PM (2002) *Nat Rev Cancer* 2:289–300.
- Böschner C, Böhmeier W, Cheredi E, Vande Woude GF (2003) *Nat Rev Mol Cell Biol* 4:915–925.
- Clark J, Menon S, Jhavar S, Fekhr P, Edwards S, Foster CS, Eeles R, Manji FL, Phillips DH, Crundwell M, et al. (2007) *Oncogene* 26:2667–2673.

- Nada G, Heath KE, Reeves HL, Li D, Giono LE, Kimmelman AC, Gluckman MJ, Narko J, Eng FJ, Chan AM, et al. (2001) *Science* 294:2563–2566.
- Marcelli M, Ittmann M, Mariani S, Sutherland R, Nigam R, Murthy I, Zhao Y, DiConcilio D, Puzosdu E, Eisen A, et al. (2000) *Cancer Res* 60:944–949.
- Foster CS, Fakoner A, Dodson AR, Norman AB, Dennis N, Fletcher A, Southgate C, Dowe A, Desmukh D, Jhavar S, et al. (2004) *Oncogene* 23:5871–5879.
- Antipenko A, Himmelen JP, van Leyen K, Nardi-Dei V, Lesniak J, Barton WA, Rajshankar KR, Lu M, Hoernne C, Puschel AW, et al. (2003) *Nature* 39:589–598.
- Barberic D, Arigliani S, Cazzaza A, Corso S, Giordano S, Love CA, Jones EY, Comoglio PM, Tamagnone L (2004) *FASEB J* 18:592–594.
- Oinuma I, Katoh H, Negishi M (2006) *J Neurosci* 24:11473–11480.
- Oinuma I, Katoh H, Negishi M (2006) *J Cell Biol* 173:601–613.
- Vakis HG, Li W, Guan KL (2002) *Genes Dev* 16:836–845.
- Humphrey PA, Zhu X, Zarnegar R, Swanson PE, Ratliff TL, Vollmer RT, Day ML (1995) *Am J Pathol* 147:386–396.
- Knudsen BS, Gmyrek GA, Inra J, Scherr DS, Vaughan ED, Natus DM, Kattan MW, Gerald WL, Vande Woude GF (2002) *Oncology* 63:1113–1117.
- Peitjean A, Mathe E, Kato S, Ishikawa C, Tavtigian SV, Hainaut P, Olivier M (2007) *Hum Mutat* 28:622–629.
- Davies H, Bignell GR, Cox C, Stephens P, Edkins S, Clegg S, Teague J, Woffendin H, Garnett MJ, Bottomley W, et al. (2002) *Nature* 417:949–954.
- Bos JL (1989) *Cancer Res* 49:4682–4689.
- Williamson MP, Ekler PA, Knowles MA (1994) *Genes Chromosomes Cancer* 9:108–118.